Alma Mater Studiorum – Università di Bologna

DOTTORATO DI RICERCA IN

Scienze Biomediche e Neuromotorie

Ciclo XXXIII

Settore Concorsuale: 05/D1

Settore Scientifico Disciplinare: BIO/09

Cardiorespiratory control during sleep in orexin deficient mice

Presentata da: Sara Alvente

Coordinatore Dottorato

Prof. Pietro Cortelli

Supervisore

Prof.ssa Giovanna Zoccoli

Co- Supervisore

Prof. Franco Trevisani

Esame finale anno 2020

INDEX

ABSTRACT

Introduction: Orexins (ORXs) are neuropeptides produced by a small neuronal population localized in the lateral hypothalamic area. Despite the restricted localization, ORX neurons widely project through the entire neuroaxis, except the cerebellum, thus suggesting the involvement of ORXs in the coordination of many biological functions. The role of ORXs in the regulation of the wake-sleep and feeding behaviours is well known, but less is known about their involvement in thermoregulation and in the regulation of the cardiovascular and respiratory variables, depending on the wake-sleep states. The loss of ORX neurons entails narcolepsy type 1 (NT1), a neurological disorder characterized by excessive daytime sleepiness and cataplectic attacks. Moreover, increased arterial pressure (AP) during sleep, blunted AP differences between sleep and wakefulness (W) and increased occurrence rate of sleep apneas have been reported in ORX-deficient (ORX-KO) mouse models of NT1 and confirmed in some studies on NT1 patients. Therefore, few studies have been described an interaction between ambient temperature (Ta) and breathing in mice and humans.

Aims: the first experiment aimed to explore the autonomic mechanisms of cardiovascular control during sleep in an ORX-knock out (ORX-KO) mouse model of NT1. The second experiment investigated the role of ORXs in the modulation of respiratory variables in the different states of the wake-sleep cycle, as a function of Ta. Moreover, a second aim was to verify whether the increase in sleep apnea occurrence rate in ORX-KO mice depended on the exposure to different Ta (20°C vs 30°C).

Methods: To explore the autonomic cardiovascular mechanisms in ORX-KO mice during sleep, 13 male ORX-KO mice were compared with 12 congenic wild-type (WT) mice. The electroencephalogram, electromyogram, and AP of the mice were recorded in the light (rest) period during intraperitoneal infusions of selective autonomic blockers, such as atropine methyl nitrate, atenolol, or prazosin, to block muscarinic cholinergic, β1-adrenergic, or α1-adrenergic receptors, respectively. Saline was infused as control. To investigate the role of ORXs in breathing phenotype during the wake-sleep states as function of Ta, respiratory variables of 9 male ORX-KO and 8 congenic WT mice were studied at thermoneutrality (Ta=30°C) or during mild cold exposure (Ta=20°C) inside a whole-body plethysmography chamber. The wake-sleep states were scored non-invasively, using a previously validated technique.

Results: ORX-KO had significantly higher AP values during REM sleep, smaller decreases in AP from W to both non-rapid-eye-movement (NREM) sleep or REM sleep, and greater increases in AP from NREM sleep to REM sleep compared to WT. These differences remain unchanged after atropine infusion; conversely, they were abolished by prazosin and also by atenolol, with the exception of the blunted AP decrease from W to REM sleep in ORX-KO. In the second experiment, we found that in both WT and ORX-KO, Ta significantly affected ventilatory period (VP) and minute ventilation (V_E) values during NREM and REM sleep. The occurrence rate of sleep apneas in NREM sleep was significantly reduced at Ta=20°C compared with Ta=30°C. No significant differences were found in respiratory regulation during sleep between WT and ORX-KO mice, except for sigh occurrence rate, which was significantly increased at Ta=20°C compared with Ta=30°C in WT mice, but not in ORX-KO mice.

Conclusion: The results of the first experiment support the hypothesis that alterations in sympathetic control of the heart and resistance vessels are sufficient to mediate sleep-related alterations of AP due to ORX-deficiency in a mouse model of NT1. Moreover, the second experiment do not support a main role for ORXs in the modulation of respiratory regulation as a function of Ta, during sleep, except for sigh occurrence rate. However, we showed that the sleep apnea occurrence rate critically depends on Ta, without any significant effect of ORXs.

1 THE HYPOCRETIN/OREXIN SYSTEM

1.1 The Peptides, the Receptors and the Anatomic organization

Orexin A and B (ORX-A, ORX-B), also called Hypocretin 1 and 2, are two neuropeptides discovered in 1998 by two independent research groups, and produced in the lateral area of hypothalamus (LHA) (De Lecea et al., 1998; Sakurai et al., 1998). Orexins/Hypocretins are considered the most pleiotropic family of hypothalamic neuropeptides because they are involved in the regulation of several biological processes, such as sleep, energy expenditure, cardiovascular functions, pain and neuroendocrine regulation (Milbank & López, 2019).

The first group that described these neuropeptides, led by Gregor Sutcliffe, used the directional tag polymerase chain reaction (PCR) subtraction to identify a novel mRNA with restrictive expression in dorsal and lateral hypothalamus. This mRNA encoded a protein of 130 amino acid, identified as the precursor of two different peptides. These peptides shared substantial amino acid identities with each other and with the gut hormone secretin. For the sequence homology with secretin and for their hypothalamic origin, they were named Hypocretin-1 and Hypocretin-2 (De Lecea et al., 1998).

In parallel, Masashi Yanagisawa and its group, while characterizing ligands for orphaned G-protein-coupled cell surface receptors (GPCRs), identified two novel peptides that bind to two related orphaned GPCRs (Hypocretin/-orexin receptor-1 and Hypocretin/Orexin receptor-2). Yanagisawa and colleagues determined that those peptides were originated from a common precursor in the lateral hypothalamus and, considering its hypothalamic locations, they suggested a potential role in feeding behaviour. In line with this, they demonstrated that intracerebroventricular (ICV) infusions of these peptides increased food intake in non-fasted rats whereas fasting increased the expression of those peptides. Therefore, considering their orexinergic activity, the researchers named these peptides Orexin-A (ORX-A) and Orexin-B (ORX-B), from the Greek *orexis,* meaning appetite (Sakurai et al., 1998).

Although “hypocretins” and “orexins” (ORXs) are synonymous for the same neuropeptides, the orexin nomenclature will be used throughout this thesis, to avoid confusion.

ORX-A is a 33-amino acid peptide of 3562 Da, with an N-terminal pyroglutamyl residue, two sets of intrachain disulfide bonds and C-terminal amidation (Sakurai et al., 1998). This structure, predicted from cDNA sequence, is completely conserved among several mammalian

species (human, sheep, dog, cow, mouse, rat, and pig). ORX-B is a 28-amino acid C-terminally amidated linear peptide of 2937 Da, with the C-terminal half very similar to that of the ORX-A (73%), whereas the N-terminal half is more variable. ORX-B is 46% (13/28) identical in sequence to ORX-A. Mouse ORX-B was predicted to be identical to rat ORX-B, whereas human ORX-B has two amino acid substitutions compared to the rodent sequence within the 28-residue stretch. ORX-B also has a high degree of sequence similarity among species (Sakurai, 1999).

Both ORXs derive from a common 130-residue (rodent) or 131-residue (human) precursor polypeptide, called prepro-orexin (prepro-ORX), by proteolytic processing (Sakurai et al., 1999). The human prepro-ORX gene is located on chromosome 17q21 and consists of two exons and one intron (818-bp) distributed over 1432bp of the human genome (Sakurai et al., 1999). The exon 1 (143-bp) includes the 5'-untranslated region and the first 7 residues of the secretory signal sequence, while the exon 2 (473-bp) contains a portion of the open reading frame and the 102-bp 3'-untranslated region. The expression of the prepro-ORX gene depends of many physiological factors, such as sleep or fasting (Hirano et al., 2018; Wall & Volkoff, 2013).

A study performed on transgenic mice demonstrated that the human prepro-ORX fragment, which contains the whole length of the 5'-noncoding region and a 3149-bp 5'-flanking region of exon 1, is sufficient to allow the expression of the Escherichia coli β-galactosidase (LacZ) gene in ORX neurons without ectopic expression, and contains all the necessary elements for appropriate expression of that gene (Sakurai et al., 1999). This fragment, functioning as a promoter, has been used to observe the consequences of the expression of exogenous molecules in ORX neurons of transgenic mice and to establish several transgenic lines, e.g., ORX neurons-ablated (ORX-AB) rats and mice (Beuckmann et al., 2004; Hara et al., 2001), mice with ORX neurons expressing green fluorescent protein (Yamanaka, Muraki, et al., 2003) or calcium-sensitive fluorescent protein (Yellow cameleon Yc2.1) (Tsujino & Sakurai, 2009).

ORXs produce excitatory post-synaptic responses by binding to two GPCRs, named ORX-1 receptor (OX1R) and ORX-2 receptor (OX2R), which have 64% amino acid overlapping (Sakurai et al., 1998). Both the receptors' genes are highly conserved between species; the amino acid identity between the human and the rat homologues of each receptor is 94% and 95% for OX1R and OX2R, respectively (Ohno & Sakurai, 2008). Binding experiments using Chinese Hamster Ovary (CHO) cells, expressing selectively the human OX1R or OX2R c-

DNA, demonstrated different affinity of those receptors to ORX-A or ORX-B. In particular, OX1R had a highest affinity for ORX-A and OX2R had similar elevated affinity for both the neuropeptides (Sakurai et al., 1998).

GPCRs transmit information into cells by activating heterotrimeric G-protein, that are composed of an α, β and γ subunits. Binding of ORXs to OX1R or OX2R activates two different G-protein subtypes, which produces the different effects of ORXs in specific neurons. OX1R is coupled exclusively to the $Gq/_{11}$ subclass, which induces the activation of phospholipase C and the triggering of the phosphatidylinositol cascade, whereas OX2R may couple to Gi and/or $Gq/_{11}$ subtypes (Sakurai, 1999; Zhu et al., 2003).

In situ hybridization studies have demonstrated that both orexin receptors (OXRs) mRNAs are expressed in the central nervous system in regions with dense orexin innervations. Molecular and immunohistochemistry studies have shown that OX1R and OX2R have a different and complementary distribution throughout the rat brain (Marcus et al., 2001). Outside the hypothalamus, OX1R mRNA has been found in tenia tecta, hippocampus, dorsal raphe nucleus, and locus coeruleus (LC). OX2R mRNA is expressed in the cerebral cortex, nucleus accumbens, subthalamic nucleus, paraventricular thalamic nuclei and the raphe nuclei. Within the hypothalamus, OX1R mRNA has a main distribution in the anterior hypothalamic area and ventromedial hypothalamic nucleus (VMH), while high levels of OX2R mRNA are found in the dorsomedial hypothalamus (DMH), in the arcuate nucleus (ARC), paraventricular nucleus (PVN) and tuberomammillary nucleus (TMN) (Ohno & Sakurai, 2008). The dorsal raphe (DR) and ventral tegmental area (VTA) express both ORXRs (Marcus et al., 2001). The wide distribution of the OXRs confirms the pleiotropic role of the orexinergic neurotransmitters.

ORXs are produced by a small population (3000 in the rat brain, 50000 in the human brain) of neurons located in the perifornical nucleus, LHA and dorsal hypothalamic area (Peyron et al., 1998). The ORX neurons have different size (cell body diameter 15-40 μm) and shape (multipolar, fusiform or spherical). Apart from ORXs, ORX neurons also produce and secret galanin, prolactin, neuronal activity regulated pentraxin (NARP), glutamate and the inhibitory peptide dynorphin. Whereas glutamate is packaged separately from ORXs, dynorphin is packaged in the same vesicles that contain ORXs and is co-released with them. The overall effect of the co-releasing is variable, depending of the expression of OXRs or dynorphin receptors on the postsynaptic membrane (Arrigoni et al., 2019).

Although ORX neurons represent a relatively small population of cells, they diffusely project from the hypothalamic regions to the entire neuroaxis, excluding the cerebellum (Nambu et al., 1999; Peyron et al., 1998). Studies performed with genetic encoded retrograde tracer or from appositions of anterogradely labelled terminals, have identified the inputs to ORX neurons, that originate from a wide variety of brain regions. The largest inputs derive from other areas of the hypothalamus and from regions involved in the emotion and autonomic control, such as the infralimbic cortex, lateral septum, and the bed nucleus of the stria terminalis (BST). This anatomical organization suggests that the activity of ORX neurons influences multiple brain areas and that ORXs are involved in the regulation of multiple physiological processes (Sakurai et al., 2005; Yoshida et al., 2006).

The study of ORX neurons' efferent and afferent systems and the characterization of genetically modified animal models, have suggested that ORX neurons are involved in the regulation of the feeding behaviour and energy metabolism and in the maintenance of the wakefulness (W); moreover, they are related to other systems that regulate emotions, reward and energy homeostasis. Lack of ORXs leads to narcolepsy, a disabling sleep disorder characterized by excessive daytime sleepiness and abnormal rapid-eye-movement (REM) sleep manifestations including sleep paralysis, cataplexy, hallucinations and sleep onset REM sleep periods (Scammell, 2003).

1.2 Orexins, sleep and wakefulness

The symptoms and the pathophysiology of narcolepsy have suggested a crucial role of ORXs in the maintenance and consolidation of W state. As discussed above, ORX neurons are localized exclusively in LHA and posterior hypothalamus and, despite their specific localization, they project through the entire neuroaxis, with the exception of cerebellum (Peyron et al., 1998). ORX neurons densely innervate the PVN of the thalamus, the ARC of the hypothalamus and, most notably, brain stem monoaminergic regions involved in the maintenance of the arousal and in the regulation of the wake-sleep cycle, such as TMN nucleus (containing histaminergic neurons), LC (containing noradrenergic neurons) and DR (containing serotoninergic neurons) (Nambu et al., 1999). The distribution of both OXRs' mRNA reflects that of the projection sites; within mouse brain, OX1R is most abundantly expressed in the LC, while OX2R is highly expressed in the TMN (Marcus et al., 2001). The DR and VTA contain both OXRs (Marcus et al., 2001). These observations suggest that these nuclei are major

effector sites of ORXs. In line with these hypothesis, in vitro studies have shown that noradrenergic neurons of LC, dopaminergic neurons of VTA, serotoninergic cells of DR and histaminergic neurons of TMN are all activated by ORXs (Liu et al., 2002; Yamanaka et al., 2002). The activity of these monoaminergic neurons is synchronized and strongly associated with sleep and wakefulness: they fire tonically during W, less during NREM and cease firing during REM. Moreover, ORXs directly activate cholinergic neurons in basal forebrain (BF), that is also involved in the maintenance of arousal and attention. These observations indicate that ORX-mediated arousal results from the activation of these wake-active monoaminergic neurons and that ORX neurons might exert their excitatory influence on these wake-active neurons, sustaining their activity (Sakurai, 2007).

There are mutual projections between ORX neurons and the ventrolateral preoptic area (VLPO), that have a crucial role in non-rapid eye movement (NREM) sleep onset and maintenance. The VLPO neurons fire during sleep and decrease their firing during W. They contain the inhibitory Gamma Amino-butyric acid (GABA) and galanin neurotransmitters, and project to the major nuclei in the hypothalamus and brainstem that participate in arousal (Yoshida et al., 2006; Sakurai et al., 2005). Moreover, VLPO receives afferents from each of the major monoaminergic systems (Chou et al., 2002) and therefore, it can be inhibited by the same arousal systems that it inhibits during sleep (Saper et al., 2005). ORX neurons are inhibited by both Muscimol ($GABA_A$ receptor agonist) and Baclofen ($GABA_B$ receptor agonist), thus indicating that the VLPO might be a source of GABA-containing inhibitory projections to ORX neurons. This pathway might be important for turning off ORX neurons during sleep (Sakurai, 2007).

In vivo single unit recording studies, performed independently by two different research groups, have reported the changes in the ORX neurons' activity across sleep-wake cycle. Using unrestrained, unanaesthetised rats, Mileykovskiy and colleagues found that ORX neurons fired in active waking, while they were relatively inactive during quiet waking, with transient activation related to sensory stimuli. Moreover, ORX neurons were silent in NREM sleep and tonic period of REM sleep, with occasional burst discharge in phasic REM (Mileykovskiy et al., 2005). To understand the mechanisms by which ORX neurons are involved in the maintenance of the awake state, Lee and colleagues also recorded the activity of ORX neurons in head-fixed rats across sleep-wake cycle. They found that ORX neurons discharged during active W, in association with movements, decreased firing during quiet W and ceased firing during NREM and REM sleep, when postural muscle tone is low or absent. Interestingly, during

the transition from REM sleep to W, ORX neurons increased firing before the end of sleep, prior to the onset of electroencephalographic (EEG) activation, anticipating by several seconds the awakening (Lee et al., 2005).

Narcolepsy is a disorder characterized by the inability to maintain vigilance states, with frequent transitions between state of sleep and W. The disease is caused by a loss of ORX neurons, thus suggesting that ORX is crucial to stabilize W and to inhibit abnormal transition between each vigilance state. To explain how ORX neurons stabilize W, by interacting with the neural circuits described above, Saper et al. have considered the ORX system as a key component of a flip flop model. A "*flip-flop switch*" is a circuit that contains mutually inhibitory elements that set up a self-reinforcing loop. The activity in one of the competing sides shuts down inhibitory inputs from the other side, and therefore disinhibits its own action (Saper et al., 2005). During **W,** histaminergic neurons of TMN, noradrenergic neurons of the LC and serotonergic neurons of the DR receive excitatory influences by ORX neurons and send inhibitory feedback projections to them. The feedback circuit might maintain the activity of monoaminergic neurons, also in case of small perturbation. In fact, when the activity of the monoaminergic neurons decreases, this causes a reduction in the inhibitory influence on ORX neurons and so ORX neurons may have an increased excitatory influence on monoaminergic neurons to maintain their activity. Moreover, these monoaminergic cells send excitatory projections to the thalamus and cerebral cortex, and inhibitory projections to the VLPO sleep centre. Because VLPO neurons do not have OXRs, ORX neurons serve primarily to reinforce monoaminergic tone, instead to directly inhibit VLPO. These mechanisms might maintain wakefulness. During **sleep**, the firing of VLPO sleep-active neurons inhibits the monoaminergic cell groups, thus relieving their own inhibition. This also allows it to inhibit the activity of ORX neurons and, so, to prevent the activation of monoaminergic neurons that might interrupt sleep.

The presence of ORX neurons in this circuit stabilizes the switch and prevents unwanted transition between sleep and wake states. In fact, when ORX neurons are removed from the switch, such as in narcolepsy, the sleep-active neurons of VLPO and the monoaminergic neurons became the only players in the "flip flop system": when the activity in one of the competing sides begins to overcome the other side, this produces an abrupt transition into an alternative state. This mechanism could explain the instability of wake/sleep states in narcolepsy (Saper et al., 2005; Sakurai, 2007). Fig. 1 schematically shows the role of ORX neurons in the stabilization of wake-sleep states.

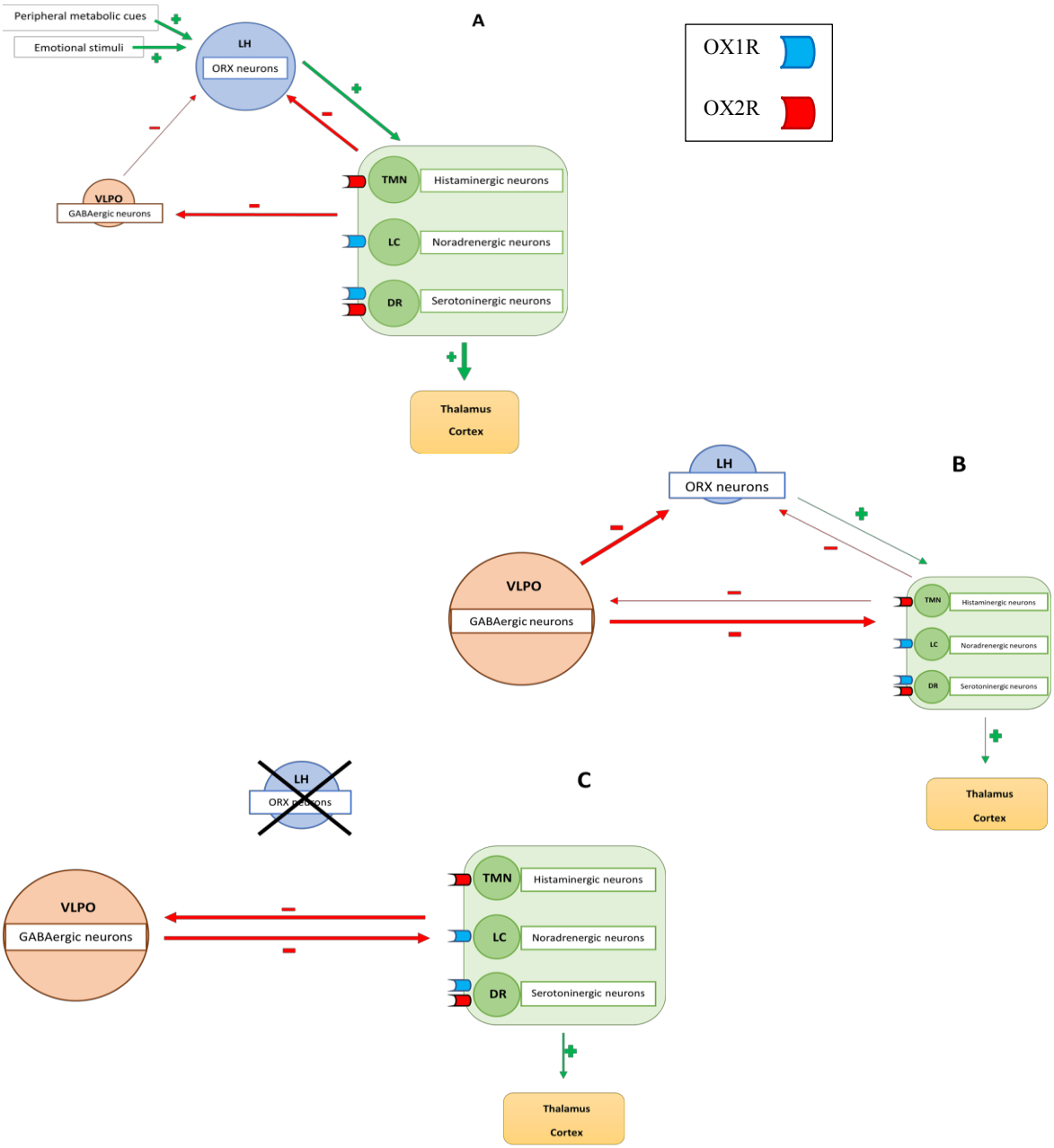

Figure 1. Role of orexin system in the stabilization of sleep and wakefulness.

The figure represents the interaction between ORX neurons, localized in the LH, monoaminergic wake-active neurons (histaminergic neurons in TMN, noradrenergic neurons in LC, and serotoninergic neurons in DR), and VLPO sleep-active centre, during the wake-sleep states. Green arrows represent excitatory input and red arrows inhibitory input. The thickness of arrows represents the strength of the input. **A. Wakefulness.** During wakefulness, the monoaminergic wake-active neurons receive excitatory influences by ORX neurons and send inhibitory projections to them. The monoaminergic cells send excitatory projections to the thalamus and cortex and inhibitory projections to the VLPO sleep centre. These mechanisms maintain wakefulness state. **B. Sleep state.** VLPO sleep-active neurons send inhibitory projections to both ORX neurons and monoaminergic neurons to stabilize sleep. **C. Narcolepsy.** If ORX neurons are removed from this system, VLPO sleep centre and monoaminergic neurons are the two only players and set up a mutually inhibitory circuit, which is instable and can cause an abrupted and unwanted transition between sleep and awake state. Orexin (ORX), tuberomammillary nucleus (TMN), locus coeruleus (LC), dorsal raphe (DR), ventrolateral preoptic area (VLPO).

ORX neurons interact with multiple neuronal systems, integrating and coordinating the afferent information about fuel stores and emotional stimuli, to produce a coherent activation of the arousal system. ORX neurons receive inputs from the limbic system, including the amygdala and other regions closely associated, which is involved in emotion, motivation, learning, and memory. These inputs might be important for regulation of ORX neurons activity upon emotional stimuli, to evoke arousal or emotional related responses, including elevation of sympathetic outflow (Ohno & Sakurai, 2008). Moreover, interaction with these regions might be implicated in the pathophysiology of cataplexy, that is generally triggered by strong positive emotion (Sakurai, 2007).

1.3 Orexins, feeding behaviour and energy balance

The hypothalamus is historically considered a key site for the maintenance of the energy homeostasis, as it coordinates and integrates metabolic, behavioral and neuroendocrine responses.

In mammals, the neurons of the LHA are important for feeding and behavioral arousal, as evidenced by the fact that animal models with injuries in this region exhibit weight loss and reduction in food intake. Therefore, the LHA is considered the feeding center, also because is an important component of the autonomic nervous system which extensively projects within the hypothalamus and throughout the entire neuroaxis and coordinates all the multiple processes necessary to induce environmentally appropriate feeding-related behaviors (Willie et al., 2001).

One of the first functions ascribed to ORXs, also considering their hypothalamic origin, was the regulation of feeding behaviour. Their feeding promoting effect was supported by several studies: central administration of ORXs in rats, in early light phase, promoted food intake in a dose-dependent manner (Sakurai et al., 1998), the expression of prepro-ORX was increased during fasting (Sakurai et al., 1998; Wall & Volkoff, 2013) and, moreover, ORXs neurons increased their firing in condition of negative energy balance (Burdakov et al., 2005; Yamanaka, Beuckmann, et al., 2003). ORX-A has been found to induce an orexinergic effect more durable than ORX-B (ORX-A induce feeding that last for about 4hours while ORX-B for about 2h) probably due to the difference in the secondary structure of the two peptides. Due to the higher orexinergic activity of the ORX-A compared to ORX-B, it was hypothesized that OX1R was implicated in the modulation of feeding more than OX2R. Moreover,

intraperitoneally administration of a selective OX1R antagonist (SB-334867-A) inhibited feeding and increase the onset of behavioural satiety (Ishii et al., 2005; Liu et al., 2020).

ORXs promote feeding behaviour through multiple neural pathways. One of the hypothalamic nuclei involved in the feeding regulation is the ARC, which is composed by two main neuronal populations: orexigenic neurons, which co-express neuropeptide Y (NPY) and agouti-related protein (AgRP), and anorexigenic neurons, which co-express cocaine- and amphetamine-related transcript (CART) and pro-opiomelanocortin (POMC; the precursor of the alpha-melanocyte stimulating hormone, α-MSH). Due to the dense projections of ORXs neurons to the ARC (Peyron et al., 1998), several studies have suggested that ORXs exert their orexinergic activity at least partially through the stimulation of the orexinergic NPY neurons (Yamanaka et al., 2000), which express OX1Rs and are directly activate by ORXs (Arrigoni et al., 2019). While some studies have demonstrated that the feeding promoting effect of ORX-A is completely abolished by central administration of NPY-Y1 or NPY-Y5 receptors antagonists (Dube et al., 2000), other studies showed only a partial blocking effect (Yamanaka et al., 2000), thus suggesting the existence of other pathways by which ORXs exert their action. One of these additional circuits might be the inhibition of the anorexigenic POMC-expressing neurons, which also express OX1Rs. Despite the mechanism by which ORX inhibits POMC neurons is not completely understood, Ma and colleagues demonstrated that ORX decreased the electrical activity of POMC cells, primarily by modulating synaptic inputs, in particular by increasing the GABAergic afferent input and by inhibiting the glutamatergic afferent input (Ma et al., 2007).

The ARC generates also integrated regulation of metabolic balance. The connections between ORX neurons and both subsets of ARC neurons (NPY or POMC neurons) provide an indirect regulation of ORX neurons by leptin and ghrelin, which are peripheral indicators of the metabolic status. Leptin is a satiety hormone secreted by adipose tissue, that increases energy metabolism and reduces energy intake. High leptin levels suppress ORX neurons activity (Zhu et al., 2002) but the interaction between ORX and leptin is not completely understood. Moreover, less is known about the localization of leptin receptors on ORX neurons: while some studies describe a colocalization (Hakansson et al., 1999), others are not able to confirm this finding (Goforth et al., 2014; Sheng et al., 2014). Ghrelin, an orexigenic hormone which is secreted by stomach and that regulates appetite, activates directly ORX neurons (Yamanaka, Beuckmann, et al., 2003).

ORX neurons can also sense changes in extracellular glucose concentration. Electrophysiological studies on brain slices have shown that low glucose levels increase ORX neurons' activity; conversely increasing in extracellular glucose concentration directly inhibits ORX neurons by inducing a membrane hyperpolarization and the cessation of action potentials (Fig.2) (Yamanaka, Beuckmann, et al., 2003; Burdakov et al., 2005). ORX neurons are considered as functional glucosensors because their electrical activity is more inhibited when their metabolic state is low whereas their response to glucose is reduced by high energy levels (ATP, lactate, pyruvate) (Venner et al., 2011).

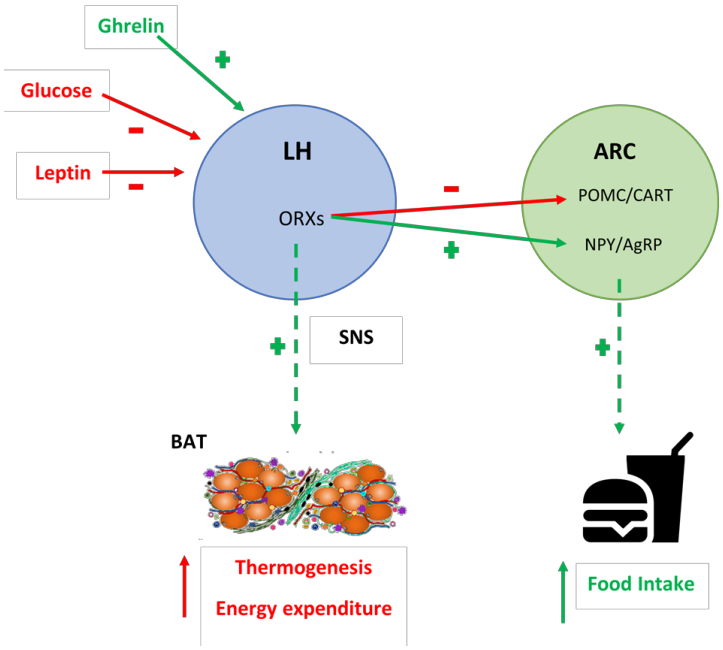

Figure 2. Role of ORX system in the regulation of feeding behaviour and energy balance.

ORX neurons in the LH area promote feeding behaviour, at least in part, through the stimulation of NPY/AgRP neurons and through the inhibition of the POMC/CART neurons, both located in the ARC. Moreover, ORX neurons control energy homeostasis through sensing the peripheral levels of metabolites, such as glucose, leptin and ghrelin and modulate energy expenditure, at least in part, by increasing BAT thermogenesis through the sympathetic nervous system. Green arrows represent excitatory input and red arrows inhibitory input. (Lateral hypothalamic area (LH area), Neuropeptide Y/Agouti Related Protein (NPY/AgRP), pro-opiomelanocortin/ cocaine- and amphetamine- related transcript (POMC/CART), arcuate nucleus (ARC), brown adipose tissue (BAT).

ORXs not only increase food intake but are also implicated in the control of energy balance, by increasing energy expenditure. Daily energy expenditure includes three different components, such as basal metabolic rate (BMR), non-exercise thermogenesis and motor activity. Mice that lack ORX neurons display a decrease in physical activity during dark period (active period for mice) (Hara et al., 2001) and injection of ORX-A in the third ventricle of mice brain increases

their BMR by increasing oxygen consumption (Lubkin & Stricker-Krongrad, 1998). ORXs also stimulate sympathetic outflow, as suggested by the increase in mean arterial blood pressure and heart rate (HR) following the ICV injection of ORX in rats' brain (Shirasaka et al., 1999), and these effects generally result in an increased energy consumption. Moreover, chemogenetic activation of the ORX neurons increases non-exercise thermogenesis during periods of spontaneous physical activity and prevents the inactivity that usually follows a high fat diet meal (Arrigoni et al., 2019).

Increasing in ORX signalling causes a decrease in body weight and prevents late onset obesity in double receptor knock out mice (Funato et al., 2009), while ORX-ataxin-3 mice, which are ORX neurons ablated, show a decreased food intake combined with development of late onset obesity (Hara et al., 2001). The severity of the obese phenotype depends on the genetic background of the mice. In fact, ORX-ataxin-3 mice show a metabolic disruption more severe than prepro-ORX knockout (ORX-KO) mice studied by Chemelli et al. (Chemelli et al., 1999). This difference could depend on the complete absence of the ORX neurons in ORX-ataxin-3 mice. In fact, as mentioned above, ORX neurons express also other neuropeptides or modulatory factors such as dynorphin, which may influence feeding behaviour. In line with this, Ghule et al. demonstrated that the lack of dynorphin causes uncoupling between energy intake and body weight gain (Ghule et al., 2020).

In agreement with the studies on mouse models with dysregulation of the ORX system, human studies have demonstrated that narcoleptic patients have a higher incidence of obesity compared to the average population. Moreover, they show a decreased caloric intake combined with and increased body mass index (BMI), suggesting an impairment in energy balance with reduced energy expenditure and BMR (Schuld et al., 2000).

ORXs have also a key role in the maintenance of consolidated W, an essential state for supporting feeding behaviour. During starvation, there are low levels of glucose and leptin, together with high ghrelin levels. The low energetic availability directly modulates activity of ORX neurons to maintain W, because proper maintenance of arousal during fasting is essential to allow food seeking behaviour and animal's survival. ORX-ataxin-3 mice fail to respond to fasting with increase in W and activity (Yamanaka, Beuckmann, et al., 2003). Furthermore, it has been reported that after 48-h of fasting, prepro-orexin mRNA was up-regulated compared with the fed control in rats (Sakurai et al., 1998). These findings suggest that ORX neurons are crucial to maintain the arousal during the period in which energy stores are low and indicate

that ORX neurons are an important link between energy balance and arousal (Tsujino & Sakurai, 2009).

1.4 Orexins and thermoregulation

The maintenance of the energy homeostasis requires a perfect balance between energy intake and energy expenditure. While energy intake is represented by caloric intake of food and beverage, energy expenditure depends on locomotor activity, on the thermic effect of the food and on thermogenesis. Thermogenesis, defined as *obligatory,* is represented by BMR and is sufficient to preserve body temperature (Tb) when the organism is in its range of thermoneutrality. When the organism is facing temperature below the thermoneutrality, it quickly responds trough an activation of heat saving mechanisms, such as piloerection and vasoconstriction. However, this response is limited and requires additional mechanisms, called *facultative or adaptive* thermogenesis, that includes *shivering* and *non-shivering thermogenesis*. In mammals, most of the non-shivering thermogenesis takes place in the brown adipose tissue (BAT) (Milbank & López, 2019). Several studies on genetic modified mouse models have demonstrated that ORXs promote energy expenditure, through the increasing of motor activity and/or BMR (Hara et al., 2001; Lubkin & Stricker-Krongrad, 1998) but also through the modulation of BAT thermogenesis (Fig. 2). ORXs and OX1R are also important for BAT development, differentiation, and function, as demonstrated by Sellayah and colleagues (Sellayah & Sikder, 2012; Sellayah et al., 2011) in ORX-KO mice. These mice showed an increase in body weight and a lower accumulation of triglyceride in BAT, compared to wild type (WT) control mice. Moreover, both OX1R and OX2R knockout mice showed the same phenotype of ORX-KO mice, due to the orexin-mediated dysfunction of BAT with consequent impairment of thermogenesis and accumulation of energy stores in the body.

Morphological analysis have also shown that ORX neurons are implicated in the modulation of the BAT thermogenesis through the sympathetic nervous system (Milbank & López, 2019). ORX-containing fibers and OXRs have been described in many regions, including the rostral raphe pallidus (rRPa) region of the ventromedial medulla, a key site of sympathetic and somatic premotor neurons involved in the control of thermal effectors (Morrison & Nakamura, 2011). The neurons of rRPa are involved in the regulation of Tb and in controlling BAT thermogenesis. Accordingly, injection of 12pmol of ORX-A into rRPa produces large and continued increasing in BAT sympathetic outflow and in BAT thermogenesis (Tupone et al., 2011). Moreover, the

stimulation of ORX neurons by means of bicuculline microinjection (a GABA-A antagonist) into the LHA, in anesthetized and artificially ventilated rats, induces a significant increase in BAT temperature and in BAT sympathetic nerve activity , in HR and in blood pressure (BP) (Cerri & Morrison, 2005).

Several studies have explored the intricate connection between orexinergic system and thermoregulation. Monda and colleagues were the first to demonstrate that ICV administration of ORX-A induces an increase not only in the firing of the sympathetic nerve to BAT, but also in HR and Tb (Monda et al., 2001). Moreover, Székely end colleagues have shown that ICV injection of ORX-A in rats could induce a short-lasting hypothermia, followed by a longer lasting hyperthermia. On the other hand, ORX-B directly causes hypothermia (Székely et al., 2002). Studies on ORX-KO and ORX-neurons-ablated (ORX-AB) mice have also shown that these mice have a Tb comparable to that of WT littermates (Zhang et al., 2010). However, ORX-KO mice showed elevated Tb during sleep (Mochizuki et al., 2006) and ORX-AB mice had an attenuated drop of Tb when the animals fell asleep (Zhang et al., 2007). Accordingly, narcolepsy patients showed a smaller drop in Tb during sleep rather than control subjects (Mosko et al., 1983).

Recently, Kuwaki and his group have investigated the role of ORX in the stress-induced hyperthermia, subjecting ORX-KO and ORX-AB mice to different kind of stressors. They found that ORX-AB mice, but not ORX-KO mice, showed the expected blunting in handling stress-induced hyperthermia (Zhang et al., 2010). Moreover, they found that the uncoupling protein-1 (UCP-1), a key protein involved in non-shivering thermogenesis, did not increase in the BAT of ORX.AB mice, although BAT functionality was preserved (Zhang et al., 2010). Using other two different kind of stressor, such as environmental cold exposure and brain prostaglandin E2 (PGE2) injections, which mimic inflammatory fever, they also found that only ORX-AB mice exhibited a blunted PGE2-induced fever and intolerance to cold (5°C) exposure (Takahashi et al., 2013). All these results suggest that ORX producing neurons, but not ORX itself, are important in the stress-induced thermogenic response.

ORXs could also have a protective role in aging-associated impaired thermogenesis (Sellayah & Sikder, 2014). However, the mechanisms underlying the increasing in fat mass induced by aging are still poorly understood. Sellayah and Sikder have shown that aging is associated with a compromised differentiation of BAT, morphologic abnormalities, and thermogenic dysfunctions in mice (Sellayah & Sikder, 2014). Aged mice showed an interscapular brown

region progressively invaded by white-like adipocytes and failed to mobilize the energetic reserves from brown adipocyte, thus producing an impairment in the regulation of basal thermogenesis. Interestingly, the administration of ORX-A reversed these effects, increasing core Tb, improving cold tolerance, and reducing adiposity; conversely, ORX-AB mice showed stronger brown-fat dysfunction. These results suggest that ORX signalling has also a role in the aging-associated thermogenesis and lead to speculate that ORX system could be a potential target of interventions to reverse the age-associated fat mass increase.

1.5 Orexins and respiratory control

It has been known for a long time that LHA is involved in both breathing and cognitive arousal. In 1950s, Redgate and Gellhorn studied the involvement of the LHA in the regulation of breathing by using high-frequency currents to produce localised lesions in the LHA of lightly anaesthetised cats. Through the monitoring the rate and depth of respiration, they observed that the lesions resulted in a rapid decrease in the rate and/or depth of respiration, and these effects increased with the size and number of lateral hypothalamic lesions (Redgate & Gellhorn, 1958). Moreover, the injection of barbiturates, that inhibited lateral hypothalamic activity, also reduced respiratory activity. Based on these results, Redgate and Gellhorn suggested that impulses from the LHA elicited an increased respiratory activity. These findings have been also supported by recent immunohistochemical evidences that have revealed that ORX-A immunoreactive nerve fibers project to different areas involved in breathing control, such as Kolliker–Fuse nucleus, dorsal and rostral ventrolateral medulla (RVLM), pre-Bötzinger complex, the nucleus tractus solitarii (NTS), raphe nuclei, hypoglossal nuclei, and phrenic nuclei. All these areas are critical for respiratory rhythmogenesis, respiratory activities regulation, and upper airway and diaphragm movements control (Han, 2012). In line with this, the expression of both OXRs mRNA is also found in many respiratory nuclei in the brainstem with a pattern matching that of ORX-containing axon terminals (Marcus et al., 2001).

The effects of ORX-A on tidal volume (i.e. the amount of air inhaled or exhaled during normal ventilation) (Vt) and ventilatory period (VP) have been studied in mice by Zhang and colleagues through administration of ORX-A in lateral ventricle and cisterna magna. Injections in lateral ventricle induced a dose-dependent increase in respiratory frequency, Vt, BP, and HR. Effects were present few seconds after the administration and lasted 10–40 min, depending on the dose. The minimum dose that evoked a significant response was 0.03 nmol for Vt and

respiratory frequency, or 0.3 nmol for BP and HR, suggesting that respiratory changes were not secondary to the cardiovascular response. Moreover, intracisternal administration of ORX-A also induced similar changes, except for respiratory frequency, that didn't change even at the highest dose (Zhang et al., 2005).

The study of mice with genetic deletion of the gene encoding prepro-ORX (ORX-KO) has allowed to better understand the link between the ORX system, breathing control and chemo-responsiveness. These mice were moderately obese and showed an attenuated fight-or-flight response when exposed to stressors, including diminished cardiovascular, respiratory, and behavioural responses (Kayaba et al., 2003), although basal ventilation was not significantly altered in ORX-KO mice, compared to that in control mice. Similar responses were observed in ORX-ataxin-3 mice exposed to air jet stress (Zhang et al., 2006). These findings suggested that ORX might be a master switch, which elicits multiples changes in behaviour and autonomic outputs, regulating respiration only in a stress condition.

ORX system is extremely important for the appropriate respiratory stimulation during hypercapnia. Using patch-clamp recordings, Williams et al. demonstrated that the ORX neurons were intrinsically sensitive to the extracellular levels of CO_2 and H^+ (Williams et al., 2007), key chemical variables controlled by breathing. Physiological acidosis causes an increase in ORX neurons firing rate while alkalosis produces a decrease in their firing rate. These effects might be mediated, at least in part, by the TASK-like tandem-pore K+ channels (Williams et al., 2007), and by other acid-sensing channels.

In vivo studies have shown that the ORX system participates in the regulation of respiration and the CO_2 central chemoreflex. The amplitude of the hypercapnic (5% CO2–21% O2 and 10% CO2–21% O2) and hypoxic (15% O2) ventilatory responses in both ORX-KO and control mice depends clearly on the behavioural state. Nakamura and colleagues found that, compared to control mice, ORX-KO mice had an attenuated responses to hypercapnia during W but not during sleep periods; this is in line with the notion that ORX neurons fire more during W (Nakamura et al., 2007). No differences were found between the two genotypes in the ventilatory responses to hypoxia, suggesting that ORXs are not involved in the hypoxic response, even during W and that the abnormal hypercapnic responses in ORX-KO mice may be vigilance-state-dependent (Kuwaki, 2008).

To better understand the possible involvement of ORX in acute respiratory chemoreflex during W, Deng et al. performed ICV administration of ORX-A and ORX-B or OX1R antagonist (SB-

334867) in ORX-KO mice and control mice. They found that ORX-B increased spontaneous ventilation more than ORX-A, mainly through OX2R. Moreover, the administration of either ORX-A or ORX-B partially restored the hypercapnic chemoreflex in ORX-KO mice. Conversely, blockage of OXR1 by SB-334867 blunted hypercapnic chemoreflex of the control mice, indicating that OX1R are necessary for chemoreflex control (Deng et al., 2007). This study also confirmed that in mice ORXs are not involved in ventilatory hypoxic response. Selective inhibition of both OXRs by Almorexant, an orally administered dual OXRs antagonist, in unanaesthetised rats, induced a decrease in CO_2 response only in W and only during the dark (active) period of the diurnal cycle. Moreover, Almorexant also decreased W and increased NREM and REM sleep during the dark period, thus suggesting that the ORX system have a critical role in central chemoreception in a vigilance state-dependent manner and the sleep–wake difference in the CO_2 response can be in large part attributed to ORXs (Li & Nattie, 2010).

In narcoleptic patients there is also evidence of an impaired chemo-responsiveness. However, in contrast to results obtained on ORX-KO model, narcoleptic patients showed a significant decrease in hypoxic responsiveness, unrelated to BMI, age or sex, but not in hypercapnic responsiveness, suggesting that, in humans, ORX-A is not the key factor contributing to chemo-responsiveness (Han et al., 2010).

ORXs might also get involved in the mechanisms of stabilization of breathing. Respiratory long-term facilitation (LTF) is a physiologic augmentation of respiratory motor output that occurs also after the end of hypoxic stimuli and is presumed to prevent sleep apneas. Terada et al. showed that LTF is absent in ORX-KO mice (Terada et al., 2008), which is in line with the finding that ORX-KO mice had more frequent sleep apneas (Nakamura et al., 2007). Narcolepsy is also characterized by a higher frequency of sleep apneas compared to healthy controls (Chokroverty, 1986). The high incidence of apneas could induce sleep fragmentation and hypoxia, thus compromising the ventilatory responsiveness of these patient. In humans, the most common type of sleep apnea is OSA (Obstructive Sleep Apnea), characterized by a complete or partial obstruction of the upper airway during sleep. The prevalence of OSAs in narcolepsy patients ranges from 2% to 68% (Sansa et al., 2010), with a marked variability among studies, due to the different definitions of OSAs, or to the use of a small study's group (Hoshino et al., 2019). Increased BMI facilitates airway obstruction and frequently correlates with OSA. Narcoleptic patients have often increased BMI, and this may predispose to co-morbid OSA. OSAs have been divided into two patterns of pathophysiology: non-stage specific

OSAs and REM-related OSAs, with the latter associated with adverse cardiovascular and metabolic events, such as hypertension, increased insulin resistance, impairment of human spatial navigational memory, and non-dipping nocturnal BP (Alzoubaidi & Mokhlesi, 2016). A recent study performed by Hoshino and colleagues has confirmed a high prevalence of REM-related OSA in adult narcoleptic patients with OSA. These results might reflect the pathophysiological characteristics of narcolepsy (Hoshino et al., 2019).

1.6 Orexins and cardiovascular regulation

As discussed above, ORXs are involved in the regulation of many biological functions, such as feeding behaviour and energy metabolism, maintenance of W and they are essential for the physiological response to stressor. Moreover, an integrate and coordinate autonomic response that also involves the cardiovascular system, is essential to stay awake and actively interact with the external environments.

Both ORX neurons and receptors are found in neuronal sites that are importantly involved in cardiovascular autonomic regulation, e.g. NTS, RVLM, medullary raphe and the premotor centres of the PVN (Li & Nattie, 2014). The distribution of OXRs reflects the projection of ORX neurons. The OX1R and OX2R mRNA is differentially distributed through the central autonomic network. OX2R mRNA is expressed in the PVN, which contains two subtype of neurons populations: magnocellular (type 1) and parvocellular (type 2). The pre-autonomic parvocellular neurons send long descending projections to several areas within the central nervous system involved in cardiovascular regulation. Between these, the dorsal vagal complex, in the dorsomedial medulla, which contains vagal preganglionic neurons, the NTS, where baroreceptor and chemoreceptor afferents end, the RVLM, which is a central site for the generation of sympathetic tone for the vasculature, and the intermediolateral column of the spinal cord, which is the site of sympathetic preganglionic motor neurons involved in the regulation of BP and HR (Shirasaka et al., 2003). Shirasaka and colleagues showed that ORXs directly excited type 1 and type 2 neurons of the PVN (Shirasaka et al., 2001). The functional significance of the depolarizing effects of orexins on PVN neurons has not been established, however it has been shown that electrical or chemical stimulation of the PVN increases BP and renal sympathetic nerve activity (RSNA) in conscious rats (Kannan et al., 1989).

The cardiovascular effects of ORXs were first demonstrate in 1999 by Shirasaka and colleagues. They showed that ICV administration of ORX-A (0.3 – 3 nmol) produced a dose-dependent increase in mean arterial pressure (MAP), HR and RSNA in conscious unrestrained rats. Significant correlations were observed between RSNA and HR or MAP, thus suggesting that the increases in HR and MAP were due to an ORX-A dependent increase in sympathetic outflow. These increases were also observed in anesthetized rats, thus indicating that these effects were not due to increases in rat's locomotion or stress. The central administration of ORX-B also produced an increase in MAP and HR but, in contrast to ORX-A, it did not determine increase in RSNA. All the cardiovascular and sympathetic responses induced by ORX-A were greater than those induced by ORX-B (Shirasaka et al., 1999).

Shirasaka and colleagues also showed that central administration of both ORX-A and ORX-B increased plasma norepinephrine (NE), with effects being longer with ORX-A; moreover, a high dose of ORX-A also increased plasma epinephrine (Epi) levels, suggesting an involvement of the sympatho-adrenomedullary system (SA system) in cardiovascular responses. Therefore, the large response induced by ORX-A, compared with that induced by ORX-B, may be due to activation of the SA system in addition to an increased sympathetic outflow (Shirasaka et al., 1999). Similar results were found in conscious rabbit, in which ICV, but not intravenous, administration of ORX-A evoked a dose-dependent increase in MAP and RSNA, as well as in circulating plasma levels of Epi, vasopressin and glucose concentration (Matsumura et al., 2001).

The increase in MAP and HR can also be evoked in anesthetized rats by the injection of ORX-A in the cisterna magna (Chen et al., 2000) or in the subarachnoid space of the thoracic spinal cord (Shahid et al., 2011). This reflects the distribution of ORX terminals in autonomic centres all the way down to the spinal cord and indicates that ORX can produce cardiovascular responses by acting at multiple levels into the neuroaxis. Focal injection of ORXs allowed to identify additional sites involved in cardiovascular regulation, such as the pressor area of RVLM (Chen et al., 2000) and medullary raphe (Ciriello et al., 2003). The cardiovascular effects of ORX-A injections on NTS are still controversial and depend on the dosage. Smith and colleagues showed that injections of low doses (10 pM–10 nM) of ORX-A produced a significant increase in MAP and HR (Smith et al., 2002), whereas high doses (25–250 mM) decreased MAP and HR, and potentiated bradycardia after the activation of baroreflex (De Oliveira et al., 2003). On the contrary, Shih and colleagues demonstrated that bilateral microinjections of ORX-A or ORX-B produced bidirectional and dose-dependent

cardiovascular effects. Indeed, at a low dose (5 pmol) ORXs decreased arterial pressure, HR, and power density of the vasomotor components of BP signals, an experimental index for sympathetic neurogenic vasomotor outflow, whereas at a higher dose (>20 pmol) they evoked cardiovascular excitatory responses. The bidirectional action of ORXs might be due to different concentrations of nitric oxide (NO), an important neuromodulator for the cardiovascular regulation in NTS. Low doses of ORXs stimulate NO synthase to produce low concentration of NO, that potentiates glutamatergic excitatory postsynaptic potentials, decreasing BP. Conversely, high doses of ORXs induce the increased release of NO, which, in turn, increases BP through potentiation of GABAergic inhibitory pathways (Shih & Chuang, 2007).

ORX-A participates in the short-term regulation of BP but not in the long-term regulation. Chronic ICV infusions of ORX-A for 14 days in conscious rats increase the systolic BP, but the values returned to baseline levels at day 14 (Lin et al., 2002).

1.7 Orexins and integrated autonomic control

The perifornical area (PFA) of the hypothalamus, that contains the highest density of ORX-neurons, is known as “defense area”. Defense reaction is defined as an increase in arousal level and sympathetic outflow to deal with the imminent danger. Defense reaction is associate with increase in BP, HR, respiratory frequency, and resistance in most vascular beds, and by a decrease in resistances in skeletal muscle and airway blood vessels (Kayaba et al., 2003). Anatomical and physiological evidence support the role of ORXs in this response: Kuwaki and his group demonstrated an attenuated response in both anaesthetized and conscious ORXs-deficient mice. They reported that the increases in BP, HR, respiratory frequency and ß-band power of electroencephalogram (an index of cortical arousal), induced by the stimulation of PFA with bicuculline, were attenuated in ORX-KO (Kayaba et al., 2003) and, in a similar way, the increases in BP, HR, and respiratory minute volume and vascular dilatation in skeletal muscle were reduced in mice that lack ORX neurons (ORX-AB) (Zhang et al., 2006).
Moreover, ORX-AB mice showed an attenuated suppression of the baroreceptor reflex during the defense response, thus suggesting that ORXs are involved in the inhibition of baroreflex only during this response (Kuwaki, 2015).

The study of the role of ORXs in cardiovascular regulation in narcoleptic patients has led to results that are not in full agreement with those obtained in mice. The autonomic regulation in

human narcolepsy type 1 (NT1) has been little explored. In 1982, Sachs and Kaijser reported a disrupted autonomic control in narcoleptic patients. The subjects involved in their study (n=9) showed an attenuation of some autonomic reflexes, i.e. subnormal changes in BP and HR in handgrip test (in which the increase in HR depends on the inhibition of vagal efferent and the increase in blood flow is mediated by β-adrenergic vasodilatation) and Valsalva maneuver (in which patients maintain a constant expiratory rate by blowing through a mouthpiece that permits a slow air flow). Conversely, diving reflex (in which bradycardia is elicited by an increase in vagal activity) and the orthostatic test (in which the increase in BP depends on sympathetic vasoconstriction) were similar in narcoleptic patients and controls. This pattern, in which only some reflexes are compromised, but not others, suggested that the autonomic impairment had central origin, while the function of peripheral nerves was preserved (Sachs & Kaijser, 1982). However, these results were not confirmed by subsequent study performed by Hublin et al, suggesting that the abnormalities reported in Sachs' study might be due to an insufficient standardization of tests' conditions, rather than a defect in the autonomic control (Hublin et al., 1994). Moreover, Grimaldi et al. also excluded abnormal cardiovascular responses to head-up tilt test, Valsalva maneuver, deep breathing and isometric handgrip tests in narcoleptic patients (Grimaldi et al., 2010).

As discussed earlier, ORX neurons play a key role in the maintenance of W state. The relationship between wake-sleep states and cardiovascular regulation has been studied in both mouse models with ORX deficiency and in NT1 patients. However, the results are still controversial. Some studies suggest that narcolepsy affects the ability to modulate BP during sleep. Grimaldi and colleagues showed a significantly reduced night-time decrease in BP ("non-dipping" pattern) in patients with narcolepsy (Grimaldi et al., 2012). This pattern was accompanied by sleep fragmentation and/or other pathologic sleep phenomena. The "non-dipping profile" has also been identified by Dauvilliers et al. (Dauvilliers et al., 2007). Also, in narcoleptic mice the dip in BP that normally exists between W and NREM sleep, is reduced, as is the rise of the BP when waking up from sleep (Bastianini et al., 2011; Lo Martire et al., 2012). However, the comparison between narcoleptic patients and subjects with insomnia evidenced no significant difference in "non-dipping profile" between groups. Moreover, the change in nocturnal BP did not correlate with the ORX levels in cerebrospinal fluid (CSF) of narcoleptic patients, thus suggesting that it is not the lack of ORX itself to lead to the abnormalities in nocturnal BP but it might be caused by the disruption of sleep architecture (Sieminski & Partinen, 2016).

1.8 Loss of function: Narcolepsy

Narcolepsy is a rare and disabling sleep disorder, described for the first time by Jean Baptiste Gélieneau in 1880. This disease is one of the most common causes of chronic sleepiness and is characterized by dysregulation of sleep-wake behaviour, resulting in the inability to maintain vigilance states, pathological intrusion of REM sleep into W and frequent transition between states of sleep and W (Sakurai, 2007).

The exact prevalence of narcolepsy is not known, but some studies estimate that in Europe narcolepsy affects between 20 and 47 people out of 100000 inhabitants (Ohayon et al., 2002), with no gender difference. The onset of symptoms in narcoleptic patients follows a bimodal distribution, with a first peak appearing between 10-20 years and a second peak between 35-40 years (Dauvilliers et al., 2007). The gap between the onset of the symptoms and the diagnosis is 5-15 years, and narcolepsy can be undiagnosed or misdiagnosed in many patients. Interestingly, gender seemed to impact the timeliness of diagnosis. Despite women report more occurrences of cataplexy and have greater objective sleepiness, they receive a diagnosis more delayed than men. One explanation for this may be that women are less forthcoming with their symptoms, opting to self-medicate, or because they are less affected in their daily lives than men (Won et al., 2014).

The disease is characterized by chronic daytime sleepiness, occurring daily and typically every 2 hours. The intensity varies across the day and between individuals. Sleepiness is exacerbated by periods of inactivity. The sleep episodes are sudden and irresistible, despite the desperate efforts to fight the urge to sleep. They are usually short, although their duration can increase with passive activities or, in case of severe sleepiness, also during activities that need concentration, such as work, study or driving. Sleep episodes are frequently associated with dreaming; and can restore normal wakefulness for up to several hours (Dauvilliers et al., 2007; Scammell, 2015).

Narcolepsy is also characterized by abnormal manifestations of REM sleep, which normally occurs during the usual sleep period, and includes vivid dreams, rapid eye movement and paralysis of all skeletal muscles, except for those involved in respiration. However, in narcoleptic patients REM sleep can intrude in wakefulness at any time of the day. The most dramatic consequence of REM intrusion is cataplexy, that is characterized by a sudden, partial

or complete paralysis of voluntary muscle, triggered by strong positive or negative emotional stimuli, with preserved consciousness. The duration of the cataplectic episodes varies from few seconds to several minutes. Sixty percent of narcoleptic subjects develops cataplexy. All striated muscles, except diaphragm, can be affected, causing the individual to collapse. Partial cataplexy can be limited to facial and neck muscles or involves limb, while severe episodes produce bilateral and generalized loss of muscles control, sufficient to cause a fall. The frequency of cataplectic episodes varies from less than one episode per year to several episodes per day. Patients can occasionally have a "status cataplecticus", which is characterized by continuous cataplectic episodes lasting several hours (Dauvilliers et al., 2007).

Other symptoms associated to dysregulation of REM sleep include sleep paralysis and sleep-related hallucinations. These symptoms are not specific and, thus, less diagnostically informative, because are present in about 50% of narcoleptic patients but also in about 20% of general population (Scammell, 2015). Sleep paralysis is similar to cataplectic attack but can occur at awakening (mainly from REM sleep) or at sleep onset. These episodes can be associated to a sensation of fear, suffocation and/or hallucinations. Disturbing hallucinations can occur at the onset of sleep (hypnagogic hallucinations) or at awakening (hypnopompic hallucinations). Typical hallucinations are visual, tactile, auditory, or even vestibular. The duration of both sleep paralysis and hallucination is rarely more than 1 or 2 minutes (Dauvilliers et al., 2007; Scammell, 2015).

The most recent International Classification of Sleep Disorder (3rd version, ICSD-3) now recognizes two subtypes of narcolepsy. NT1 represents the classical clinical syndrome, characterized by excessive daytime sleepiness, cataplexy and absent or very low levels of ORX-A in CSF. Conversely, narcolepsy type 2 (NT2) is characterized by absence of cataplexy and normal levels of ORX-A in CSF. Cataplexy is specific to NT1 and is the best diagnostic marker of the disease (Dauvilliers et al., 2007; Scammell, 2015). Thus, the diagnosis of NT1 is straightforward, while NT2 is difficult to diagnose (Scammell, 2015; Reading, 2019).

NT1 often includes other symptoms directly related to reduction in hypocretin signalling, such as the dysregulation of the feeding behaviour. Narcoleptic patients tend to gain excessive weight and have also higher BMI than normal subjects (in adult patients BMI is 15% above average), possibly due to the low metabolic rate. Moreover, narcolepsy shows an increased prevalence of non-insulin-dependent diabetes, sleep apnea syndrome, sleepwalking and REM sleep behaviour disorders. In addition, depression has been reported in 18-37% of cases but is

difficult to understand if it is related to a neuropathologic state or to the effect of narcolepsy on patients' life (Dauvilliers et al., 2007; Scammell, 2015).

Studies performed in genetically modified animal models demonstrated that ORX system plays a key role in NT1. After a linkage analysis of dogs with autosomal recessive narcolepsy, Lin and colleagues found a null mutation in the OX2R gene (Lin et al., 1999). Meanwhile, Yanagisawa's group found that mice lacking the prepro-ORX gene (ORX-KO) showed a phenotype resembling human NT1 (Chemelli et al., 1999). These findings were confirmed also in narcoleptic subjects with cataplexy, in which approximately 90% of them had no detectable ORX-A in their CSF (Nishino et al., 2000; Mignot et al., 2002). Post-mortem studies confirmed that the markedly decrease in CSF ORX-A levels resulted from a loss of ORX-producing neuron. Peyron et al, found no detectable prepro-ORX mRNA in the hypothalamus of the narcoleptic/cataplectic subjects (Peyron et al., 2000), and a 90% reduction in the number of ORX immunoreactive neurons was found by Thannickal and colleagues. Interesting, this reduction was highly selective and was greater in the brain of narcoleptic subject with cataplexy than in patients without cataplexy (Thannickal et al., 2000).

Despite of the results in animal studies, the process that causes the selective loss of ORX neurons in NT1 is still unknown. However, an auto-immunological mechanism has been proposed, based on the tight association between narcolepsy and human leukocyte antigen (HLA). HLA genes encode proteins that can present antigens to T cells, and this interaction triggers the immune response against those cells that contain the specific antigen. Many autoimmune diseases are associated with HLA genes (Liblau, 2018). More than 98% of subjects with NT1, and about 50% of people with NT2, carry HLA-DQB1*06:02 (Scammell, 2015). This HLA haplotype confers an increased risk of narcolepsy of 200-fold; the homozygotes for this allele have doubled risk compared to heterozygotes. Variations in other class II or class I alleles also contribute to genetic susceptibility (Reading, 2019).

Narcolepsy is usually sporadic, and the onset of the symptoms follows a seasonal peak, in late spring. This observation suggests that the disease may be triggered by other infections, such as Streptococci or respiratory winter viruses. In the winter of 2009-2010, the administration of Pandemrix, a vaccine against swine's flu H1N1, caused an increase of new cases of narcolepsy by a factor of 5-14 in children and teenagers and by a factor of 2-7 in adults. Observational studies showed that the risk of narcolepsy was elevated for 2 years after the Pandemrix vaccination. All the subjects were positive for HLA-DQB1*06:02 and developed the symptoms

few months after the vaccination. However, an increased risk of narcolepsy was reported also in China, where natural H1N1 infection was common but no vaccination was administered (Sarkanen et al., 2018). These findings support the hypothesis of an autoimmune process underlying narcolepsy. The mechanism of cell death in NT1 is most likely T-cell mediated with activation of helper T cells (CD4+), that secret cytokines, and killer T cells (CD8+) that lyse target cells through the secretion of cytotoxic granules (Liblau, 2018). Recent study by Latorre and colleagues has identified the presence of a specific type of autoreactive immune cell, called CD4+ memory T cell, in the blood samples of 19 narcoleptic patients. These cells target and recognize self-antigens expressed by ORX producing neurons, and this recognition led to T-cell proliferation and activation, and to production of cytokines (Latorre et al., 2018). CD4+ memory T cells were present also in 3 out of 13 control subjects, but their level was low, and the proportion of reactive T cells was ten times less than in narcoleptic group. Furthermore, reactive T cells were found also in NT2 patients, which are not ORX-deficient. Although these findings represent an important point to understand the pathophysiology of narcolepsy, the precise mechanisms by which T-cell subtypes lead to death of ORX neurons remains only speculative (Latorre et al., 2018; Liblau, 2018).

The diagnosis of narcolepsy is based on the clinical history of the patient, which gives information about sleep quality, presence of cataplexy or sleep paralysis and the level of daytime sleepiness. After the anamnesis, is essential to confirm the diagnosis with night-time polysomnography, followed by multiple sleep latency test (MSLT). Polysomnography helps the clinician to exclude other potential causes of daytime sleepiness and to check if the patient sleep at least 6 hours before MSLT. Narcoleptic patients show fragmented and light sleep, a shortened REM sleep latency (< 15 minutes) and an augmentation in slow-wave sleep at the end of the night (Dauvilliers et al., 2007b). During MSLT, the subject is encouraged every 2 hours to fall asleep for 20 minutes, starting at least 1,5 h after awakening. People with narcolepsy usually fall asleep in less than 8 minutes and have REM sleep in at least two of MSLT. A sleep-onset REM period (SOREMP) is defined as the occurrence of REM sleep within 15 minutes of sleep onset. A positive MSLT is defined by a short sleep-onset latency plus at least two SOREMPs. The presence of the HLA-DQB1*0602 genotype in patients can only support the diagnosis. Since narcolepsy is characterized by a selective loss of ORX neurons, the diagnosis should be confirmed by measurement of ORX-A levels in the CSF, which must be lower than 110 pg/ml or one third of mean values obtained in normal subjects (Dauvilliers et al., 2007; Scammell, 2015).

1.9 Mouse models of orexin deficiency

In the last decades, genetically engineered mice have been used as models to study the effects of ORX system disfunction and to explore the mechanism at the basis of narcolepsy.

In 1999, Chemelli and colleagues developed a prepro-ORX knockout mouse (**ORX-KO**) model by using the homologous recombination strategy to introduce a null mutation in the mouse prepro-ORX gene, the precursor gene that encodes for both ORX-A and ORX-B. To target that gene, the researchers constructed a targeting vector to replace exon-1 with nuclear *lac-Z* and *neo* cassettes by homologous recombination in embryonic stem cells (Chemelli et al., 1999). This mouse model congenitally lacks ORX peptides, whereas ORX neurons and the other neurotransmitters co-released with ORX, are preserved. ORX-KO mice reproduce many narcoleptic characteristics. Compared to control mice, ORX-KO are hypersomnolent during active dark period and show a fragmented W, with direct transitions into REM sleep. Moreover, during dark phase, they have transient episodes of behavioural arrest, that resemble cataplectic attack. A consensus report has defined mouse cataplexy as an abrupt episode of nuchal atonia lasting at least 10 s, preceded by at least 40s of W, with mouse immobile and θ activity dominating the electroencephalogram (Scammell et al., 2009). Mouse cataplexy can be enhanced by social interaction and motor activity, such as grooming, burrowing or climbing (Chemelli et al., 1999). Finally, ORX-KO mice show a short phasic high-amplitude bursts of pointed theta waves (7 Hz) during either cataplexy-like episode or REM sleep (Bastianini et al., 2012).

The association between ORX system and narcolepsy came from studies on canine model with mutations in OX2R (Lin et al., 1999). Willie and colleagues developed an OX2R knockout (**OX2R-KO**) mouse model by using a homologous recombination strategy to introduce a null mutation in the OX2R gene. Like narcoleptic Dobermans, OX2R knockout mice were only mildly symptomatic. They showed disrupted wakefulness and abnormal attacks of NREM sleep. However, in contrast to ORX-KO mice, OX2R-KO mice were only mildly affected (Willie et al., 2003).

In 2001, Hara and colleagues developed a genetically engineered mouse model in which ORX-containing neurons were specifically ablated (**ORX-AB**) (Hara et al., 2001). This mouse model was developed by introducing a truncated Machado-Joseph disease gene product (ataxin-3)

with an expanded polyglutamine stretch expressed under the control of the ORX promoter. The ORX neurons of the ORX-AB mice degenerate postnatally, with a drastic reduction occurring within 2 weeks after birth. At 12 weeks of age, more than 99% of ORX neurons were lost and at 15 weeks of age, nearly no ORX neurons could be found in the hypothalamic regions (Hara et al., 2001). This model recapitulates the development of human pathology, characterized by the loss of orexinergic neurons at postnatal age. As ORX-KO mice, ORX-AB mice also exhibit a phenotype like human narcolepsy. They show narcoleptic behavioural arrest and a disruption of the wake-sleep cycle like those observed in ORX-KO mice. Moreover, ORX-AB mice show a late-onset obesity despite hypophagia that may reflect a reduction in energy expenditure. This metabolic abnormality was greater than that observed in ORX-KO mice. ORX neurons contain not only orexin, but also other neuropeptides or modulatory factors, which may be involved in metabolism regulation. The loss of these molecules in ORX-AB mice may explain the metabolic differences observed between the mouse models (Hara et al., 2001).

In the last decade, Tabuchi and colleagues created a genetically modified mouse model with a conditional ablation of ORX neurons, which had closer fidelity to narcolepsy phenotype. This mouse model allows the study of the relationship between the number of ORX neurons and narcolepsy symptoms and, so, the progression of the disease. To produce the specific degeneration of ORX neurons in adulthood, the conditional mouse model (ORX-tTA; TetO DTA mice) has been developed by using Tet-off (Tet-O) system, in which the expression of diphtheria Toxin A (DTA) in ORX neurons was controlled by doxycycline (DOX). ORX-tTA (Orexin-tetracycline-controlled Transcriptional Activator) mice (Tabuchi et al., 2013), in which tTA is expressed in ORX neurons and is driven by human prepro-ORX promoter, are bred with TetO DTA mice to create a double transgenic mice **ORX-tTA; TetO DTA**. The administration of DOX to these mice blocks the tTA from binding to the TetO, and disables the expression of DTA (Black et al., 2018). These double transgenic mice showed an increase in body weight and fragmentation of wake-sleep states, the latter of which depended on the number of ORX-neuron ablated. Also, the frequency of cataplectic attack in this model was exacerbated by the increased loss of ORX-neurons, thus suggesting that the symptomatology of narcolepsy is related to the number of remaining ORX neurons (Tabuchi et al., 2014). The conditional control of ORX neurons degeneration has been proposed as model of both NT1 or NT2, depending on the extent of the ablation (Black et al., 2018).

2 SLEEP-DEPENDENT REGULATION OF CARDIORESPIRATORY SYSTEM

2.1 Arterial pressure regulation

The maintenance of the arterial pressure (AP) within a physiological range is one of the most important goals for the cardiovascular system, because it primarily determines the blood flow to all the body's tissues. Therefore, its value is finely regulated by complex control mechanisms that interact at different levels. This regulation acts on three different levels: a local control (self-regulation), a systemic mechanism (baroreflex) and a central autonomic control.

Local control allows each organ to change its own vascular resistance and self-regulate its blood flow, independently from change on AP. Local control is exerted by myogenic and metabolic mechanisms.

The smooth muscles of small arterial vessels contract in response to an increase in the transmural pressure. The rise in the transmural pressure increases the degree of muscles 'contraction by opening more membrane calcium channels. Thus, this myogenic response increases resistances and, in turn, increases arterial AP (Koeppen et al., 2010).

Moreover, the blood flow directed to a specific tissue depends on the metabolic activity of that tissue. Thus, in case of inadequate oxygen supply, the tissue produces vasodilator metabolites (mainly lactic acid, carbon dioxide, hydrogen ions and nitric oxide) that favours an increase in blood flow. However, an excessive increase in blood flow removes faster vasodilator catabolites, determining a vasoconstriction (Koeppen et al., 2010).

The **baroreflex** (or **baroreceptor reflex**) is a negative feedback system involved in the short-term regulation of AP. It is activated quickly by any changes in AP (Dampney, 2017). The baroreflex acts to reduce the fluctuations of AP and consists of three different components: a system of stretch-sensitive receptors, a centre that receives and integrates all the afferent information and an effector's system. The specialized stretch-sensitive receptors, known as baroreceptors, are mainly located in the wall of the aortic arch and carotid sinuses, and reveal change in AP value by means of the stretching of the vessel's wall. The central pathways that regulate the baroreflex activity are located within the medulla oblongata (Guyenet, 2006). The glutamatergic afferents that originate from baroreceptors in the aortic arch and carotid sinus,

terminate in the NTS and synapse with second-order glutamatergic excitatory neurons that, in turn, synapse with GABAergic inhibitory neurons within the caudal ventrolateral medulla (CVLM). There, the baroreceptor inputs activate the CVLM GABAergic neurons, that project to sympathetic premotor neurons within RVLM. Finally, the RVLM neurons project directly to sympathetic preganglionic neurons in the intermediolateral cell column (IML) in the spinal cord, using glutamate as their primary neurotransmitter (Guyenet, 2006; Dampney, 2017). In RVLM are localized different subtypes of sympathetic premotor neurons and each one of these regulates the sympathetic outflow to different vascular beds. Not all vascular beds are equally affected by baroreceptor inputs, e.g. renal or skeletal muscle vessels are strongly affected by baroreflex, while the sympathetic outflow to vascular skin is poorly affected (Wallin & Charkoudian, 2007). When changes of AP occur, NTS produces compensatory responses by modulating sympathetic and parasympathetic nervous system activity on the heart and sympathetic activity on resistances. For example, a rise in BP produces an increase in the baroreceptors stretching and, in turn, an increase in their activity. Thus, NTS inhibits sympathetic activity and promotes parasympathetic activity, with consequent reduction of HR, of vascular resistances and venous return. Moreover, there is a decrease in the stroke volume, given by the reduction of the sympathetic activity on the ventricles, thus resulting in a decrease of AP (Koeppen et al., 2010).

As described above, baroreflex is activated instantly by change of AP. However, if the stimuli causing AP changes operate for many days, producing the same increase, the baroreceptors adapt to this new condition. Thus, in subjects with hypertension, baroreflex continues to oppose the change in AP, but at higher level. This is called “reset of baroreflex” (Vander et al., 1986).

In districts such as heart and brain, that have an extremely limited tolerance to insufficient blood supply, self-regulation prevails, counteracting higher regulatory systems to maintain the blood flow adequate to their energy needs.

Central autonomic control represents the highest level of cardiovascular regulation. It is an anticipatory mechanism and is performed by some structures of the central nervous system, such as the cerebral cortex and the diencephalon (thalamus and hypothalamus).

This feed-forward mechanism is important to prepare the body to a specific and physiological, situation, such as exercise or sexual activity, by modifying the cardiovascular variables before need.

2.2 Autonomic nervous system and cardiovascular control

Both the sympathetic and parasympathetic branches of the autonomic nervous system (ANS) are strongly involved in the cardiovascular regulation and provide a rapid and sensitive support of the blood flow. Although both ANS divisions are involved in hemodynamic control, the distribution of sympathetic and parasympathetic afferents in the cardiovascular system is not uniform. Indeed, while the sympathetic innervation is spread to all the cardiovascular areas, including myocardium and vessels' endothelium, the parasympathetic branch, by vagi nerves, send inputs only to the heart (Mason, 1968).

HR is intrinsically generated in the heart, through action potentials generated by the pacemaker cells. In a complete absence of hormonal or nervous influences, HR is about 100 beats per minute. However, the sinoatrial node is normally influenced by both ANS' branches. Stimulation of the sympathetic nervous system causes an increase in the pacemaker activity and, in turn, in HR, whereas the parasympathetic activity causes an opposite effect. In resting condition, the parasympathetic influence is stronger than sympathetic. For this reason, the normal HR is approximately 70 beats per minute, so well below 100 beats per minute (Vander et al., 1986).

Norepinephrine released by sympathetic fibres activates **β1-receptors**, expressed in cardiac muscle cells and on autorhythmic cells of SA and atrioventricular (AV) nodes. The activation of these receptors produces an inotropic and chronotropic effect. *Atenolol* is a selective β1-adrenergic receptor antagonist. It is a hydrophilic molecule with limited blood-brain barrier transport. It blocks sympathetic nervous activity to the heart.

Acetylcholine, released by parasympathetic fibres, activates **muscarinic receptors,** that are G protein-coupled receptors. In the heart, the most important muscarinic receptors' subtype is represented by M2, mostly located in the atria. The activation of M2 produces a decrease in HR and inhibits the impulse conduction through the AV node. These receptors are also distributed in the endothelium of the coronary vasculature and their activation leads to vasodilation (Saternos et al., 2018). *Atropine methyl nitrate* is a muscarinic receptors antagonist and blocks parasympathetic nervous activity to the heart, thus producing an increase in HR.

Most vessels receive only a sympathetic innervation, thus the sympathetic division of the ANS is mainly involved in the regulation of vasoconstriction and blood flow. Norepinephrine,

released by sympathetic fibres on blood vessels acts primarily on **α1 receptors** and causes vasoconstriction (Campbell & Jialal, 2020). *Prazosin hydrochloride* is a selective α1-receptor antagonist that blocks sympathetic vasoconstrictor activity in arterioles and veins. This results in a decrease of peripheral vascular resistance and in a reduction of venous return to the heart. The administration of prazosin usually does not increase HR. Prazosin may also act in the central nervous system to suppress sympathetic outflow.

2.3 The wake-sleep cycle: an overview

Sleep is a heterogeneous behaviour, defined as a rapidly reversible state of inactivity with reduced responsiveness to external stimuli, that follow a circadian rhythm. Despite the great amount of time spent sleeping by all the animals, the mechanisms and the purposes underlying sleep are still incompletely understood.

Within sleep, two separate states can be recognized, non-rapid eye movement (NREM) sleep and rapid eye movement (REM) sleep, each one with specific electroencephalographic (EEG), electromyographic (EMG) and electrooculographic (EOG) characteristics.

NREM sleep is characterized by a high-voltage slow waves, and a synchronous EEG activity, with typical waveforms, i.e. K complexes and sleep spindles, associated with a low muscle EMG tone and minimal physiological activity. According to the updated American Academy of Sleep Medicine classification, in human NREM sleep can be divided in three stages (stages I, II, III), that correspond to an increase of sleep depth, based on the EEG characteristics (Schulz, 2008).

REM sleep, or paradoxical sleep, is associated to bursts of rapid eye movements, low amplitude and mixed frequency in EEG, and suppression of the muscle tone. The absence of EMG activity may be interrupted by phasic phenomena of muscle activity, defined as twitches. In REM sleep, dreaming is common. The abrupted transition from REM sleep to W is typical of narcolepsy.

EEG, EMG and EOG characteristics allow also to distinguish sleep states from W, that is characterized by a low-voltage mixed-frequency EEG and by a great muscle activity and eye movements.

In mouse, which is the mammalian model of choice for the study of complex behaviour, the EOG is not considered for the discrimination of each behavioural states. As in human, the wake-

sleep cycle in mice is characterized by three different states, which cyclically alternate. In mice, W is characterized by desynchronized EEG and high EMG tone; NREM sleep is characterized by synchronized EEG activity, with predominant δ waves (1-4 Hz) components, with occasional sleep spindles and K complexes and low muscle tone; REM sleep is characterized, even in mice, by muscle atonia and high frequency EEG activity, with predominant θ waves (4-12 Hz).

All the wake-sleep states are associated with profound changes in the regulation of many physiological behaviours, including cardiovascular and respiratory functions. Changes in BP, heart period (HP, the reciprocal of HR) and respiratory variables occur during NREM and REM sleep and during transitions between states, reflecting the complex interaction between several neuronal groups located in the hypothalamus and brainstem. These neurons receive inputs from monoaminergic, cholinergic and ORX neurons that, in turn, modulate sympathetic and cardiovagal output, respiratory pattern, and chemosensitivity through the continuous interactions between cortical state and subcortical circuits. Studies in rodents using combined techniques have provided new information on the brainstem mechanisms controlling wake-sleep cycle, arousal, cardiovascular and respiratory control. These findings have also a clinical importance in the comprehension of the pathophysiology of sleep-related cardiovascular and respiratory disorders, including narcolepsy (Benarroch, 2019).

The following paragraphs will briefly review the physiological changes of the cardiovascular and respiratory variables across wake-sleep states.

2.4 Cardiorespiratory changes during NREM sleep

NREM sleep is a state associated to a relative autonomic stability, with a minimal motor activity and energy expenditure. During NREM sleep, cardiovascular and respiratory variables are maintained to lower levels, compared to those on W. In the transition between W to NREM sleep, the contribution of the parasympathetic branch of the ANS becomes predominant, compared to that of sympathetic branch, accordingly to the low metabolic and somatic activity of this state (Amici et al., 2014).

The cardiovascular changes during NREM sleep in human and experimental animals has been extensively reviewed in *Silvani & Dampney, 2013* and in *Silvani, 2008.*

During the transition between W and NREM sleep, which is the typical entrance into sleep, in human and rodents the BP decrease by approximately 10%, while HP increase. The decrease in BP value is not found in other species, such as cats, rabbits or pigs (Silvani, 2008). Microarousal during NREM sleep are followed by a transient stereotyped sequence of cardiovascular changes: first there is a decrease in HP, followed by an increase in BP; then HP returns at or above baseline level and, finally, BP returns to baseline (Silvani & Dampney, 2013).

High values of BP during NREM sleep and/or a blunted decrease (<10%) of that is defined as "non-dipping pattern", which is considered a predictive marker of cardiovascular risk. However, despite the clinical significance of the haemodynamic changes, the autonomic mechanisms underlying the cardiovascular regulation during sleep are still poorly understood (Silvani & Dampney, 2013).

Different hypotheses have been raised to explain the changes in BP and HP during NREM sleep. First, it has been hypothesized that the cardiovascular variations were related to changes in posture or to the decrease in somatic motor activity. However, in human, the BP decreases gradually during the different NREM sleep stages, when increase the sleep depth and the subjects remain in the same position, thus suggesting that the change in posture was not enough to explain the cardiovascular modifications (Carrington et al., 2005).

Another explanation for the sleep-related cardiovascular changes could be modifications in the activity of the ANS. Studies in human (Somers et al., 1993) and rats (Miki et al., 2003) found a decrease in the sympathetic activity directed to skeletal muscle and to renal vessels, respectively. Moreover, our recent study in mice has suggested that the decrease in BP was due to a reduction in sympathetic vasoconstriction activity. Indeed, we found that only prazosin, which is an α1-blocker and mediates the sympathetic vasoconstriction, blunted the decrease in BP in the W-NREM transition, while no effects on BP occurred by blunting the increase in HP with atenolol (β1-blocker) or atropine methyl nitrate (muscarinic blocker) administration (Lo Martire et al., 2018).

An early study on cats attributed the increase in HP to the increase in parasympathetic activity to the heart (Baust & Bohnert, 1969). However, our findings suggested that the increase in HP depended on balanced parasympathetic activation and sympathetic withdrawal. Indeed, both administration of atropine methyl nitrate and atenolol, that exert their action on parasympathetic

and on sympathetic control of the heart, respectively, had significant effects on the increase in HP during the transition between W and NREM sleep (Lo Martire et al., 2018).

The sleep-related changes in BP depend on two neural mechanisms, such as baroreflex and the central autonomic commands, which elicit their effects by acting on both sympathetic and parasympathetic branches of the ANS. The baroreflex operates a negative feedback control to keep constant the BP value in spite of perturbations, while central autonomic commands operate to prepare the body to face dangerous situations by means of anticipatory feed-forward control (for further details please refer to the paragraph "*Arterial pressure regulation*"). These two systems interact continuously, but their actions and their relationship change, based on body needs and behavioural states (Amici et al., 2014).

The hemodynamic changes occurring during NREM sleep could be explained by a change in sensitivity or by a resetting of the baroreflex, compared to W. However, the latter phenomenon is more supported by experimental studies on animal models and humans (Silvani, 2008). During NREM sleep, the increase in HP and the decrease in the vascular resistance that entail the decrease in BP, do not follow the logic of the baroreflex in W. In this sleep state, the baroreflex resets to lower values BP, HP and sympathetic nerve activity, and this contributed to the great stability of the cardiovascular variables observed during this state (Silvani, 2008). The resetting has been reported in human (Bristow et al., 1969) and in rats (Nagura et al., 2004). In rats, there was a strong positive correlation between the mean values of renal sympathetic activity and HR with BP values (Miki et al., 2003), suggesting that the NREM sleep-related cardiovascular changes may result primarily from central autonomic commands (Silvani, 2008), and be permitted by resetting of the arterial baroreflex (Silvani, 2008). Increases in the gain of sensitivity of baroreflex have been reported during NREM sleep in human (Smyth et al., 1969) although the underlying mechanisms remain unclear and the results in other species are contrasting. Our recent study on mice suggests that increase cardiac baroreflex sensitivity is due mainly to increased fluctuations in parasympathetic activity (Lo Martire et al., 2018).

The central mechanisms responsible for the baroreflex resetting are not fully understood yet. It has been hypothesized that the NTS, in which the primary afferent fibres from arterial baroreceptors end, could exert an important role in this mechanism. Study on rats has confirmed that the responsiveness of the NTS neurons to a baroreceptor input increases during low-frequency high- amplitude EEG waves, which are characteristic of NREM sleep, while decrease with low-amplitude high-frequency EEG waves, typical of arousal (Tang & Dworkin, 2010).

The NTS receives several inputs from different brain areas, such as cortex, amygdala, hypothalamus, midbrain, medulla and PBN (Dampney, 1994). The available evidences suggest that the PBN could be an important baroreflex modulator during NREMS, because of its strong projections to the NTS and because it contains neuronal populations that fire accordingly to sleep states (Silvani & Dampney, 2013). Moreover, PBN receives projections from VLPO, an important area for the induction and maintenance of NREM sleep (Sherin et al., 1998; Lu et al., 2000). The inhibitory GABAergic neurons of the core of VLPO, which fire during NREM sleep, project also to the PVN, which contains neuronal populations that regulate the sympathetic outflow, thus inducing a decrease in SNA (Uschakov et al., 2006).

During sleep states also respiratory variables, such as minute ventilation (V_E) and tidal volume (Vt), undergo modifications. This could be the result of the loss and/or downregulation of the voluntary control of the ventilatory muscles and of the change in both the resistance of the upper airways and chemosensitivity. During the transition between W and NREM sleep, breathing is characterized by a large instability, with fluctuations of V_E and Vt (Amici et al., 2014). This is the result of a mismatch in timing combined to downregulation in important breathing control mechanisms. Indeed, in the early stages (stages 1 and 2) of NREM sleep, brief breathing interruptions are common also in healthy subjects (Douglas, 2010). Conversely, breathing becomes regular in deep NREM sleep (stages 3 and 4), airway resistance increases, ventilation decreases, and Vt slightly increases, with an overall reduction of ventilation. It has also been observed an increase and a decrease in alveolar and arterial CO_2 and O_2 partial pressure, according to the reduction of the metabolic rate in NREM sleep.

Moreover, the response to a mechanical respiratory load are the same of W, thus indicating that in NREM sleep the proprioceptive reflexes of the intercostal muscles pulmonary inflation and deflation reflexes are normal (Amici et al., 2013).

During the sleep states, many of the inputs that are capable to regulate breathing during W (e.g. receptors in the limb muscles and joints, receptors for ouch or temperature, inputs from limbic system) are absent and/or downregulated. Therefore, in NREM sleep the respiratory control is dominated by chemical inputs. Thus, subject that lacking chemoreceptor control show normal breathing during W, but seriously hypoventilate during NREM sleep (Amici et al., 2013). During sleep there is a reduced chemosensitivity (Douglas, White, Weil, Pickett, Martin, et al., 1982). The hypoxic ventilatory responses are reduced during stage 2 and 3 of NREM sleep compared with W; therefore, breathing stimulation during sleep require a major decrease in O_2,

compared to W. However, the reduction of hypoxic response seems to be sex-dependent, as studies on men and women show different results (Douglas, White, Weil, Pickett, Martin, et al., 1982). The levels of CO_2 are the main regulators of breathing during sleep. However, ventilatory responses to hypercapnia are also reduced during sleep compared with W (Douglas, White, Weil, Pickett, & Zwillich, 1982), but less than the responses to hypoxia. Therefore, people can tolerate higher CO_2 levels and lower levels of minute ventilation during sleep compared to W. Depending on the metabolic conditions, in NREM sleep V_E is reduced by 1 to 2 L/minute, and the partial pressure of CO_2 in the blood increases by 3 to 8 mm Hg, compared with W (Skatrud et al., 1988).

2.5 Cardiorespiratory changes during REM sleep

REM sleep is a state characterized by profound instability. During REM sleep, posture control is lost, thermoregulation is impaired or suppressed, the activity of ANS is instable, breathing becomes irregular and sudden fluctuations in cardiovascular variables occur. Thus, functional variability is the key feature of the cardiovascular control in this sleep state (Amici et al., 2014).

During REM sleep, the mean value of BP increases compared to NREM sleep in humans (Somers et al., 1993), rats (Miki et al., 2003) and rabbits (Cianci et al., 1991). This increase has not been confirmed in lambs (Fewell, 1993), that show no significant changes in mean BP value, and in dogs (Schneider et al., 1997) and pigs (Zinkovska et al., 1996), in which the BP value decrease during the transition between NREM and REM sleep states. Moreover, different inbred mouse strains show a reduction or no significant changes in BP during the NREM-REM sleep transition (Campen et al., 2002), whereas in cats changes in BP depend on the duration of the recovery period (Sei et al., 1989). These discrepancies in both among and within species are consistent with the heterogeneity not only of NREM sleep but also of the REM sleep itself (Miki et al., 2003; Silvani, 2008).

The changes in mean BP are not always accompanied with coherent changes in the others cardiovascular variables, such as HP and vascular conductance. Increase in BP was associated with increase in HR in some (Somers et al., 1993), but not all (Iellamo et al., 2004), human studies, and discrepancies are found also in other species, such as cats (Sei et al., 1994), rats and different inbred mouse strains (Campen et al., 2002), in which was described a decrease, increase or no change in HR.

Moreover, discordant results were found in the relationship between the changes in BP and cardiac output (CO) during the transition between NREM and REM sleep. Indeed, studies on human have found a non-significant increase in CO, while a decrease was shown in both lambs (Fewell, 1993) and cats (Mancia et al., 1971).

Due to the lack of a coherent and consistent changes in BP, HR and CO, the modifications in the vascular conductance appear to be involved in the haemodynamic changes across sleep states (Silvani, 2008). Vascular conductance appears to decrease or increase depending on species and on the tissue. In cats, it has been reported an increase in the conductance of splanchnic and renal vessels and a decreased conductance in skeletal muscles perfused by the iliac artery (Mancia et al., 1971). Moreover, studies on rats showed an increased vascular conductance in the mesenteric and renal vessels and a decreased conductance in the iliac artery. Taken together, these results suggest that in REM sleep there is a rearrangement of the sympathetic nerve activity directed to de different vascular districts (Silvani, 2008).

The main autonomic features of REM sleep are fluctuations of sympathetic and parasympathetic activity, which cause cardiovascular instability. These events are loosely associated with bursts of rapid eye movements, myoclonic twitches, breathing irregularities and ponto-geniculo-occipital waves (Amici et al., 2014). Several findings indicate that the haemodynamic pattern of REM sleep is not related to changes in baroreflex properties. First, the changes in baroreflex gain during the transition between NREM and REM sleep states transition, do not occur in both humans and in animal models (Silvani, 2008). Moreover, also sinoaortic denervation (SAD) experiments provide contrasting results. Indeed, in cats (Baccelli et al., 1978), the vasoconstriction of the iliac artery found during REM sleep becomes a vasodilation after SAD, while in rats, the SAD causes a reduction or an increase in BP according to a shorter or longer post-operative recovery, respectively (Silveira et al., 2008; Sei et al., 1999). Finally, in rats, the reductions of renal SNA and of HR, which occur during the transition between NREM and REM sleep, appear before the increase in BP, so it does not represent a baroreflex response (Miki et al., 2003). In sum, these results suggest that the cardiovascular changes during REM sleep are modulated by the baroreflex but are not mainly caused by changes in its properties (Silvani, 2008).

Some evidence suggested that the cardiovascular parameters during REMS are regulated by central commands. Cats subjected to decerebration showed a REMS-like condition, that is characterized by a decrease in BP and HR due to a decreased SNA directed to the heart and to

cutaneous, splanchnic and renal vessels (Futuro-Neto & Coote, 1982). Moreover, these events are accompanied by an increase in the SNA directed to skeletal muscle vessels, regardless of vagotomy or SAD (Silvani, 2008). Accordingly, the phasic increases that occur in BP during REM are accompanied by tachycardia, as expected by central autonomic control (Amici et al., 2014). All these results suggest that during REM sleep the central autonomic command exert its control con cardiovascular variables by modifying the SNA directed to the different cardiovascular effectors (Silvani, 2008).

Our recent study on mice demonstrated that the increase in BP during the transition between NREM and REM sleep depended on an increase in both sympathetic vasoconstriction and sympathetic activity on heart. Indeed, the increase in BP is blunted with the administration of both prazosin (α1-blocker), that acts on vascular resistances, and atenolol (β1-blocker), that acts on the heart. Moreover, we also found that the decrease of HP during this transition is blunted by administration of atropine methyl nitrate (muscarinic blocker) and virtually abolished by atenolol, which would indicate a role of both parasympathetic withdrawal and sympathetic activation or an exclusive role of sympathetic activation, respectively. However, further analysis will have to be done to explain this mismatch (Lo Martire et al., 2018).

The cardiovascular changes that occur during REM sleep onset, may be due to the activity of REM sleep-on and/or REM sleep-off neurons. The neurons in the sublaterodorsal nucleus (SLD) project to the lateral paragigantocellular nucleus in the medulla, which, together with SLD, is strongly excited during REM sleep. The lateral paragigantocellular nucleus overlaps the sympathoexcitatory areas of RVLM and RVMM (Dampney, 1994). The projections from SLD and RVLM/RVMM make synapses with sympathetic preganglionic neurons that increase skeletal muscle sympathetic activity (Silvani & Dampney, 2013). Finally, the regulation of SNA to different vascular beds, is also exerted by the ventrolateral periaqueductal gray (vlPAG) and by the lateral periaqueductal gray, which include different groups of sympathoinhibitory and sympathoexcitatory neurons, respectively (Silvani & Dampney, 2013).

As mentioned above, REM sleep is also characterized by an extreme breathing irregularity, due to alteration in the automatic control mechanisms of respiration. The respiratory rhythm is irregular, with the average frequency increasing or decreasing compared to the rate reached during NREM sleep in eupnea or polypnea, respectively (Amici et al., 2013). The respiratory activity of the intercostal muscles is diminished. Experiments performed by Millman et al. (Millman et al., 1988) and Gould et al. (Gould et al., 1988) on human subjects, showed that the

phasic REM sleep events, that are coupled with bursts of rapid eye movements and abrupt increase in BP, were also associated with a reduction in total breath time (Tt), no change in inspiratory time and a reduction in Vt. The respiratory changes during phasic REM sleep events were more pronounced during hypercapnia, because of the inhibition of abdominal breathing movements. This may contribute to the decrease in the hypercapnic ventilatory response during REM sleep, as described in dogs during phasic REM sleep (Sullivan et al., 1979; Schäfer & Schläfke, 1998). The response to hypoxia also decreased to less than one third of the waking value and this could explain the REM-sleep-related hypoxemia found in normal subjects and in patients with cardiovascular diseases (Douglas, White, Weil, Pickett, Martin, et al., 1982).

During transition from W to sleep and particularly during REM sleep, there is a reduced tonic activation of dilator muscles of the upper airway, which could predispose to obstructive sleep apnea (Mezzanotte et al., 1996), that is a common findings also in narcolepsy.

3 EFFECTS OF AMBIENT TEMPERATURE ON SLEEP AND RESPIRATORY REGULATION

It is well known that the ambient temperature (Ta) exerts complex influences on wake sleep behaviour and breathing pattern. Several studies performed on human and animals have clarified the role of different environmental temperatures on the wake-sleep cycle. Thermoneutrality is defined as a range in Ta within which body temperature (Tb) is maintained at its set point by minimal values of rates of oxygen consumption (V_{O2}) or basal metabolic level (Mortola & Maskrey, 2011).

In humans, deviations of Ta from thermoneutrality increase the time spent in W and modify the sleep structure. The decrease in sleeping is greater at higher Ta than lower Ta (Parmeggiani, 1986). In humans, the exposure to a hot environment disrupts sleep significantly, increasing time spent in W and reducing amounts of NREM and REM sleep (Karacan et al., 1978).

In mice, the range of thermoneutrality is approximately 28 – 31°C (Ganeshan & Chawla, 2017). When the animals are housed at a warm Ta (30°C), there is an increasing in time spent in both NREM and REM sleep, whereas exposure to cold temperatures (10 or 18°C) reduces sleep (Roussel et al., 1984). In order to evaluate the effects of Ta on sleep pattern, Jhaveri et al. performed a study on C57BL/6J mice that were exposed to different environmental temperatures (22, 26, and 30°C) in three different conditions: control condition, after sleep deprivation (SD), and after infection with influenza virus (Jhaveri et al., 2007). The results showed that, in control conditions, mice spent more time in NREM sleep at 30°C compared to 26°C and spent more time in REM sleep at 26°C compared to 22°C. The length of NREM sleep bouts was longer in mice exposed to 30°C compared to 26°C, but the number of bouts did not differ significantly between the two Ta. Moreover, higher temperature promotes the depth and consolidation of sleep after SD (Jhaveri et al., 2007).

The maintenance of an adequate tissue oxygenation and a constant Tb is the highest priorities for animal's survival. Mammals can maintain Tb into a limited range by using endogenous mechanisms of heat loss and heat production. Ventilation contributes to the regulation of ˙Tb, and, at the same time, is susceptible to changes in Ta and Tb. The complex interweaving between Tb and respiratory regulation has been studied extensively in adult mammals (Mortola & Frappell, 2000). In many species, including humans, the exposure to cold environment causes an increase in V_{O2}, with a proportional increase in both Vt and breathing rate. Conversely,

during heat exposure, the breathing pattern is rapid and shallow (thermal polypnea or panting), to allow heat loss without affecting alveolar ventilation. However, during a severe heat stress, the breathing becomes deep and slow and there is a severe respiratory alkalosis (Mortola & Frappell, 2000).

The relation between Ta and breathing regulation has been studied also in mice. Hodges et al. found that, in WT mice, the reduction in Ta entailed a decrease in ventilatory period (VP) values, and an increase in Vt values. However, the relationship between the changes in the breathing pattern and Ta has been investigated without considering the wake-sleep state (Hodges & Richerson, 2008).

Recently, Valham and colleagues have been performed a study in human subjects to investigate the effect of Ta on sleep and sleep apneas in patients with obstructive sleep apnea. They found that the subjects slept longer and had better sleep efficiency at a room temperature of 16°C compared to 24°C, but obstructive sleep apnea occurrence rate was more severe at this Ta (Valham et al., 2012). These findings suggest that the comprehension of the intricate connections between Ta, sleep and breathing is important also from a clinical point of view.

4 AIM OF THE RESEARCH

This research aims to explore, for the first time, the integrative role of ORXs in the autonomic control of the cardiovascular functions and in respiratory regulation, as a function of ambient temperature (Ta), during different sleep states in mice.

ORX-producing neurons widely project through the entire neuroaxis (Peyron et al., 1998), thus supporting the pleiotropic role of ORXs in the regulation and coordination of multiple physiological functions. Indeed, the loss of ORX neurons promotes narcolepsy in both humans (Peyron et al., 2000) and mouse models (Chemelli et al., 1999; Hara et al., 2001). While their involvement in the maintenance of W and in the control of feeding behaviour has been extensively studied, less is known about the role of ORX system in the regulation of the autonomic mechanisms involved in cardiovascular control and breathing function during the wake-sleep cycle in mice.

Sleep exerts strong effects on cardiovascular control. During the transition between W and NREM sleep, BP decreases by approximately 10% while HP increases (Silvani, 2008). A blunted reduction (<10%) of BP during the W-NREM sleep transition has been reported to be highly frequent in several morbid conditions, such as narcolepsy. The "non-dipping" profile has been identified in both narcoleptic patients (Dauvilliers et al., 2007; Grimaldi et al., 2012) and mouse models of narcolepsy (Bastianini et al., 2011; Lo Martire et al., 2012). The reduction in the nocturnal BP decline is associated with higher cardiovascular risk and with other impairments, such as certain secondary forms of hypertension, renal function damage and disruption of the autonomic nervous system (Birkenhäger & van den Meiracker, 2007). Despite its clinical relevance, the autonomic mechanisms responsible of non-dipping profile are still unclear. The aim of the **first experiment** presented here was to explore the autonomic mechanisms of cardiovascular control during sleep in an ORX-deficient mouse model of NT1. To reach out the goal, we recorded BP and HP (Silvani et al., 2009) in mice lacking ORXs (ORX-KO) and control WT mice under long-term continuous infusions of selective sympathetic and parasympathetic autonomic blockers; experiments were performed using an innovative infusion technique developed in our laboratory (Lo Martire et al., 2018).

An interaction between respiratory modulation and Ta was described in WT mice (Hodges & Richerson, 2008; Hodges et al., 2008), in which reduced Ta (25°C, moderate cold stress) decreased VP values and increased Vt values. However, these changes were described without considering the wake-sleep state. The **second experiment**, described in detail in *Berteotti et al.*,

2020, was designed to investigate if ORXs may modulate respiratory variables in the different states of wake-sleep cycle, as a function of Ta To this aim, we measured Vt, VP, and V_E in ORX-KO mice exposed to different Ta (mild-cold stress: 20°C; thermoneutrality: 30°C) (Berteotti et al., 2020). Moreover, studies reported a higher frequency of sleep apneas in ORX-KO mice, suggesting a key role of ORXs in respiratory regulation during sleep (Nakamura et al., 2007). Sleep apneas have also been found to be associated with NT1 in adult patients (Chokroverty, 1986; Hoshino et al., 2019). In light of these findings, a second aim of this experiment was to verify whether the increase in sleep apnea occurrence rate in ORX-KO mice depended on the exposure to different Ta (20°C Vs. 30 °C) (Berteotti et al., 2020).

In the following sections, the two main experiments will be treated separately to better highlight the experimental characteristics and the results of each one.

FIRST EXPERIMENT

Explore the autonomic mechanisms of cardiovascular control during sleep in an ORX-deficient mouse model of NT1.

5 MATERIAL AND METHODS

5.1 Ethical approval

The study protocol was performed according to the guidelines of the Animal Welfare Committee of the University of Bologna, Italy (D. Lgs 26 of 2014) and complied with the European Directive 2010/63/EU for animal experiments. All efforts were made to minimize animal suffering.

5.2 Mice and genotyping

Experiments were performed on 13 male mice homozygous for a null mutation of the orexin gene (ORX-KO) (Chemelli et al., 1999), and congenic (≥ 10 generations of backcrossing) to C57BI/6J strain. Mouse colony was expanded at the Department of Biomedical and Neuromotor Sciences of the University of Bologna, Italy. Mice were housed at 23°C, with a 12:12 hours light-dark cycle (light on at 9am) and free access to water and food (4RF21 diet, Mucedola, Settimo Milanese, Italy).

Data obtained in this study were compared to those found on 12 male wild-type (WT) mice congenic to C57BI/6J and already published by *Lo Martire et al., 2018*. Mice were matched for age (33.6 ± 0.4 vs. 32.3 ± 1.5 weeks of age, mean ± SEM, P = 0.413, t-test; ORX-KO vs WT, respectively). The experimental groups were not matched for body weight, which was significantly higher in ORX-KO than in WT (34.5 ± 0.7 g vs. 31.7 ± 0.7 g, P = 0.012, t-test).

ORX-KO mice were maintained by heterozygote × homozygote or homozygote × homozygote mating. These breeding strategies did not yield ORX-KO and WT littermates but reduced the generation of heterozygote mice and, therefore, the number of animals employed for experimentation. The genotype of ORX-KO mice was assessed in the Centre for Applied Biomedical Research – CRBA, S. Orsola University Hospital, Bologna, Italy. DNA was extracted from bioptic tissue, taken through a non-invasive procedure performed under general anaesthesia, amplified by polymerase chain reaction, and resolved by gel electrophoresis.

Primers sequences used were:

5’-TCACCCCCTTGGGATAGCCCTTCC-3’ (common, 5’)

5’-GACGACGGCCTCAGACTTCTTGGG-3’ (wild-type HCRT allele, 3’)

5’-CCGCTATCAGGACATAGCGTTGGC-3’ (null mutation of HCRT gene, 3’)

as previously described (Bastianini et al., 2011; Chemelli et al., 1999).

5.3 Surgery

Mice were instrumented with electroencephalographic (EEG) and electromyographic (EMG) electrodes, a telemetric AP transducer (TA11PA-C10, DSI, Tilburg, Netherlands; weight 1.4 g) and an intraperitoneal (IP) catheter for drugs’ infusion. Please refer to the “*Data Supplement*” for full details on the materials and methods.

Surgery was performed under general anaesthesia (ISOFLO, Esteve Spa, Milano. Italy,1.8-2.4% in oxygen, inhalation route) with mouse’s body temperature maintained at 37°C by using a heating pad (Homeothermic blanket Control Unit, Harvard Apparatus) and intra-operative analgesia (10 μL of Norocarp dissolved in 1 ml of saline; 0.2 ml subcutaneously, Pfizer, Italy, Latina).

All procedures were performed in sterile conditions; the surgical tools were sterilized for 15 minutes at 121°C in an autoclave (Beta 35 Easy-lock, PBI, Milano, Italy), the IP catheter and the telemetric BP transducer were sterilized in a solution of peracetic acid (CidexOpa®, Johnson & Johnson Medical, Rome, Italy) and the EEG and EMG were placed under an UV lamp for almost 15 minutes.

The right inguinal area, the skin above the head and the left sub-costal area of the mice were shaved and sterilized with iodine solution.

The surgery consisted in three different steps. The **first step** consisted in the implantation of a telemetric AP transducer connected to a catheter inserted into the abdominal aorta via femoral artery (Tank et al., 2004; Silvani et al., 2009; Lo Martire et al., 2018). The transducer was calibrated with a high-precision manometer (PCE-P05, PCE, Lucca, Italy) before implantation. One cm of the skin in the right inguinal region of the mouse was cut to create a subcutaneous pocket in the right flank of the animal. Using a Zeiss microscope with 16 magnification, the femoral artery was carefully dissected from the femoral vein and femoral nerve, by removing the connective tissue. Once isolated, two silk suture threads (Softsilk 5-0, United States

Surgical, CT, USA) were proximally and distally placed below the arterial segment of interest. The distal thread was permanently knotted, to prevent the retrograde blood flow, while the proximal one was only pulled by another operator to clamp the femoral artery and to temporarily arrest the blood flow.

The catheter was inserted in the distal portion of the artery, between the suture threads, through a hole made by a 90° bent needle (25 G). The tip of the catheter was placed between the iliac bifurcation and the renal arteries for about 2 cm. After the insertion, the threads were both tied in order to secure the catheter to the artery. Then, the telemetric transducer was switched on by using a magnet to verify its correct functioning via radio waves. The battery of the transducer was inserted into the subcutaneous pocket previously created in the right flank of the mouse and fixed with surgical glue (3M Vetbond, 3M Animal Care Products, USA). Finally, suture stitches and an antiseptic ointment (Betadine 10%, Viatris, Milan, Italy) were applied to the skin incision.

The **second step** of the surgery consisted in the implantation of a silicone IP catheter (Silclear Degania, Defries Industries, Australia. Length: 82mm; volume 20 μL approx) to allow for drugs' infusion, as previously described (Lo Martire et al., 2018).

Two incisions were made to create a subcutaneous tunnel, the former on the skin under the left sub-costal margin and the second on the skin of the head. One end of the catheter was inserted into the peritoneal cavity, through a small cut made first in the abdominal muscles and then in the peritoneal wall muscles. The other end was tunnelled subcutaneously towards the mouse head. After that, the tip of the catheter was sutured with the peritoneal wall by using 5-0 suture threads and the patency of the catheter was verified. The end of the catheter on the mouse's head was plugged with a cut and blunted 22G needle. Finally, the sub-costal incision was sutured with 3-0 suture threads and the antiseptic ointment was applied.

In the **third step** of the surgery the mouse was placed on the stereotaxic apparatus (51600 Lab Standard™ Stereotaxic Instrument) in order to fix its head. Electrodes for the recording of the differential EEG and EMG signals were implanted. The periosteum was removed, and the bone surface was cleaned. A drop of hydrogen peroxide was applied locally to better highlight the cranial sutures and the anterior and posterior crossing points, called Bregma and Lambda, respectively. These points were considered as a reference to make 4 holes, at 1 mm of depth, 2 on the left and 2 on the right hemisphere, 1 mm anteriorly and 1 mm laterally with the respect to bregma and to lambda. Two stainless-steel screws (2.4 mm length, Plastics One, Roanoke,

VA, USA), welded to a pair of Teflon-coated stainless-steel wires (Cooner Wire, Chatsworth, CA, USA) were placed in the right holes, while two free stainless-steel anchor screws were placed in the left holes (Fig. 3). All the screws were fixed to the bone by using dental cement (Rely X ARC, 3M ESPE, Segrate, Milan - Italy). A second pair of electrodes was inserted bilaterally in the nuchal muscles to obtain a differential EMG signal. All electrodes on the mouse's head were incorporated in a miniature acrylic cap (Respal NF, SPD, Mulazzano, Italy) light enough (1.5g approx.) to avoid any impairment of the posture of the animal.

At the end of the surgical procedure, an antibiotic solution (30 µL of Veterinary Rubrocillin, Intervet, Schering-Plow Animal Health, Milan – Italy, dissolved in 0.8 ml of sterile saline) was administered subcutaneously to prevent infections and to rehydrate the animal.

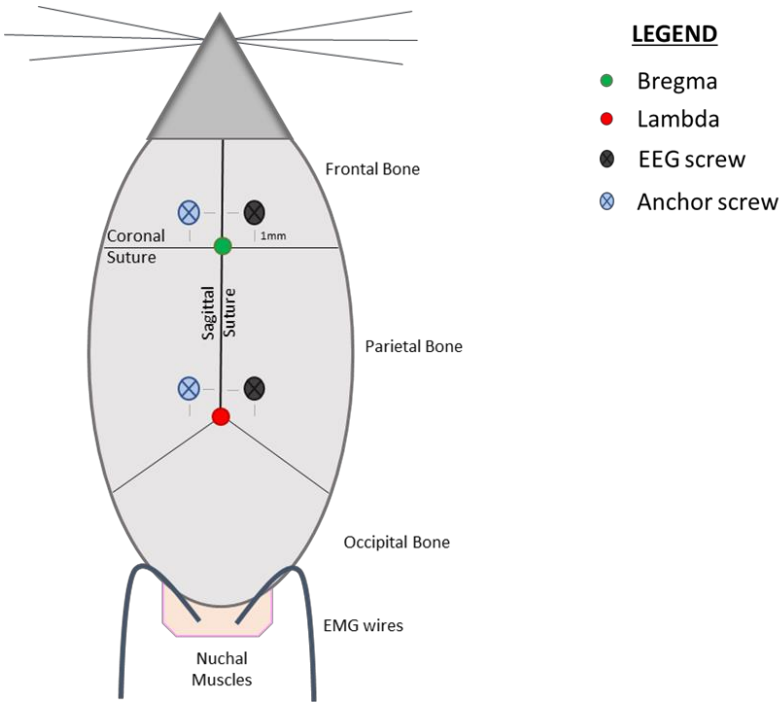

Figure 3. Schematic diagram of the positioning of the EEG screws and EMG wires on the mouse's head.

Screws for the recording of the EEG signals are placed on the right of the sagittal suture while anchor screws are placed on the left of that. EMG wires are placed inside the nuchal muscles.

5.4 Overview of the experimental protocol

The week of the surgery was followed by two weeks of recovery. During this period, each mouse was left in single cage with Ta set al 25°C, light-dark cycle 12:12 and free access to water and food. The last seven days of recovery included the habituation to the recording and to the infusion apparatus, that allowed the recording of sleep and cardiovascular variables and drugs' infusion, simultaneously. The infusion apparatus consisted in the intermediate portion of the infusion catheter (Segment M), which had a length 28 cm, internal diameter of 0.58 mm and volume of 75 μL. Segment M was connected to the IP catheter by means of a 22G blunt needle, filled with sterile saline, closed with a piece of polyethylene tube, and stitched to the recording cable, to prevent twisting. The experimental protocol consisted in a 48 hours recording of the sleep variables in physiological conditions (with no infusion, 12:12 hours light-dark cycle, Ta set at 25°C and free access to food and water) to obtain information about basal wake-sleep cycle.

The weeks of recovery were followed by three weeks of infusions and recording sessions, that were performed during the first 8 hours of the light cycle (from 9 am to 4 pm). During each week, were performed one infusion of vehicle (saline; control infusion) and, after one day of recovery, one infusion with the chosen drug.

After the last recording session, mice were sacrificed by anaesthetic overdose (isoflurane 4% in O2) and autopsied to check the correct insertion of the IP catheter's tip in the peritoneal cavity.

The experimental protocol was described in detail by Lo Martire et al., 2018 and it is shown in Fig. 4.

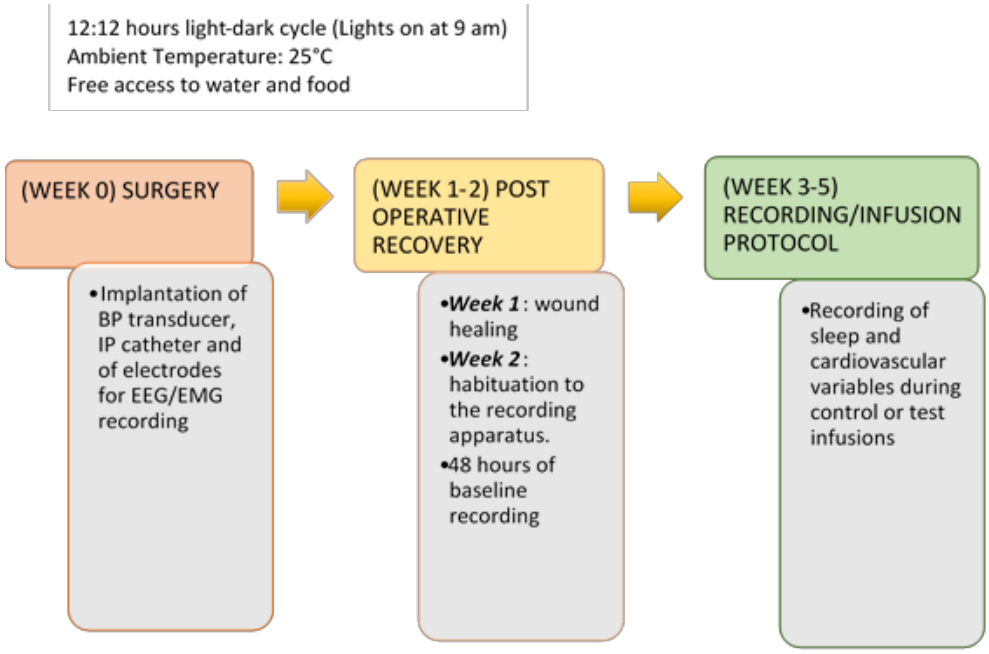

Figure 4. **Experimental schedule of the first experiment.**

Please refer to "Overview of the experimental protocol" for full details.

5.5 Drugs preparation and infusion

The preparation and infusion of the drugs were described in detail by Lo Martire et al., 2018.

Atropine methyl nitrate (SML0732, Sigma-Aldrich, St Louis, MO, USA), a muscarinic acetylcholine receptor antagonist, was infused at 0.5 mg/mL to block parasympathetic nervous activity on the heart.

Atenolol (A7655, Sigma-Aldrich, St Louis, MO, USA), a β1-adrenergic receptor antagonist, was infused at 0.25 mg/mL to block sympathetic nervous system activity on the heart.

Prazosin hydrochloride (P7791, Sigma-Aldrich, St Louis, MO, USA), an α1-adrenoceptor antagonist, was infused at 0.25 mg/mL to block sympathetic vasoconstrictor activity. Each drug was dissolved in sterile saline before each recording session.

Mice were not weighted before each recording session to avoid stress for the animal, due to handling and cable/tubing disconnection, with consequences on sleep and cardiovascular variables during the subsequent recordings. For this reason, drugs' concentrations and infusion rate were not scaled to the mouse weight but were selected arbitrarily. Nonetheless, based on

the average body weight measured at surgery and on an infusion rate of 100 µL/h, the concentrations of the drugs administered during each infusion were 20% lower than that considered safe and were also effective on the different branch of ANS as single bolus injections (Baudrie et al., 2007; Gross et al., 2005; Laude et al., 2008).

The set-up for intraperitoneal infusion is illustrated in Fig.5.

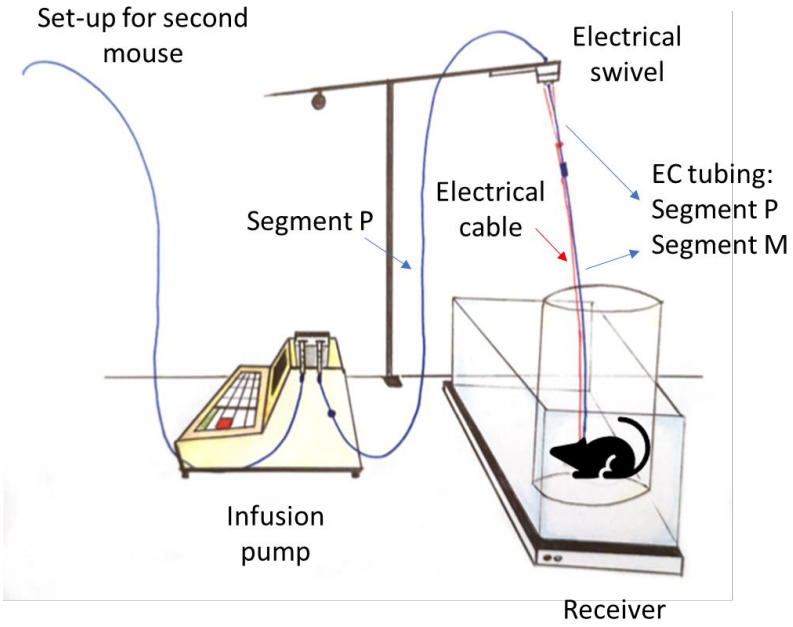

Figure 5. Experimental set-up for continuous intraperitoneal (IP) infusion in mice.

The figure shows the experimental set-up for IP infusion in two mice at the same time, with the simultaneous recording of sleep (via electrical cable) and cardiovascular (via receiver) variables. EC: extracorporeal. Figure modified from *Lo Martire et al., 2018.*

The segment M of the catheter was connected to a remote infusion pump (model 22 multiple syringe pump, Harvard Apparatus, Holliston, MA, USA) by means of a long upper catheter (Segment P, Smiths Medical, Ashford, UK). Segment P had a length of 160 cm, internal diameter of 0.86 mm and volume of approximately 1.3 ml. Before the connection, segment P was sterilized and was pre-filled with either sterile saline or drug solutions, based on the experimental schedule.

The free end of segment P was passed through a hole of the electrical swivel and connected to a syringe, which was filled with distilled water and mounted on the pump. The overall weight of both segments M and P were supported by the same suspensor arm that supported the weight

of the electrical cable and swivel. An air bubble was introduced at the end of segment P to avoid mixing of the distilled water in the syringe with the saline/drug solutions in segment P. Before the start of each recording session, an infusion of saline or drug solution was performed at a rate of 30 μL/min for 5 min to fill segment M and the IP catheter with the same solution of the segment P. After this initial bolus loading, the syringe was filled again with distilled water and then recordings were started. Infusion of saline or drug solution was performed at 100 μL/h for 7h. The progress of the bubble along segment P was periodically measured with a caliper to check that the actual and nominal infusion rates coincided. After 7 hours, recordings were stopped; segment P was replaced with another 60cm long catheter, filled with sterile saline and having a small air bubble close to the pump, as previously described. A bolus was performed (30 μL/min for 5 min) to fill segment M and the IP catheter with saline. Finally, segment P was disconnected, and segment M was plugged. The mouse was then left undisturbed in its cage with the cable connected to the electrical swivel and segment M stitched to the cable.

The experimental set-up allowed the simultaneous recording of two mice, with the following weekly schedule:

- Monday: control infusion in the first group of mice
- Tuesday: control infusion in the second group of mice
- Wednesday: drug's infusion in the first group of mice.
- Thursday: drug's infusion in the second group of mice.

5.6 Data acquisition

Data acquisition was performed by using a software written in Labview (National Instruments, Austin, TX, USA). The acquisition of EEG, EMG and BP signals was performed as previously described (Bastianini et al., 2011), via an electrical cable connected to a rotating electrical swivel (SL2+2C/SB, Plastics One, Roanoke, VA, USA) mounted on a balanced suspension arm, that prevented the cable from twisting and allowed free movement of the mouse. The EEG and EMG signals were amplified and filtered (EEG: 0.3–100 Hz with 50 Hz notch filter; EMG: 100–1000 Hz with 50 Hz notch filter; 7P511J amplifiers, Grass, West Warwick, RI, USA). The BP transducer transmitted telemetrically the signal to a receiver (RPC-1, DSI) placed under the mouse's cage. The receiver also produced an activity signal (ACT) by quantifying the displacement of the transducer during the movement of the animal. The calibration of the BP transducer was performed with a high-precision manometer (PCE P05, PCE Italy, Gragnano,

Lucca, Italy) before the implantation and after the end of the experimental protocol. All signals were digitized at 16-bit (PCI-6224 board, National Instruments, Austin, TX, USA). EEG and EMG signals were down sampled at 128 Hz and stored together with the BP signal at 1024 Hz.

5.7 Data analysis

5.7.1 Discrimination of the wake-sleep states

Data analysis was performed with a custom-made software written in Matlab (Mathworks, Natick, MA, USA). Sleep scoring was performed on 4-s epochs, based on visual analysis of raw EEG and EMG signals, using a validated semi-automatic algorithm (SCOPRISM) (Bastianini et al., 2014). The analysis was performed by trained investigators following published criteria (Silvani et al., 2009):

- W was scored when EMG tone was high and EEG was at low voltage, with δ (0.5-4Hz) and θ (6-9 Hz) frequency waves.

- NREM sleep was scored when EMG tone was lower than in W and EEG was at high voltage, with a prevalence of δ frequency waves.

- REM sleep was scored when EMG showed muscular atonia with occasional muscle twitches and low voltage EEG with a prevalence of θ frequency waves.

Sleep architecture was assessed by computing the percentage of recording time spent in each wake-sleep state and the average latency from the end of a W episode to the onset of the subsequent REM sleep episode. Cataplexy-like episodes were scored according to consensus criteria. Episode duration, REM sleep latency and cataplexy-like episodes were analysed taking into account only episodes with duration ≥ 12 s as previously described (Bastianini et al., 2011).

5.7.2 Analysis of the cardiovascular variables

While performing the visual identification of wake-sleep states, the investigator identified the 4-s epochs in which the AP signal had insufficient quality to allow an accurate automatic determination of the systolic and diastolic AP and of heart period (HP, reciprocal of HR). Values of HP were computed as the time intervals between the onset of successive systolic upstrokes of blood pressure (Silvani et al., 2012). A following semiautomated analysis was performed by using a software developed in Matlab, to identify the 4-s epochs in which there

were errors in the automatic detection of the minima and maxima of the pulse waves that produced artefactual values of HP, systolic AP, diastolic AP, or mean AP greater than twice the respective median values or lower than 10 % of the respective median values. Non-physiological fluctuations were excluded manually from the analysis.

Subsequently, beat-to-beat values of systolic AP, diastolic AP, mean AP and HP were computed from the raw BP signal in each artefact-free 4-s epoch (Silvani et al., 2009).

The values of mean AP (MAP, the average AP in each cardiac cycle) and HP were computed from the raw AP signal for each heartbeat and averaged for each wake-sleep state and each mouse.

Fig.6 shows an example of raw EEG, EMG, AP, and ACT signals.

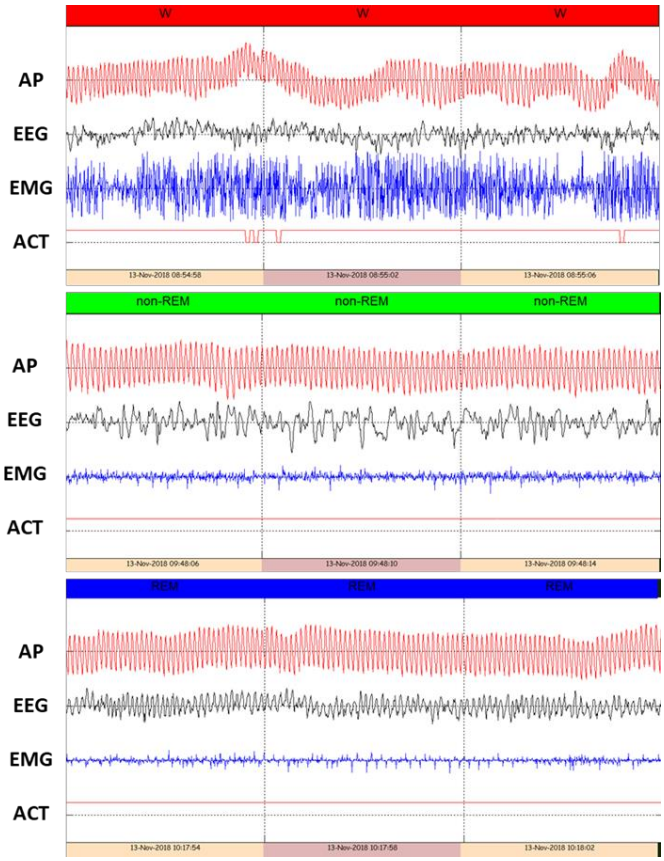

Figure 6. **Example of raw tracing obtained during each wake-sleep state.**

The automatic scoring procedure classified the behavioural state (top of each window) for each 4-s epoch; this classification is then confirmed or denied by the investigator.

W: Wakefulness, non-REM: Non-rapid Eye Movement Sleep; REM: Rapid Eye Movement Sleep, AP: Arterial Pressure; EEG: electroencephalogram; EMG: electromyogram of nuchal muscles; ACT: Activity.

5.8 Statistical analysis

The statistical analysis was performed with SPSS Statistics (IBM Corp., Armonk, NY, USA) with the level of significance set at $P < 0.05$. The normality of the data distribution was tested by means of Kolmogorov-Smirnov test. To simplify interpretation of the results, we preliminarily tested for systematic differences in MAP and HP among vehicle infusions of different control recording sessions. A 3-way mixed-model analysis of variance (ANOVA) with the mouse group (2 levels), recording session (3 levels), and wake-sleep state (3 levels) as factors did not detect significant main effects or interactions of the recording session (data not shown). The results obtained during the different control/saline sessions were, therefore, averaged for each mouse. Three-way mixed model ANOVAs were then performed on MAP and HP with mouse group (2 levels), drugs/vehicle (4 levels: average control session, atropine methyl nitrate, atenolol, and prazosin), and wake-sleep state (3 levels) as factors. In case of significance of the 3-way interaction, simple effects of the mouse group were assessed with independent-sample t-tests. The data on sleep structure were analysed with 2-way ANOVA with the mouse group (2 levels) and drugs/vehicle (4 levels, cf. above) as factors. In case of significant effects of the drugs/vehicle factor without significant interactions, the effect of each drug was compared with that of the average of vehicle infusion sessions with ANOVA simple contrasts. The Huynh-Feldt correction was applied if the ANOVA sphericity assumption was not met. All data are reported as means ± SEM.

Because of battery failure of telemetric AP transducers, we lost data from at least one infusion in 4 WT mice and in 2 ORX-KO mice. Thus, ANOVAs were performed with a sample size of 8 WT vs 11 ORX-KO mice with the complete infusion set. Simple effects of the mouse group were analysed with t-tests with sample sizes of 12 WT vs 13 ORX-KO mice for average vehicle infusions, of 10 WT vs 12 ORX-KO mice for atropine methyl nitrate and atenolol infusions, and of 10 WT vs 13 ORX-KO mice for prazosin infusions. A statistical power analysis was performed based on the effect size of the difference in MAP during REM sleep previously reported between ORX-KO and WT mice (Bastianini et al., 2011). This analysis indicated that sample sizes of 10 vs 12 mice afforded a 99% power with alpha level at $P < 0.05$ and two-tailed independent-sample t-test.

6 RESULTS

The effects of autonomic receptor blockers on MAP, as a function of the wake-sleep state in ORX-KO and WT mice are shown in Fig. 7. ANOVA revealed a significant 3-way interaction of mouse groups, drugs, and wake-sleep states (P = 0.001), significant 2-way interactions between wake-sleep states and either mouse groups or drugs, and significant main effects of drugs and wake-sleep states (all P < 0.001). No significant main effect of mouse groups (P = 0.204) and interaction between mouse groups and drugs (P = 0.639) were reported. Analysis of simple effects with t-tests indicated that MAP was significantly higher in ORX-KO than in WT mice during REM sleep in the course of saline (P = 0.018, Fig.7A) and atropine methyl nitrate (P = 0.036, Fig.7B) administration, but not during of atenolol (P = 0.131, Fig.7C) and prazosin (P = 0.074, Fig.7D) administration.

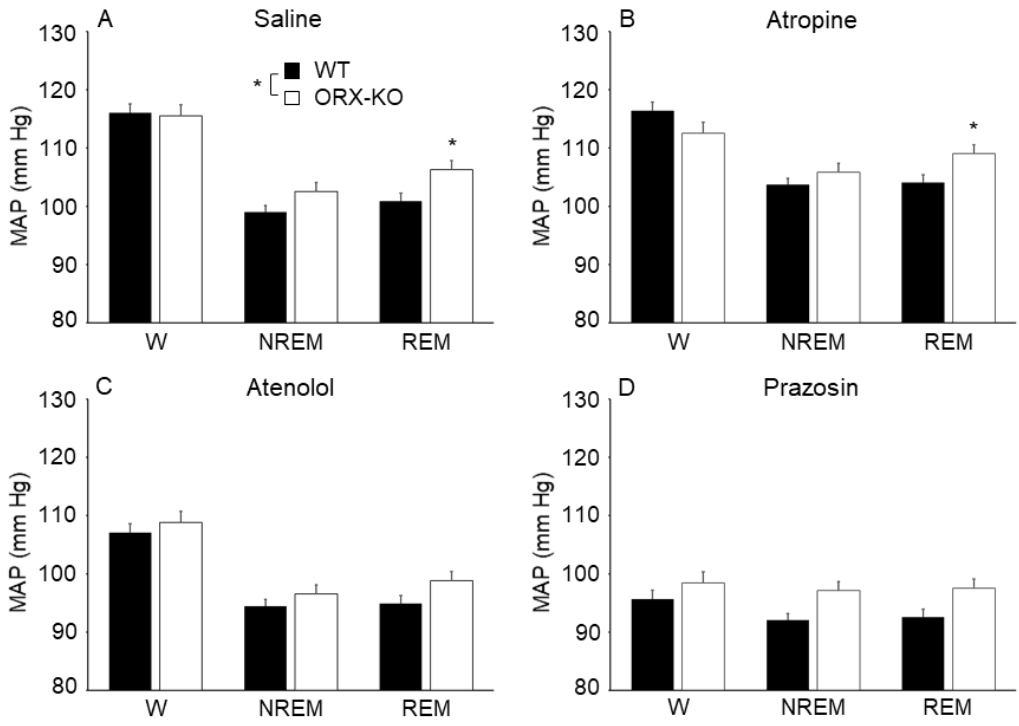

Figure 7. **Effects of autonomic receptor blockers on mean arterial pressure during wakefulness and sleep in orexin knock-out mice and wild-type controls**

MAP: mean arterial pressure. W: wakefulness. NREM: non-rapid-eye-movement sleep. REM, rapid-eye-movement sleep. WT: wild-type mice. ORX-KO: orexin knock-out mice. Atropine methyl nitrate is indicated as atropine for brevity. Data are shown as mean ± SEM. For WT mice, n = 12 (saline) or n = 10 (atropine, atenolol, and prazosin). For ORX-KO mice, n = 13 (saline and prazosin) or n= 12 (atropine and atenolol). *: P < 0.05 vs. WT (t-test).

To better characterize the significant interactions between mouse groups and wake-sleep states, a further analysis was performed on the differences in MAP (ΔMAP) between NREM sleep and W, between REM sleep and W, and between NREM sleep and REM sleep (Fig.8). During saline infusion (Fig.8A), ΔMAP between either NREM sleep or REM sleep and W was significantly blunted in ORX-KO compared with WT mice, whereas ΔMAP between NREM sleep and REM sleep was significantly enhanced in ORX-KO compared with WT mice ($P = 0.008$, $P < 0.001$, and $P = 0.047$, respectively; t-test). The significance of these differences between ORX-KO and WT mice were preserved during atropine administration ($P < 0.001$, $P < 0.001$, and $P = 0.004$, respectively; t-test) (Fig.8B). During atenolol administration (Fig.8C), only ΔMAP between REM sleep and W was still significantly blunted in ORX-KO compared with WT mice ($P = 0.039$, t-test), whereas ΔMAP between NREM sleep and W and ΔMAP between NREM sleep and REM sleep did not differ significantly between groups ($P = 0.784$ and $P = 0.130$, respectively; t-test). During prazosin administration (Fig.8D), no significant differences between ORX-KO and WT mice were observed in ΔMAP between NREM sleep and W, in ΔMAP between REM sleep and W or in ΔMAP between NREM sleep and REM sleep ($P = 0.189$, $P = 0.258$, and $P = 0.909$, respectively; t-test).

The effects of autonomic receptor blockers on HP are shown in Fig.9. ANOVA showed a significant 2-way interaction between drugs and wake-sleep states and significant main effects of the drugs and of the wake-sleep states (all $P < 0.001$). The 3-way interaction of the mouse groups, drugs, and wake-sleep states ($P = 0.311$), the 2-way interactions between mouse groups and either drugs ($P = 0.664$) or wake-sleep states ($P = 0.591$), and the main effects of mouse groups ($P = 0.925$) were not statistically significant. In the absence of significant interactions involving the mouse groups and the wake-sleep states, no further analysis was performed on simple effects of the mouse group on HP values in each wake-sleep state and on the differences in HP between wake-sleep states.

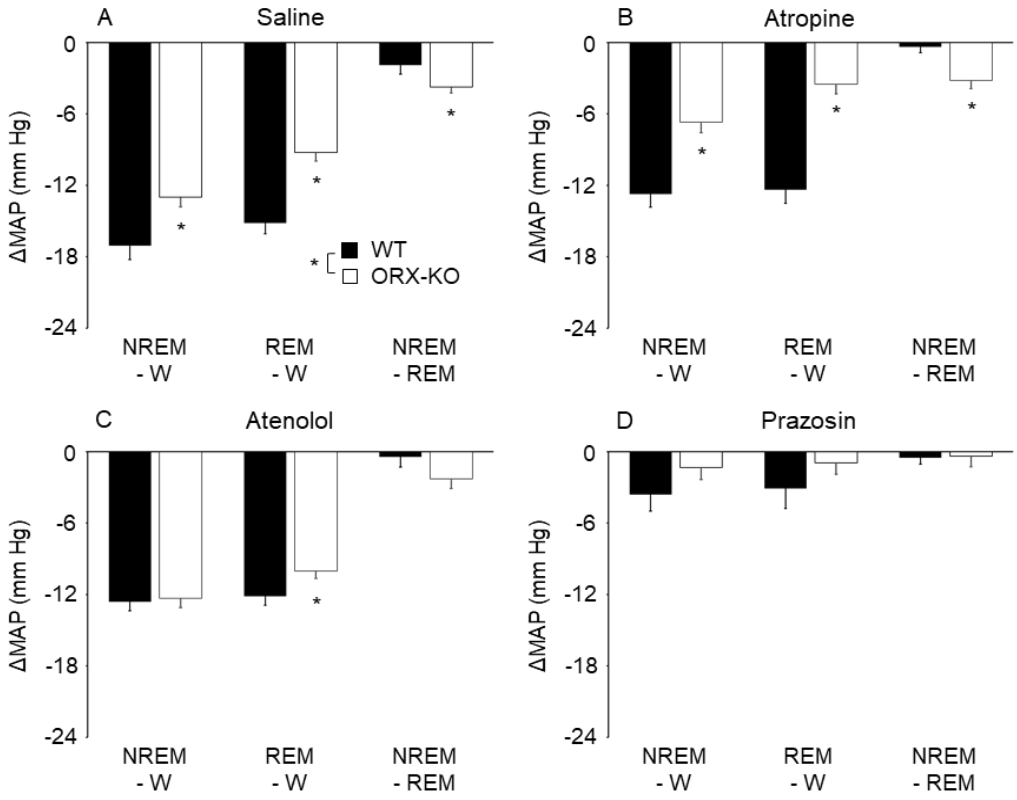

Figure 8. Effects of autonomic receptor blockers on differences in mean arterial pressure between wake-sleep states in orexin knock-out mice and wild-type controls

ΔMAP: difference in mean arterial pressure between wake-sleep states. W: wakefulness. NREM: non-rapid-eye-movement sleep. REM, rapid-eye-movement sleep. WT: wild-type mice. ORX-KO: orexin knock-out mice. Atropine methyl nitrate is indicated as atropine for brevity. Data are shown as mean ± SEM. For WT mice, n = 12 (saline) or n = 10 (atropine, atenolol, and prazosin). For ORX-KO mice, n = 13 (saline and prazosin) or n = 12 (atropine and atenolol). *: $P < 0.05$ vs. WT (t-test).

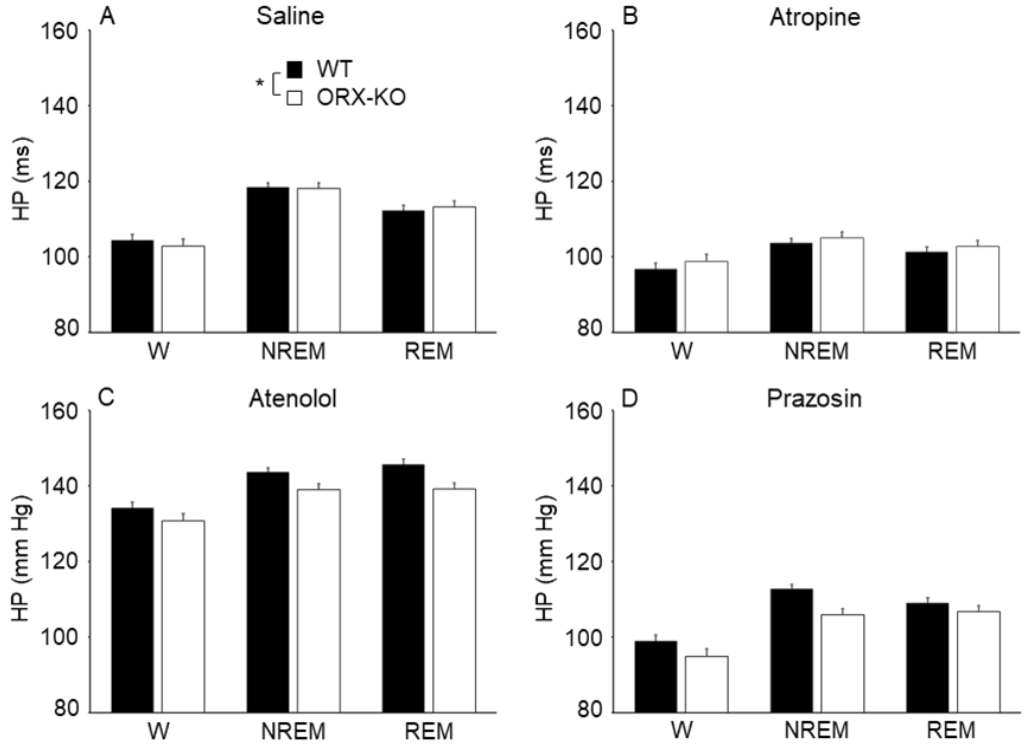

Figure 9. Effects of autonomic receptor blockers on heart period during wakefulness and sleep in orexin knock-out mice and wild-type controls

HP: heart period. W: wakefulness. NREM: non-rapid-eye-movement sleep. REM, rapid-eye-movement sleep. WT: wild-type mice. ORX-KO: orexin knock-out mice. Atropine methyl nitrate is indicated as atropine for brevity. Data are shown as mean ± SEM. For WT mice, n = 12 (saline) or n = 10 (atropine, atenolol, and prazosin). For ORX-KO mice, n = 13 (saline and prazosin) or n = 12 (atropine and atenolol). *: $P < 0.05$ vs. WT (t-test).

The effects of the drugs on the wake-sleep architecture in ORX-KO and WT mice are shown in the Table1. ANOVA did not reveal any significant interaction between drugs and mouse groups for any variable under study ($P \geq 0.148$). ORX-KO significantly differed from WT mice in terms of lower mean duration of W and REM sleep episodes and of shorter REM sleep latency ($P = 0.001$, $P = 0.025$, and $P = 0.005$, respectively; ANOVA main effects). Drugs significantly affected the percentage of recording time spent in REM sleep ($P = 0.002$, ANOVA main effect), which was significantly lower during atropine methyl nitrate than during saline administration ($P < 0.001$, ANOVA simple contrast). Drugs also significantly affected the average duration of W, NREM sleep and REM sleep episodes and REM sleep latency ($P \leq 0.006$, ANOVA main effects). Each of these variables was significantly lower during the administration of all drugs than during saline administration ($P \leq 0.040$, ANOVA simple

contrasts). Cataplexy-like episodes did not occur during the recordings, except for 1 episode in 1 ORX-KO mouse, during prazosin infusion.

		Saline		Atropine		Atenolol		Prazosin	
		WT	ORX-KO	WT	ORX-KO	WT	ORX-KO	WT	ORX-KO
W	%	32±2	31±2	31±3	34±4	33±1	31±1	33±2	28±2
	D (s)	116±11	83±7*	71±8†	54±4*†	83±5†	70±6*†	79±7†	44±6*†
NREM	%	56±2	57±2	60±3	59±3	56±1	59±1	56±2	62±2
	D (s)	76±4	71±2	68±4†	57±5†	59±4†	67±4†	56±5†	54±5†
REM	%	9±1	9±0	7±1†	6±1†	8±0	8±0	7±1	8±1
	D (s)	54±2	45±1*	55±5	42±3*	51±4	48±2*	44±5†	39±2*†
	L (s)	456±50	242±19*	315±37 †	212±30 *†	280±43 †	207±14 *†	278±44 †	154±21 *†

Table 1. Effects of autonomic receptor blockers on sleep and wakefulness in orexin knock-out mice and wild-type controls.

Atropine methyl nitrate is indicated as atropine for brevity. W: wakefulness. NREM: non-rapid-eye-movement sleep. REM, rapid-eye-movement sleep. WT: wild-type mice. ORX-KO: orexin knock-out mice. %: percentage of recording time spent in each wake-sleep state. D: episode duration. L: latency. Data are shown as mean ± SEM. For WT mice, n = 12 (saline) or n = 10 (atropine, atenolol, and prazosin). For ORX-KO mice, n = 13 (saline and prazosin) or n = 12 (atropine and atenolol). *: $P < 0.05$ vs. WT (ANOVA main effect). †: $P < 0.05$ vs. saline (ANOVA main effect and simple contrast).

7 DISCUSSION

The main findings of our study were that the sleep-related differences in AP between ORX-KO and WT mice were entirely abolished by prazosin and mostly abolished by atenolol.

During saline administration, the differences that we found in AP (Fig.7A and Fig.8A) and sleep architecture (Table 1) between ORX-KO and WT mice confirmed our previous findings obtained on younger (14-15 vs. 32-33 weeks of age) ORX-KO male mice during the light and dark periods (Bastianini et al., 2011). In our previous study, however, ORX-KO mice also showed increased AP during NREM sleep, increased HR during each wake-sleep state, and increased rate of cataplexy-like episodes compared to WT mice (Bastianini et al., 2011). These discrepancies are not unexpected. The association between alterations in cardiac control and NT1 in both human patients and animal models is still a matter of controversy and inconsistency. Furthermore, NT1 may be associated with AP values that are lower than normal in W and normal during sleep, or normal in W and higher than normal during sleep, particularly during REM sleep (Berteotti & Silvani, 2018). On the other hand, the lack of cataplexy-like episodes in ORX-KO mice in this study may have been, at least in part, because recordings were restricted to the light period.

The lack of significant differences in MAP (Fig.7D) and in ΔMAP (Fig.8D) between ORX-KO and WT mice during prazosin infusion indicates that alterations in the sympathetic control of resistance vessels may be sufficient to mediate sleep-related AP alterations due to ORX deficiency in NT1. This suggestion is strengthened by the significance of the three-way ANOVA interaction of drugs, wake-sleep states, and mouse groups, and supported by the high estimated statistical power of the tests (*cf. 5.8 Statistical analysis*). Moreover, this conclusion is in line with our previous results on WT mice, which showed that modulation of sympathetic vasoconstriction was critical for the effects of sleep on AP (Lo Martire et al., 2018). However, blunted, non-significant differences in AP between W and NREM sleep have been reported in patients with NT1 in the face of significant sleep-related decreases in sympathetic nerve activity to skeletal muscle and skin blood vessels, measured with microneurography (Donadio et al., 2014). This discrepancy may be only apparent, as data on rats indicate that sympathetic nerve activity to the kidneys also decreases from W to NREM sleep, reaches its minimum values during REM sleep (Yoshimoto et al., 2011) and causes an effective renal vasodilatation compared with wakefulness (Yoshimoto et al., 2004). These data raise the hypothesis that sleep-

related alterations in AP due to ORX deficiency in NT1 depend on an insufficient sleep-related reduction of renal sympathetic nerve activity.

In our study, the lack of significant differences in MAP (Fig.7C) and in ΔMAP (with the exception of the one in ΔMAP between W and REM sleep, Fig.8C) between ORX-KO and WT mice during atenolol administration indicates that alterations in the sympathetic control of the heart may also be sufficient for sleep-related AP alterations due to ORX deficiency in NT1. However, we did not find alterations in HP control in ORX-KO compared to WT mice (Fig. 9). Atenolol blocks the β1-adrenergic receptors that not only decrease HP, but also increase contractility in response to sympathetic nerve activity to the heart (Silvani et al., 2016). Our data thus raise the hypothesis that the sleep-related AP alterations in ORX-KO mice mainly depended on sympathetic increases in cardiac contractility.

The significantly blunted ΔMAP between W and REM sleep in ORX-KO mice during atenolol infusion, taken together with its lack in the course of prazosin infusion, may indicate that the effects of cardiac sympathetic response alterations were somewhat less robust than that of alterations in sympathetic activity to resistance vessels. Little is known about the physiological changes in cardiac sympathetic activity during sleep (Silvani, 2008). In our previous analysis of results on WT mice, we concluded that changes in sympathetic activity to the heart contributed to sleep-related changes in HP and to the increase in AP from NREM sleep to REM sleep (Lo Martire et al., 2018). However, our prior analysis, we focused on transitions from wakefulness to relatively long episodes of NREM sleep and vice versa (Lo Martire et al., 2018). Conversely, here we focused on ΔMAP between episodes of W and NREM sleep of any duration for direct comparison with our original work on cardiovascular differences between ORX-KO and WT mice (Bastianini et al., 2011).

We found that the sleep-related AP differences between ORX-KO and WT mice were fully preserved during administration of atropine methyl nitrate (Fig.7B and 8B). These results demonstrate that alterations in cardiac parasympathetic control are not necessary to explain the sleep-related AP alterations associated with ORX deficiency. This conclusion is in line with our previous analysis of data in WT mice, which indicated that changes in cardiac parasympathetic activity play a role in the sleep-related changes in HP, but not in those of AP (Lo Martire et al., 2018).

The infusion of atropine methyl nitrate, atenolol, and prazosin partially disrupted sleep architecture (Table 1). Sleep architecture changes may have resulted, at least in part, from the

substantial AP and HP changes caused by drugs 'infusion. Nevertheless, it appears unlikely that sleep structure alterations could explain our results on AP. Indeed, the sleep-related differences in AP between ORX-KO and WT mice were fully preserved during infusion of atropine methyl nitrate, which fragmented W and NREM sleep episodes, and which decreased REM sleep latency and REM sleep time. Moreover, the reduction in REM sleep episode duration, that was associated selectively with prazosin administration, was relatively small, in the order of 10-20%.

Our study has few limitations. We did not study ORX-KO mice at the same time as WT littermates, but we compared ORX-KO mice with WT control mice that had been previously studied (Lo Martire et al., 2018). However, the ORX-KO and WT mice had the same genetic background and were studied in the same facilities with an identical research protocol. This approach helped to reduce the number of animals employed for research, and was sensitive enough to confirm, during saline administration, those previously reported differences between ORX-KO and WT mice (Bastianini et al., 2011).

We estimated the alterations in sympathetic and parasympathetic activities of ORX-KO mice effects only by subtraction, evaluating differences between ORX-KO and WT mice during administration of autonomic receptor blockers. Direct measurements of autonomic nerve activity in freely behaving mice during spontaneous sleep have never been performed to our knowledge and would be challenging in these small animals. Nevertheless, our approach does not allow us to exclude central nervous system effects of prazosin and atenolol (Neil-Dwyer et al., 1981).

We did not adjust drug doses to mouse body weight. ORX-KO mice, which were significantly heavier than WT mice at surgery, may therefore have received lower doses per unit body weight than WT mice. Nevertheless, they would be expected to have enhanced the cardiovascular differences between ORX-KO and WT mice.

Our analysis of simple effects relied on a relatively large number of independent-sample t-tests. Recognizing that this may inflate type I error rate, we analysed simple effects only for MAP, for which ANOVA revealed a highly significant three-way interaction including the mouse group, and not for HP, for which such interaction was not significant.

We performed this study on ORX-KO mice, which have congenital deficiency of ORXs peptides (Chemelli et al., 1999). However, patients with NT1 lose ORX neurons after birth,

including their released co-transmitters. We cannot exclude that the study of mouse models lacking the whole orexin neurons (Hara et al., 2001; Tabuchi et al., 2014) would have yielded different results. Nevertheless, ORX-KO mice still represent the best mouse model to single out the contribution of orexin peptide deficiency to the key behavioural (Chemelli et al., 1999) and cardiovascular (Bastianini et al., 2011) features of NT1.

SECOND EXPERIMENT

Investigate whether ORXs may modulate respiratory variables during the different states of wake-sleep cycle, as a function of Ta and verify whether the increase in sleep apnea occurrence rate in ORX-KO mice depends on the exposure to different Ta (20°C Vs. 30 °C).

All the sections referred to the “Second Experiment” are published in our recent study, in which I am co-author

(Berteotti et al., 2020)

8 MATERIAL AND METHODS

8.1 Ethical approval

The study protocol was performed according to the guidelines of the Animal Welfare Committee of the University of Bologna, Italy (D. Lgs 26 of 2014) and complied with the European Directive 2010/63/EU for animal experiments. All the experiments included in this study were executed non-invasively.

8.2 Mice and genotyping

Experiments were performed on 9 male ORX-KO and 8 congenic (≥ 10 generations of backcrossing) male C57Bl/6J WT mice matched for age (44.9 ± 0.6 weeks and 45.3 ± 0.4 weeks, respectively). Mice were maintained at 23°C with a 12:12 hour light-dark cycle and free access to food (4RF21 diet, Mucedola, Settimo Milanese, Italy) and water.

Mice ORX-KO were maintained by heterozygote × heterozygote and heterozygote × homozygote mating. The genotype was assessed in the Centre for Applied Biomedical Research – CRBA, S. Orsola University Hospital, Bologna, Italy. DNA was extracted from bioptic tissue, collected through a non-invasive procedure performed under general anaesthesia, amplified by polymerase chain reaction, and resolved by gel electrophoresis.

Primers sequences used were:

5'-TCACCCCCTTGGGATAGCCCTTCC-3' (common, 5')

5'-GACGACGGCCTCAGACTTCTTGGG-3' (wild-type HCRT allele, 3')

5'-CCGCTATCAGGACATAGCGTTGGC-3' (null mutation of HCRT gene, 3')

as previously described (Bastianini et al., 2011; Chemelli et al., 1999)

8.3 Experimental protocol

The experimental protocol consisted of two recording sessions for each animal, performed with the mouse placed inside a modified whole-body plethysmography (WBP) chamber (PLY4223,

Buxco, Wilmington, NC, USA) (Fig.10) exposed either to mild cold stress (T_a = 20°C) or to thermoneutrality (Ta = 30 °C). The order of the recording sessions was randomly chosen and balanced between groups, with from 2 to 28 days' interval between the sessions. Each recording session started at lights on (9 am) for 8h, during the light period.

The mouse chamber was modified by inserting a solid 10 cm diameter Plexiglas block, which reduced the internal volume of the chamber to 0.97l. The chamber accommodated a rotating electrical swivel (SL6C/SB, Plastics One, Roanoke, VA, USA) and temperature and humidity probes (PC52–4-SX-T3 sensor, Rense Instruments, Rowley, MA, USA), (Bastianini et al., 2017). Free access to water was allowed. The differential pressure between the mouse chamber and a 2nd reference chamber was measured with a high-precision differential pressure transducer (DP103–06+ CD223 digital transducer indicator; Validyne Engineering, Northridge, CA, USA). WBP chamber was continuously purged at 1.5 l/h with air fed from a cylinder. Respiratory signals, chamber humidity and temperature were continuously recorded, digitized, and stored at 128 Hz, 4 Hz, and 4 Hz, respectively. The system was calibrated with a 100 µL micro-syringe (Hamilton, Reno, NV, USA) at the end of each recording.

Figure 10.

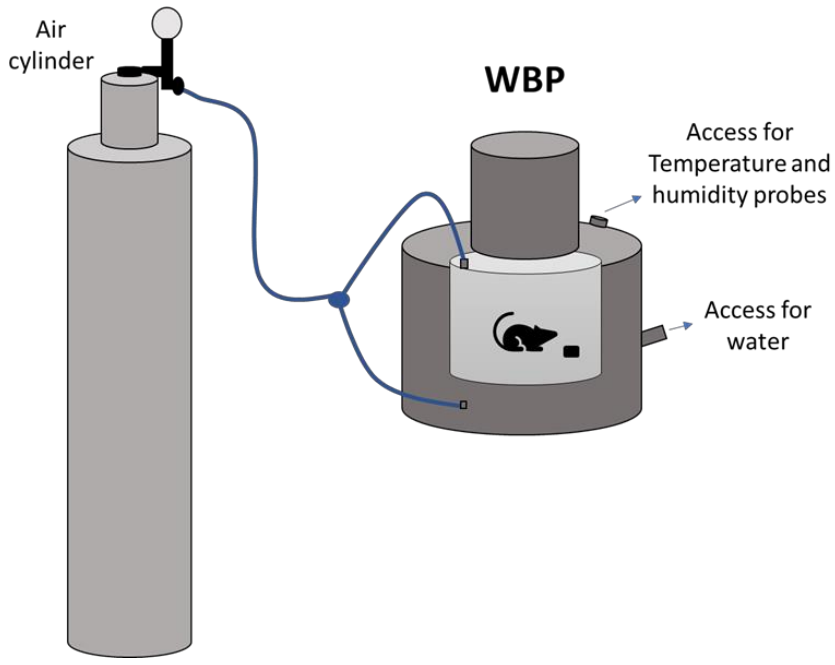

Figure 10. Schematic representation of the whole-body plethysmography (WBP) chamber.

The mouse chamber was modified to reduce the volume of the chamber to 0.97l. The chamber accommodated temperature and humidity probes. Free access to water was allowed. WBP chamber was continuously purged at 1.5 l/h with air fed from a cylinder.

At the end of both recording sessions, mice were perfused with saline followed by 4% paraformaldehyde. Brains were cryoprotected in PBS with 20% sucrose and coronally sectioned at 30 µm using a cryostat-microtome at - 22.0 °C. Free-floating hypothalamic sections were washed in 0.3% Triton X-100 in PBS for 30 min. After blocking for 90 min with 3% bovine serum albumin (Sigma Aldrich, Milan, Italy) in 0.3% Triton X-100 in PBS, sections were incubated overnight at 4°C with rabbit anti–orexin A antiserum (Phoenix Pharmaceuticals, Burlingame, CA, USA) diluted 1:5000 in 0.3% Triton X-100 in PBS and BSA 1%. Sections were then washed in 0.3% Triton X-100 in PBS for 30 min and incubated for 2 h with a Cy3-conjugated AffiniPure Donkey Anti-rabbit IgG (Jackson ImmunoResearch, West Grove, PA, USA) secondary fluorescent antibody diluted 1:200 in 0.3% Triton X-100 in PBS and BSA 1%. Sections were counterstained with Hoechst 33342 (Sigma-Aldrich, Milan, Italy) to label cell nuclei. Immunofluorescence images were captured with a Nikon Eclipse TE 2000-S inverted microscope (Nikon Corp., Kawasaki, Japan) equipped with a Nikon digital camera DS-Qi2. Control and experimental animals were processed simultaneously for staining to avoid any batch-to-batch variation. The same lot of primary antiserum was used for staining the brains of WT and ORX-KO mice (Berteotti et al., 2020).

8.4 Data analysis

8.4.1 Discrimination of wake-sleep cycle

Sleep scoring was carried out based on visual inspection of the raw respiratory tracing, with a procedure validated against gold-standard conventional EEG and EMG recording (Bastianini et al., 2017). According to previous studies, breathing analysis was restricted to stable sleep episodes ≥ 12 s (Bastianini et al., 2015; Silvani et al., 2014) because of the frequent occurrence of movement artefacts during W. The WBP sleep scoring was based on three components of the breathing trace, as frequency, amplitude, and baseline, evaluated from the visual inspection of the raw signal. Sleep analysis was performed by trained investigators following published criteria (Bastianini et al., 2017):

- W was scored when the baseline was highly irregular and individual breaths were not identifiable.

- NREMS was scored when breathing frequency and amplitude were stable and regular, and baseline was steady.

- REMS was scored when breathing frequency and amplitude were irregular, and baseline was steady.

Large pressure perturbations e.g. due to opening/closing of a door were considered as artefacts.

Fig.11 shows an example of WBP trace compared to gold-standard EEG and EMG signals.

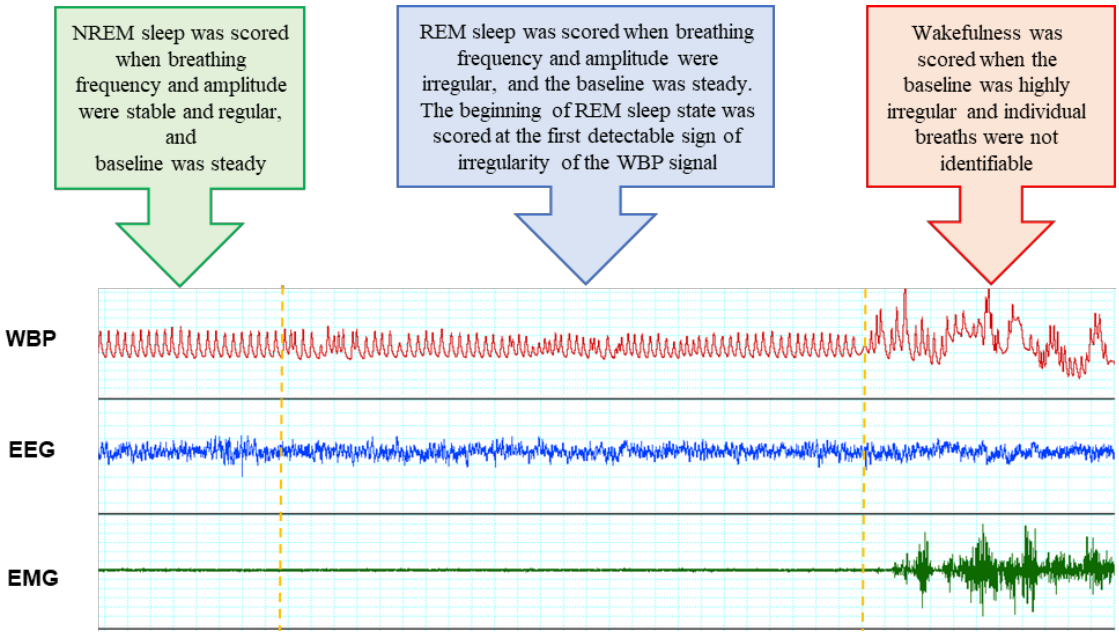

Figure 11. Representative raw tracings of the whole-body plethysmography (WBP) signals during non-rapid-eye-movement (NREM) sleep, rapid-eye-movement (REM) sleep and wakefulness (W).

For comparison, in the figure is also included the relative electroencephalographic (EEG) and electromyographic (EMG) signals, which represent the gold standard for the wake-sleep scoring (*Bastianini et al., 2017)*.

8.4.2 Analysis of breathing pattern

Breath-to-breath values of ventilatory period (VP), tidal volume (Vt), and minute ventilation (V_E) were obtained as previously described in Bastianini et al., 2017. The variability of VP and Vt was analysed with a technique already applied to respiratory physiology (Bastianini et al., 2015; Silvani et al., 2014). The short-term (breath-to-breath) and long-term variability of VP and Vt were calculated based on Poincaré plots, in which the abscissa and ordinate of each point indicate the duration (or amplitude) of the N^{th} and $(N+1)^{th}$ successive breaths, respectively. In this analysis, the short-term variability (s.d.1) of VP and Vt was estimated by standard deviation of VP and Vt values around the axis oriented with the line of identity of the

Poincaré plot, while the standard deviation of VP and Vt values around the orthogonal axis estimated long-term variability (s.d.2). The mean values of VP, Vt, V_E, and the s.d.1 and s.d.2 of VP and Vt were computed for each mouse after exclusion of the breaths with VP and/or Vt that deviated more than 3 standard deviations from the respective mean value in the whole recording (Bastianini et al., 2015). Finally, apneas and augmented breaths (sighs) were automatically detected as breaths with values of VP (apneas) or Vt (sighs) > 3 times the average values of VP or Vt, respectively, for each mouse and sleep state. The accuracy of the detection was checked on raw recordings (Bastianini et al., 2015; Silvani et al., 2014). Because sighs often precede apneas during NREM sleep, the latter have been categorized as post-sigh apneas, if they followed a sigh by ≤ 8 s, or as spontaneous apneas if they followed a sigh by > 8 s (Bastianini et al., 2019).

8.5 Statistical analysis

Statistical analysis was performed with SPSS software (SPSS, Chicago, IL, USA) with repeated measure ANOVAs (two-way, with orexin deficiency (ORX-KO vs WT) and Ta (20°C vs 30°C) as factors, or three-way, with orexin deficiency (ORX-KO vs WT), Ta (20°C vs 30°C), sleep state (NREM vs REM) or s.d.1 vs s.d.2 as factors. Independent t-test was then applied to compare the differences between the two experimental groups, whereas dependent t-test was used to compare the effect of different conditions (i.e. sleep states or Ta) on a variable which was not affected by mouse genotype (thus both experimental groups were considered as a whole). The normality of the data distribution was tested by means of Shapiro-Wilk test. Results are shown as mean ± SEM with significance at $P < 0.05$ (Berteotti et al., 2020).

9 RESULTS

To verify the validity of the ORX-KO mice used in this experiment as a model of orexin deficiency, immunoreactivity for orexin A has been performed on hypothalamic sections. As expected, the ORX-A antiserum produced no staining in the brains of ORX-KO mice, whereas it clearly labelled ORX-A in the orexinergic neurons in WT mice brains (Fig.12).

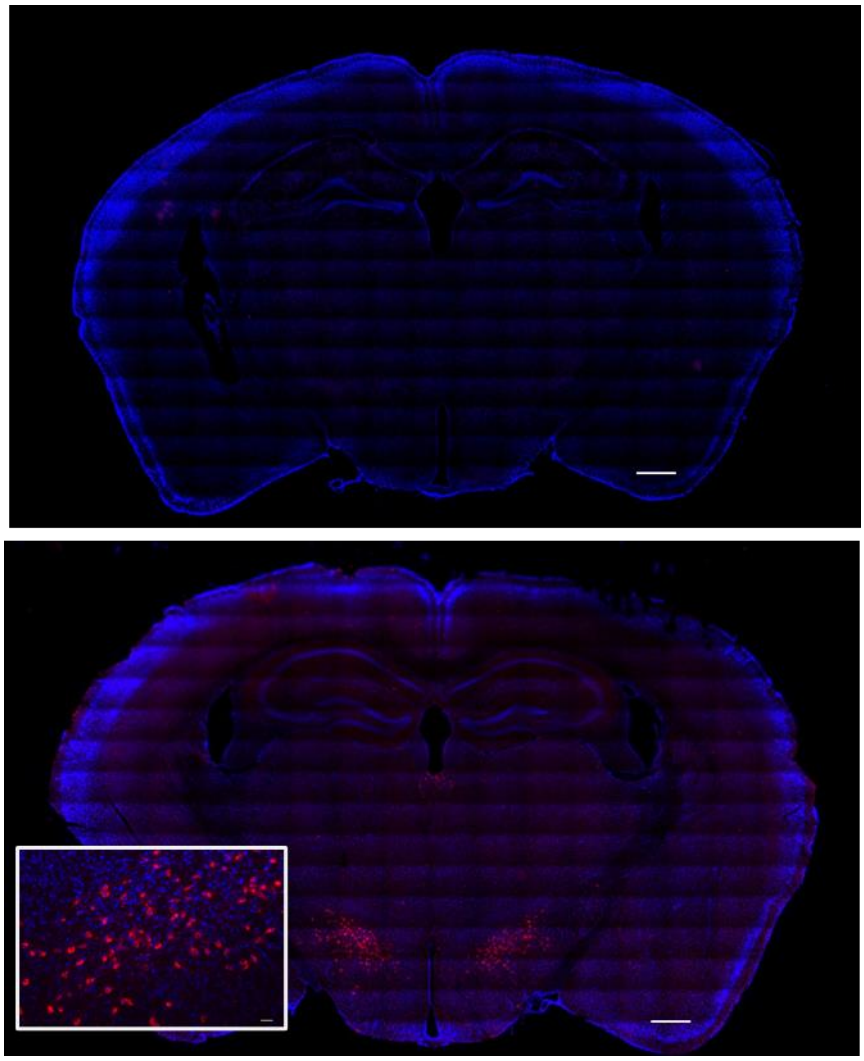

Figure 12. Representative sections of ORX-A immunostaining (red) with Hoechst nuclear counterstaining (blue) in orexin knockout (ORX-KO, top) and control wild-type (WT; bottom, with higher magnification in inset) mice.

Cells with red nucleus are ORX-A+ cells, which lack in ORX-KO mice, and cells with blue nucleus are Hoechst-stained cells. Scale bars, 500 μm (lower magnification) and 50 μm (higher magnification) (Berteotti et al., 2020).

Mice body weight was measured before each recording. The body weight of ORX-KO mice was significantly higher than that of WT mice (34.2±1.2 vs. 30.0± 0.7 g, P=0.012). As expected, sleep architecture was also affected by ORXs deficiency. Indeed, two-way ANOVA revealed that ORX-KO mice showed significant fragmentation of W (i.e. reduced episode duration) (P=0.016) and NREM sleep (P=0.028) episodes, and shorter REM sleep latency (P=0.001) compared with WT mice, irrespective of Ta (for fragmentation of W episodes P=0.991; for fragmentation of NREM sleep episodes P=0.728; for REM sleep latency P=0.0502). The two experimental groups constituted distinct clusters on a scatterplot of reduced REM sleep latency and reduced W episodes mean duration, particularly at Ta=20°C (Fig.13).

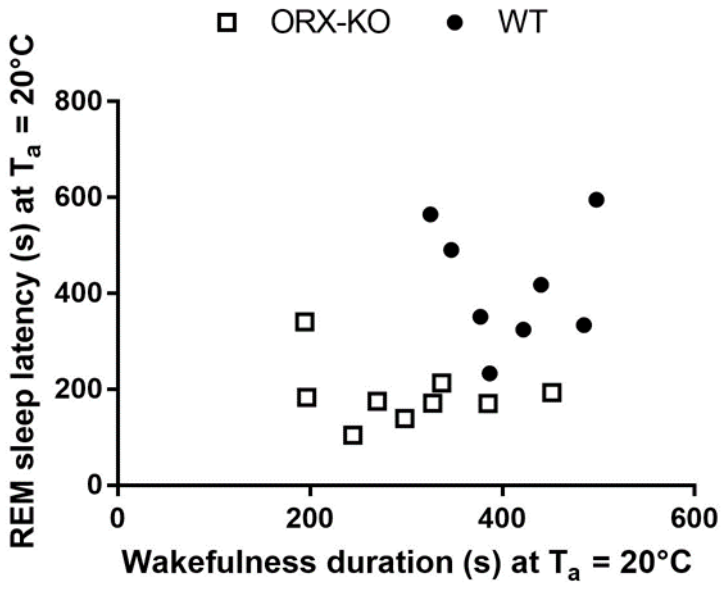

Figure 13. Scatterplot of rapid eye movement (REM) sleep latency and wakefulness (W) episode mean duration at ambient temperature (Ta) of 20°C for each ORX-KO (n=9, white symbols) and WT (n=8, black symbols) mouse under study.

In line with previous results, ORX-KO mice exhibit a significantly shorter REM sleep latency and W episodes' duration and constitute a distinct cluster from that of WT mice (Berteotti et al., 2020).

The percentage of recording time spent in W, NREM or REM sleep did not differ significantly between ORX-KO and WT mice (two-way ANOVA: P=0.746; P=0.641; P=0.561, for W, NREM and REM sleep, respectively), nor it was affected by Ta (P=0.497; P=0.452; P=0.977, for W, NREM and REM sleep, respectively) (Table 2). These results agree with those reported by previous studies on ORX-KO mice (Chemelli et al., 1999; Bastianini et al., 2011),

confirming the validity of the mice used in this experiment as an ORXs deficiency and NT1 model.

		WT		ORX-KO	
State	Measure	Ta 20°C	Ta 30°C	Ta 20°C	Ta 30°C
Wakefulness	% of Recording time	48.4 ± 1.8	54.5 ±3.1	48.9 ± 2.9	51.4 ± 4.6
	Mean episode duration (s)*	410 ± 22	446 ± 6.2	301 ± 28	338 ± 33
NREM sleep	% of Recording time	47.3 ± 1.5	40.8 ± 2.7	47.1 ± 2.7	44.2 ± 4.1
	Mean episode duration (s)*	206 ± 11	220 ± 17	166 ± 10	188 ± 17
REM sleep	% of Recording time	4.1 ± 0.3	4.6 ± 0.6	3.8 ± 0.3	4.3 ± 0.6
	Mean episode duration (s)*	126 ± 8	133 ± 22	100 ± 3	117 ± 11
	Latency (s)*	414 ± 45	390 ± 23	188 ± 22	275 ± 38

Table 2. **Wake-sleep architecture of WT and ORX-KO mice, as a function of Ta.**

Percentage (%) of recording time and mean episode duration of wakefulness, non-rapid eye movement (NREM) sleep and rapid eye movement (REM) sleep of ORX-KO and WT wild-type (WT) mice exposed to different ambient temperature (Ta). REM sleep latency, time from sleep onset to the first epoch of REM sleep. *Main effect of genotype, P<0.05, ANOVA (Berteotti et al., 2020).

The analysis of breathing pattern demonstrated that in both experimental groups, VP and V_E values were strongly and significantly affected by Ta (three-way ANOVA, main effect: for VP, P<0.001; for V_E, P=0.001) (Fig.14); on the contrary, Ta did not exert a significant effect on Vt (ANOVA, main effect: P=0.304). In particular, the values of VP were significantly lower and those of V_E were significantly higher at Ta=20°C than at Ta=30°C, regardless of sleep state and ORX deficiency (Ta × sleep state interaction on VP: P=0.151; Ta × ORX deficiency interaction on VP, P=0.520; Ta ×sleep state interaction on V_E: P=0.075; Ta × ORX deficiency interaction on V_E: P=0.980).

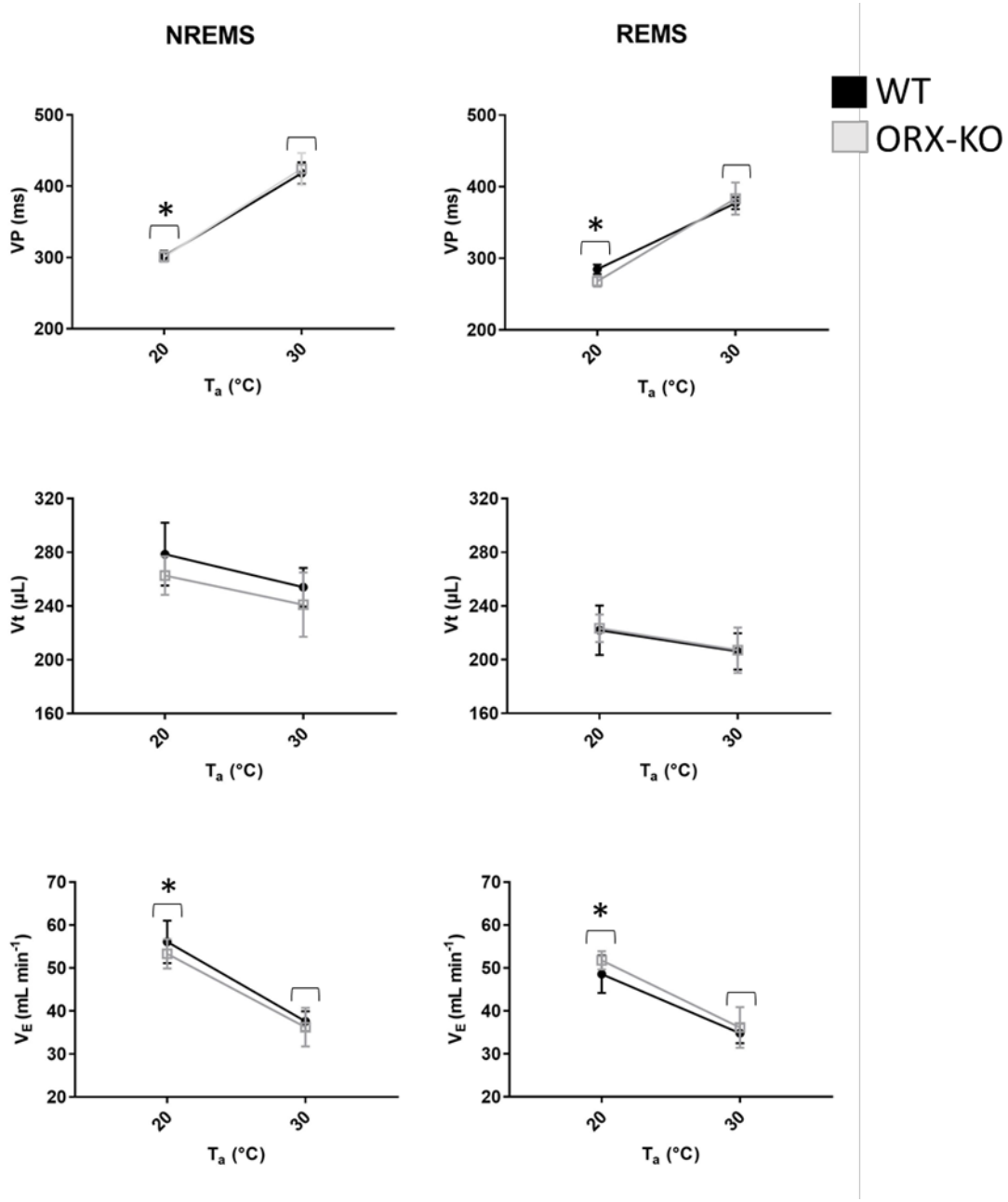

Figure 14. **Respiratory variables in mice exposed to different ambient temperatures (Ta).**

From top to bottom: ventilatory period (VP), tidal volume (Vt), minute ventilation ($V_{E)}$ of orexin knockout (ORX-KO, n=9, grey symbols) and wild-type mice (WT, n=8, black symbols) during non-rapid eye movement (NREM) sleep and rapid eye movement (REM) sleep at different ambient temperature (Ta). *Significant main effect of Ta (P<0.05, ANOVA) (Berteotti et al., 2020).

The sleep apnea occurrence rate was not significantly affected by ORX deficiency, as revealed by three-way ANOVA (P=0.185), but there was a significant interaction between Ta and sleep

state (P=0.040) on this variable. Considering both experimental groups together, dependent t-test confirmed that sleep apnea occurrence rate increased with Ta during NREM sleep but not during REM sleep (P<0.001 and P=0.730, respectively) (Fig.15).

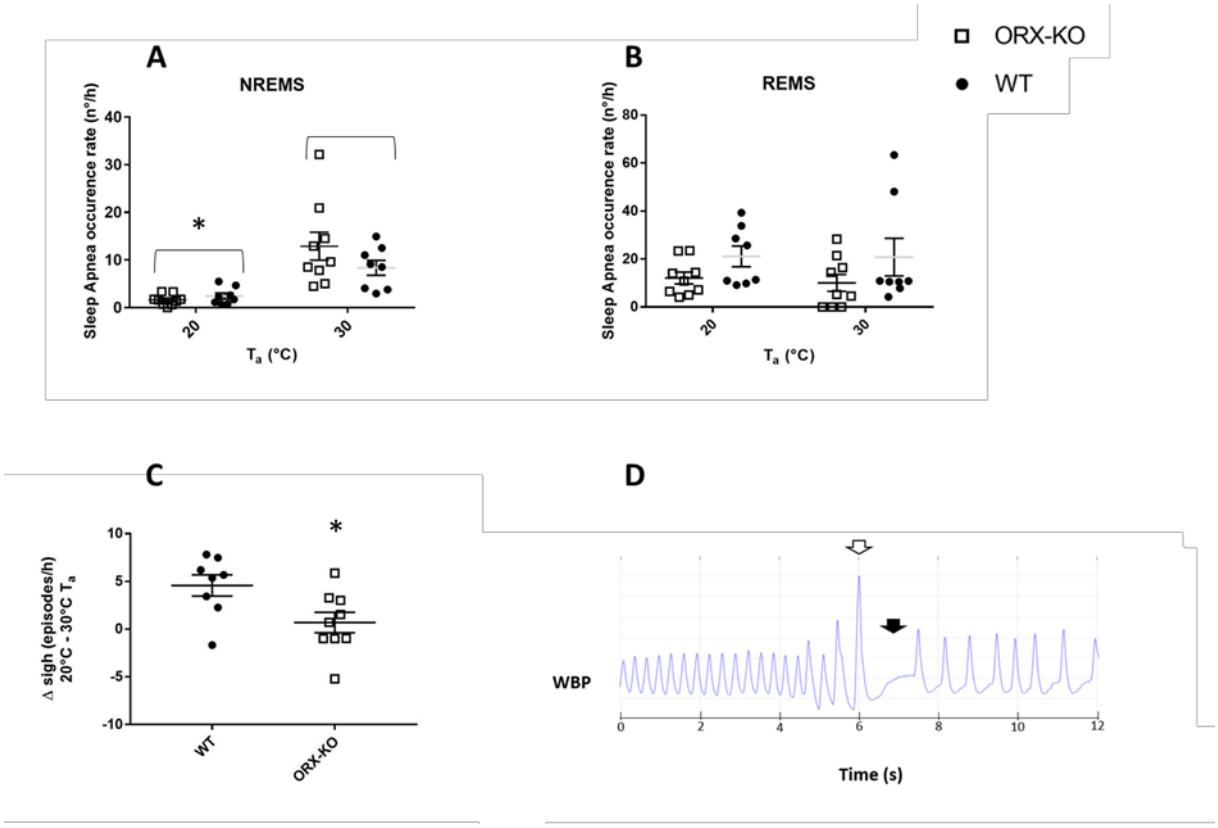

Figure 15. Graphic representation of temperature-dependent regulation of sleep apneas and augmented breaths (Sighs).

(**A,B**) Occurrence rate of sleep apnea during non-rapid eye movement (NREM) sleep and rapid eye movement (REM) sleep in orexin knockout (ORX-KO, n=9, white symbols) and wild-type (WT, n=8, black symbols) mice exposed to different ambient temperatures (Ta); *significant main effect of Ta (P<0.05, ANOVA). (**C**) Difference of sigh occurrence rate between Ta=20°C and Ta=30°C (Δsigh) during NREM sleep in ORX-KO and WT mice; *P<0.05 versus WT, independent t-test. (**D**) Raw tracing of the whole-body plethysmography (WBP) signal during NREM sleep. The black arrow indicates a sleep apnea; the white arrow indicates a sigh (Berteotti et al., 2020).

Further categorization of NREM sleep apneas as post-sigh or spontaneous, based on the temporal distance between the apnea and the preceding sigh (Table 3) indicated that the occurrence rate of both post-sigh and spontaneous sleep apneas significantly increased with Ta (dependent t-test: P<0.001 and P=0.032, respectively).

		WT		ORX-KO	
State	Measure	Ta 20°C	Ta 30°C	Ta 20°C	Ta 30°C
NREM sleep	Post-sigh apneas (episodes/h) *	0.8 ± 0.3	3.8 ± 0.8	0.5 ± 0.3	5.3 ± 1.0
	Spontaneous apneas (episodes/h) *	1.1 ± 0.4	3.3 ± 0.8	0.8 ± 0.2	5.1 ± 2.5

Table 3. **Occurrence rate of post-sigh and spontaneous apneas during non-rapid eye movement (NREM) sleep in WT and ORX-KO mice exposed to different ambient temperature (Ta).**

Sleep apneas were categorized as post-sigh if they followed a sigh by ≤8 s, or as spontaneous if they followed a sigh by >8 s. *Main effect of Ta, P<0.001 for post-sigh apneas; P=0.039 for spontaneous apneas, ANOVA (Berteotti et al., 2020).

In mice, sighs occur almost exclusively during NREM sleep (Bastianini et al., 2019), thus the analysis of their occurrence rate was restricted to this sleep state. Two-way ANOVA revealed a significant interaction between ORX deficiency and Ta on this variable (two-way ANOVA, P=0.024). Sighs were significantly increased at Ta=20°C compared with Ta=30°C in WT mice (12.7±2.3 versus 8.2± 1.8 episodes/h, respectively; paired t-test, P=0.005), whereas no significant difference were showed in ORX-KO mice (7.9±1.2 versus 7.2±0.8 episodes/h, respectively; paired t-test, P=0.539). To better clarify the interaction between ORX deficiency and Ta, the difference between sigh occurrence rate at Ta=20°C and that at Ta=30°C (Δsigh) was calculated for each mouse. Δsigh was positive and was significantly lower in ORX-KO compared with WT mice (independent t-test, P=0.024) (Fig. 15C). Sleep apneas and sighs are extreme events of VP and Vt variability, respectively.

As discussed in *Materials and Methods* section (*c.f. 8.4.2 Analysis of breathing pattern*), the overall variability of VP and Vt was analysed with a technique already used in previous studies (Bastianini et al., 2015; Silvani et al., 2014) that protects the results from the effects of extreme values of breathing variables. Three-way ANOVA showed a significant main effect of Ta on VP variability (P<0.001), but it did not reveal any significant effect of ORX deficiency (P=0.968). In particular, considering both the experimental group together, the short-term

(breath-to-breath, s.d.1) and the long-term (s.d.2) variability of VP were significantly lower at Ta=20°C than at Ta=30°C both in NREM sleep (dependent t-test, P<0.001 for s.d.1 and P<0.001 for s.d.2) and in REM sleep (dependent t-test, P<0.001 for s.d.1 and P<0.001 for s.d.2) (Fig. 16).

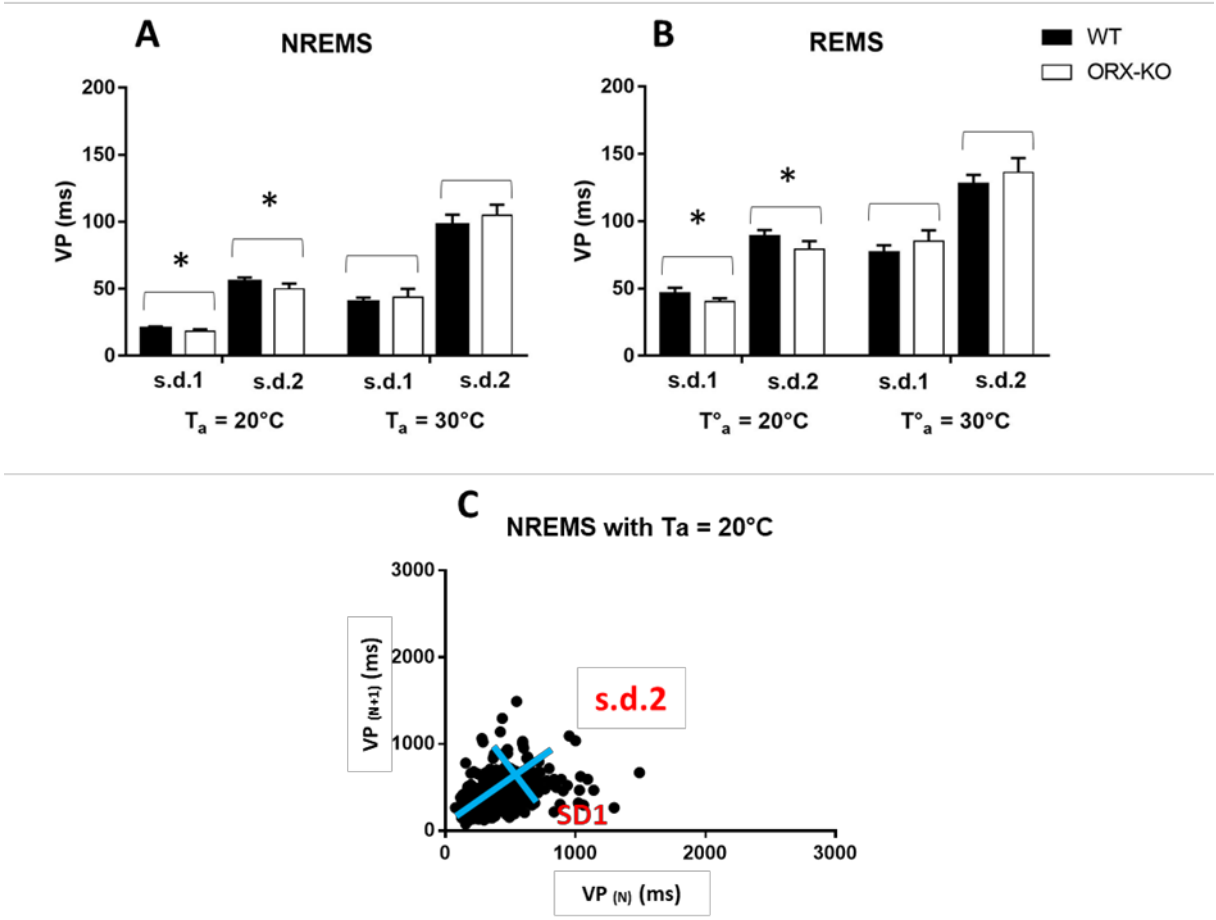

Figure 16. **Variability of ventilatory period (VP) during sleep.**

(**A,B**) Values (means ± SEM.) of indexes of the short-term (s.d.1) and long-term (s.d.2) variability of VP, which quantify variability along the axes highlighted graphically in panel **C**, for non-rapid eye movements (NREM) sleep and rapid eye movement (REM) sleep, respectively. WT, n=8; ORX-KO, n=9. *Significant main effect of Ta (P<0.05, ANOVA). (**C**) Representative Poincaré plots of VP of each breath (N) versus the following breath (N+1) during NREM sleep in a representative orexin knockout (ORX-KO) mouse recorded at ambient temperature (Ta) of 20°C (Berteotti et al., 2020).

Three-way ANOVA of Vt variability did not show significant main effects of Ta (P=0.085) and ORX deficiency (P=0.738), whereas it reveals a significant Ta × Vt variability interaction (P=0.005). In particular, the s.d.2 of VT was significantly lower at Ta=20°C than at Ta=30°C in NREM sleep (dependent t-test, P=0.003) (Fig. 17).

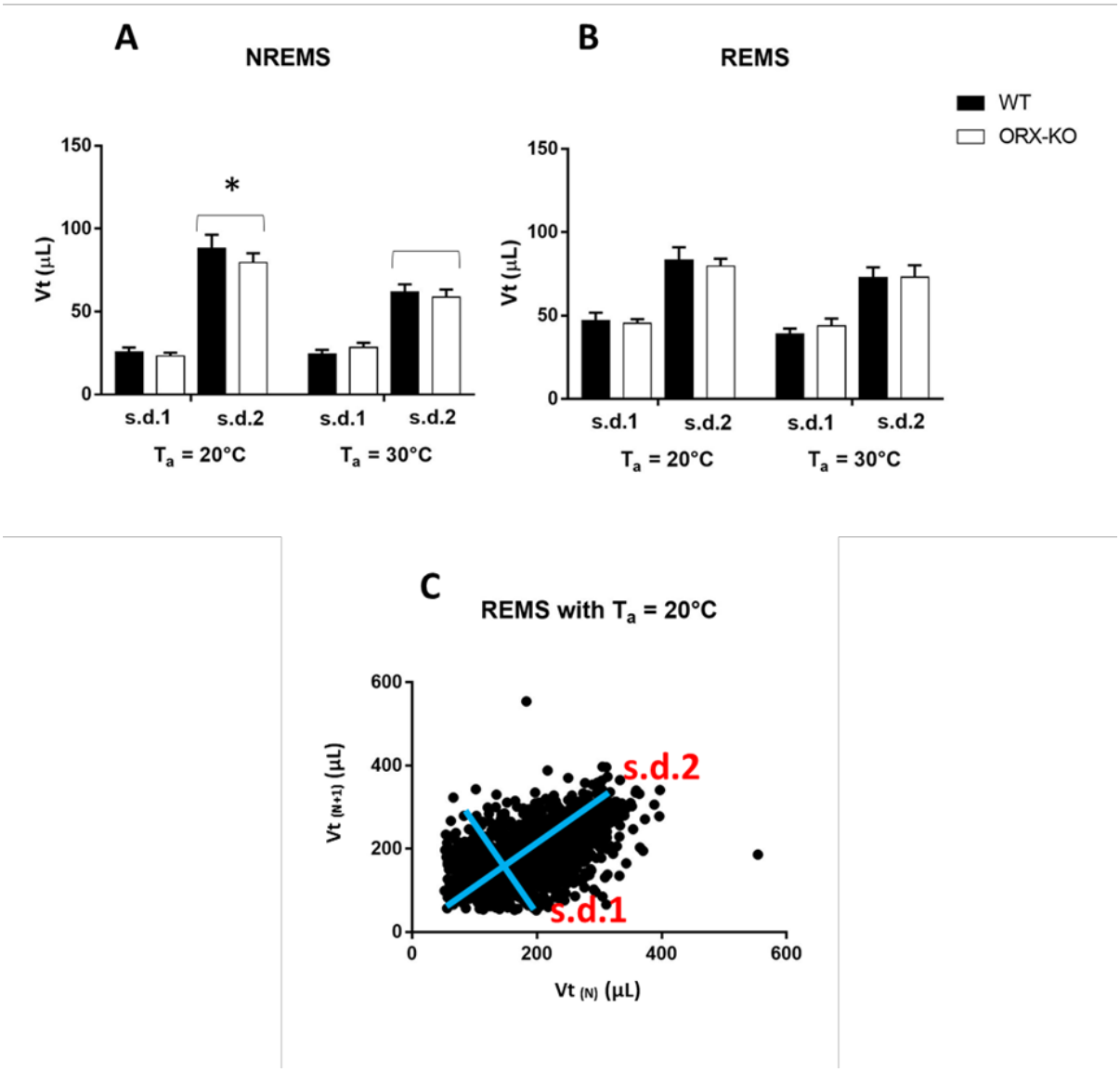

Figure 17. **Variability of tidal volume (Vt) during sleep.**

(**A, B**) Values (means ± SEM) of indexes of the short-term (s.d.1) and long-term (s.d.2) variability of Vt, which quantify variability along the axes highlighted in panel C, for non-rapid eye movement (NREM) sleep and rapid eye movement (REM) sleep, respectively. WT, n=8; ORX-KO, n=9. *Significant main effect of Ta ($P<0.05$, ANOVA). (**C**) Representative Poincaré plots of Vt of each breath (N) versus the following breath (N+1) during REM sleep in a representative orexin knockout (ORX-KO) mouse recorded at ambient temperature (Ta) of 20°C (Berteotti et al., 2020).

10 DISCUSSION

The first aim of this experiment was to investigate the role of ORXs in the respiratory regulation during sleep, as a function of Ta. The results do not support a significant role of these neuropeptides in the temperature-dependent breathing modulation during sleep, with one significant exception, represented by sighs occurrence during NREM sleep. Indeed, the difference between the sigh occurrence rate at Ta=20°C and that at Ta=30°C was significantly lower in ORX-KO mice than in WT mice during NREM sleep (Fig. 15).

Although the mechanisms responsible for the extreme respiratory events (i.e. apneas and sighs) are not completely understood yet, it has been hypothesized that sighs may be the result of an increased inspiratory reflex that can be caused either by stimulation of peripheral chemoreceptors in response to hypoxia or hypercapnia or by the activation of chest wall and pulmonary receptors in response to reduced lung compliance (Qureshi et al., 2009).

Studies performed on ORX-KO mice by Nakamura and colleagues showed that ORXs contribute to central chemoreflex sensitivity only during wakefulness, particularly in the active period, which corresponds to dark period in rodents (Nakamura et al., 2007). However, this is unlikely to explain the findings concerning sigh occurrence rate during sleep in the light (rest) period, thus suggesting that ORXs could be also involved in the integration of afferent signals from chest wall receptors.

The second aim of the experiment was to verify whether the increase in sleep apnea occurrence rate that is reported in ORX-KO mice (Nakamura et al., 2007) depended on the exposure to different Ta. This experiment showed for the first time that the occurrence rate of sleep apneas critically depends on Ta, irrespective of ORX deficiency. In particular, sleep apneas were more frequent at thermoneutrality (Ta=30°C) and reduced by mild cold exposure (Ta=20°C). The conclusion that effects of Ta on breathing do not significantly depend on ORXs is in line with our previous results showing that the effects of Ta on sleep-dependent cardiovascular changes are the same in ORX-AB mice, lacking ORX neurons, and in WT controls (Lo Martire et al., 2012). It is well known that ORX neurons produce and co-release other neurotransmitters, together with ORXs. More experiments are needed to understand whether these co-transmitters play a role in the adaptive breathing responses to different values of Ta. ORX-AB mice exhibited an intolerance to cold exposure (5°C), suggesting that ORX neurons are important in driving the cold defence responses (Takahashi et al., 2013). In particular, in ORX-AB mice but not in ORX-KO mice, abdominal temperature fell rapidly and reached the endpoint of 30°C

within 50–150 min of cold exposure (Takahashi et al., 2013). These data suggest that ORX neurons, rather than ORXs themselves, participate in the homeostatic response to cold exposure. As shown in Table 2, in the present experiment Ta did not modulate the percentage of recording time spent in the different states of the wake–sleep cycle, neither in ORX-KO mice and in WT mice. However, this result is at variance with those of our previous results on ORX-AB and WT mice (Lo Martire et al., 2012), probably due to some differences between these experiments.

First, in this study, the recordings were performed with a non-invasive procedure, on non-instrumented mice with a pure C57BL/6J background, whereas previous data (Lo Martire et al., 2012) were obtained on chronically instrumented mice with a hybrid genetic background (75% C57BL/6J and 25% DBA/2J). Moreover, during this study the plethysmographic recordings were execute inside a WBP chamber only for 8 h during the light (rest) period, while in the previous study mice were recording for 48 h at each of two values of Ta, in freely moving conditions (Lo Martire et al., 2012). Thirdly, in this study mice were not habituated to the new Ta value because Ta changed acutely at the beginning of each recording session in WBP chamber, whereas in the previous study the values of Ta were changed 24 h before each recording session in the home cage (Lo Martire et al., 2012). We found that when ORX-KO and WT mice were exposed to mild cold stress (Ta=20°C), they increased breathing rate and V_E with the respect to the exposure at Ta=30°C (Fig.14). This strategy has already been described in WT mice (Hodges & Richerson, 2008), but only during wakefulness, without taking into account sleep states. Furthermore, no data are currently available regarding the adaptive response to cold exposure in narcoleptic ORX-KO mice lacking ORX peptides.

In this experiment, ORX-KO mice did not show a higher sleep apnea occurrence rate compared with WT controls (Fig. 15; Table 3). Thus, our data are in contrast with those published by Nakamura and colleagues, showing that the occurrence rate of sleep apnea is increased by the loss of ORXs (Nakamura et al., 2007). These contrasting results might be partly explained by the different experimental approach used in our study compared to previous study. Indeed, stress related to chronic instrumentation in previous report (Nakamura et al., 2007), compared with our own experiments using non-instrumented mice, might help to explain differences in sleep apnea occurrence, because this increases with corticosterone levels (Ren et al., 2012).

One interesting result of the present study is that the occurrence rate of sleep apnea during NREM sleep increased in a Ta-dependent manner. Indeed, both post-sigh and spontaneous

sleep apneas (Table 3) were less frequent in conditions of mild cold exposure (Ta=20°C) than at thermoneutrality (Ta=30°C) (Fig.15) and this finding was observed in both the experimental groups (ORX-KO and WT mice), thus suggesting that this phenomenon could be related to a specific interaction between thermoregulatory response and NREM sleep state.

11 CONCLUSION

The studies reported in this thesis explored, for the first time, the integrative role of ORXs in the autonomic control of the cardiovascular functions and in respiratory regulation as a function of ambient temperature (Ta), during different sleep states in mice.

The results obtained in the first experiment suggest that arterial pressure (AP) alterations during sleep in ORX-deficient (ORX-KO) mice result from alterations in sympathetic activity and that these alterations are sufficient to explain the sleep-related AP modification in narcolepsy type 1 (NT1). Despite some limitations (c.f. *8. Discussion*), our results shed light on possible autonomic mechanisms which relate the lack of ORXs with the sleep-dependent AP alterations that potentially contribute to cardiovascular risk in patients with NT1. This finding may be important to identify new druggable targets to rescue the physiological cardiovascular phenotype of narcoleptic patients during sleep.

The second experiment explored the role of ORXs in breathing regulation during sleep states, as a function of Ta, and investigated if the increase in sleep apnea occurrence rate, previously described in NT1 patients and mouse models, was modulated by Ta. The involvement of ORXs in breathing regulation has been little explored and the interaction between respiratory modulation and Ta was described only in WT mice, without considering the wake-sleep state (Hodges et al., 2008; Hodges & Richerson, 2008). Our results show that ORXs are not significantly involved in the Ta-dependent modulation of respiratory regulation during sleep, except for sigh occurrence rate during NREM sleep, that is increased in WT mice. However, we found that the occurrence of sleep apneas during NREM sleep critically depends on Ta, being exacerbated at thermoneutrality (Ta=30°C) and reduced by mild cold exposure (Ta=20°C), but does not depend on ORX transmission. As previously discussed , the selective involvement of ORXs in breathing regulation is compatible with contrasting effects of activation of the two different OXRs on breathing as a function of Ta and does not imply that ORXs have no effect at all on respiratory regulation. To confirm this hypothesis, it would be necessary to perform pharmacological studies targeting separately ORX action on each of the two OXRs (Berteotti et al., 2020) or to perform studies on genetic mouse models that selectively lack one or both receptors (Willie et al., 2003). Moreover, despite the lack of involvement of ORXs in the apneas occurrence rate, the significant interaction between apneas during NREM sleep and Ta is of practical interest, as it highlights the critical importance of controlling for Ta

when phenotyping mice for sleep apneas (Berteotti et al., 2020), as for others biological variables (Lo Martire et al., 2012).

In narcoleptic patients, the prevalence of obstructive sleep apneas (OSAs) ranges from 2% to 68% (Sansa et al., 2010). Moreover, REM-related OSAs are associated with adverse cardiovascular and metabolic events and with a non-dipping pattern (Alzoubaidi & Mokhlesi, 2016). Thus, an important development of our study of respiratory regulation and respiratory disorders during sleep in mouse models of narcolepsy would be represented by the possibility of characterizing sleep apneas by distinguishing them into OSAs or central sleep apneas (CSAs). To this aim, in our laboratory, we recently developed an innovative technique to detect and discriminate CSAs from OSAs, based on the simultaneous recording of EEG, EMG, diaphragmatic activity and ventilation. This new technique will allow us to study the pathophysiological mechanisms underlying OSAs in mouse model of different human diseases characterized by high prevalence of them, such as narcolepsy, and to contribute to the development of new and specific pharmacological therapies.

12 DATA SUPPLEMENT

CRAFTING OF ELECTRODES FOR ELECTROENCEPHALOGRAPHIC (EEG) (Fig. A) AND NUCHAL ELECTROMYOGRAPHIC (EMG) (Fig. B) SIGNALS RECORDING

EEG electrodes were made up of a pair of 1.2 cm stainless-steel wires covered with an insulating sheath (Cooner Wire, Chatsworth, CA, USA) welded to one end to a stainless-steel screw (length 2.4 mm and diameter 1.19 mm, Plastics One 00-96X3/32, Roanoke, VA, USA) and at the other end to a connector equipped with two terminal pins (0.5 cm wide and 0.3 cm high; 701-9925 RS Components, Cinisello Balsamo, Milano).

EMG electrodes consisted in a pair of 4 cm stainless-steel wires coated by an insulating sheath. 2-3 mm of coating was removed from one end and at 1.5cm from this end to allow electrical contact with nuchal muscles during the implantation. Then, this extremity was welded to a connector equipped with two terminal pins.

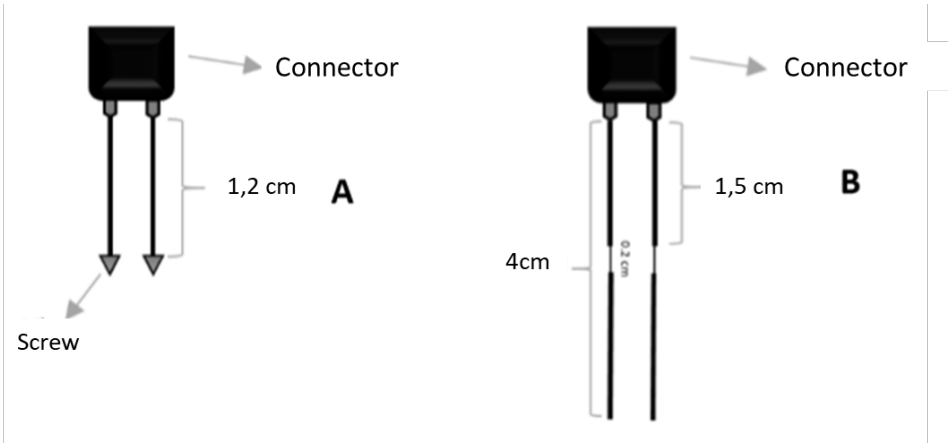

CATHETER FOR INTRAPERITONEAL INFUSIONS

The intraperitoneal catheter allowed continuous infusions of drugs or saline in freely behaving animals. The catheter was crafted using not-sterile medical-grade silicone (Silclear Degania, Defries Industries PTY LTD) and polyethylene (Fine-Bore Polyethylene-Polythene-Tubing; Smiths Medical) tubes. It consisted of three different segments, one inserted in the peritoneal cavity of the animal and two extracorporeal. Each part had specific characteristics.

- IP catheter (Fig C) was the smallest part of all the circuit. It consisted of 7 cm long silicone tube (code L-155, 0.64 x 1.19 mm) inserted in a 1.2 cm long silicone tube, serving as a connector (code L-205, 1.02 x 2.16 mm); all the structure was stabilized using silicone (Transparent Universal Silicone, Saratoga International). After all the segments were connected, one silicone enlargement (**A**) was made 1 cm above the end of L-155 silicone tube to suture, with stiches, the catheter's tip into the peritoneal wall; a second silicone enlargement **(B)** was made 5mm below the junction between L-205 and L-155 in order to clamp this space to keep under pressure a solution inside the catheter, i.e.to weight the IP catheter and to know its internal volume before implantation.

- Intermediate catheter (segment M, Fig D) was a 28 cm long polyethylene tube (code PE50; internal diameter 0.58 mm and external diameter 0.96 mm). One of its ends was connected to the IP catheter by a 22 G blunt needle with length of 1.5 cm; the other end was connected to a 2.5 cm long silicone tube (code L-205) through a silicone junction (0.5 cm). During the infusion, the segment M was connected to the upper catheter (segment P) by this junction, while, during the habituation, this end was closed by means of a piece of polyethylene tube (code PE90; internal diameter 0.86 mm and external diameter 1.52 mm) with a blind bottom. The volume of the intermediate catheter was approximatively 75 µL.

- Upper catheter (segment P, Fig E) was made by a 160 cm long polyethylene tube (PE90) and had a volume of approx. 1,3 ml. One end of the tube was connected to the flexible portion of an intravenous catheter (Delta ven; Delta Med, Medical devices, Viadana – Italy) to allow the connection of the upper catheter with a 1ml syringe, that was placed on an infusion pump. The other end was connected to a L-205 silicone piece to allow the connection with segment M.

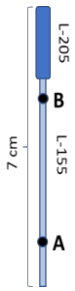

Fig C

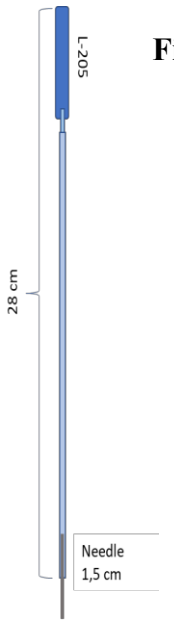

Fig D

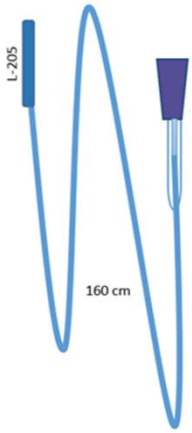

Fig E

13 REFERENCES

Alzoubaidi, M., & Mokhlesi, B. (2016). Obstructive sleep apnea during rapid eye movement sleep: clinical relevance and therapeutic implications. *Current Opinion in Pulmonary Medicine*, *22*(6), 545–554. https://doi.org/10.1097/MCP.0000000000000319

Amici, R., Bastianini, S., Berteotti, C., Cerri, M., Del Vecchio, F., Lo Martire, V., Luppi, M., Perez, E., Silvani, A., Zamboni, G., & Zoccoli, G. (2014). Sleep and bodily functions: The physiological interplay between body homeostasis and sleep homeostasis. *Archives Italiennes de Biologie*, *152*(2–3), 66–78. https://doi.org/10.12871/000298292014232

Amici, R., Cerri, M., & Parmeggiani, P. L. (2013). Overview of Physiological Processes During Sleep. *Encyclopedia of Sleep*, 385–389. https://doi.org/10.1016/B978-0-12-378610-4.00086-3

Arrigoni, E., Chee, M. J. S., & Fuller, P. M. (2019). To eat or to sleep: That is a lateral hypothalamic question. *Neuropharmacology*, *154*(November 2018), 34–49. https://doi.org/10.1016/j.neuropharm.2018.11.017

Baccelli, G., Albertini, R., Mancia, G., & Zanchetti, A. (1978). Control of regional circulations by the sino-aortic reflexes during desynchronised sleep in the cat. *Cardiovascular Research*, *12*(9), 523–528. https://doi.org/10.1093/cvr/12.9.523

Bastianini, S., Alvente, S., Berteotti, C., Bosi, M., Lo Martire, V., Silvani, A., Valli, A., & Zoccoli, G. (2019). Post-sigh sleep apneas in mice: Systematic review and data-driven definition. *Journal of Sleep Research*, e12845. https://doi.org/10.1111/jsr.12845

Bastianini, S., Alvente, S., Berteotti, C., Lo Martire, V., Silvani, A., Swoap, S. J., Valli, A., Zoccoli, G., & Cohen, G. (2017). Accurate discrimination of the wake-sleep states of mice using non-invasive whole-body plethysmography. *Scientific Reports*, *7*(August 2016), 1–10. https://doi.org/10.1038/srep41698

Bastianini, S., Berteotti, C., Gabrielli, A., Del Vecchio, F., Amici, R., Alexandre, C., Scammell, T. E., Gazea, M., Kimura, M., Lo Martire, V., Silvani, A., & Zoccoli, G. (2014). SCOPRISM: A new algorithm for automatic sleep scoring in mice. *Journal of Neuroscience Methods*, *235*, 277–284. https://doi.org/10.1016/j.jneumeth.2014.07.018

Bastianini, S., Silvani, A., Berteotti, C., Elghozi, J. L., Franzini, C., Lenzi, P., Lo Martire, V.,

& Zoccoli, G. (2011). Sleep related changes in blood pressure in hypocretin-deficient narcoleptic mice. *Sleep*, *34*(2), 213–218. https://doi.org/10.1093/sleep/34.2.213

Bastianini, S., Silvani, A., Berteotti, C., Lo Martire, V., Cohen, G., Ohtsu, H., Lin, J.-S., & Zoccoli, G. (2015). Histamine Transmission Modulates the Phenotype of Murine Narcolepsy Caused by Orexin Neuron Deficiency. *PloS One*, *10*(10), e0140520. https://doi.org/10.1371/journal.pone.0140520

Bastianini, S., Silvani, A., Berteotti, C., Lo Martire, V., & Zoccoli, G. (2012). High-amplitude theta wave bursts during REM sleep and cataplexy in hypocretin-deficient narcoleptic mice. *Journal of Sleep Research*, *21*(2), 185–188. https://doi.org/10.1111/j.1365-2869.2011.00945.x

Baudrie, V., Laude, D., & Elghozi, J. L. (2007). Optimal frequency ranges for extracting information on cardiovascular autonomic control from the blood pressure and pulse interval spectrograms in mice. *American Journal of Physiology - Regulatory Integrative and Comparative Physiology*, *292*(2), 904–912. https://doi.org/10.1152/ajpregu.00488.2006

Baust, W., & Bohnert, B. (1969). The regulation of heart rate during sleep. *Experimental Brain Research*, *7*(2), 169–180. https://doi.org/10.1007/BF00235442

Benarroch, E. E. (2019). Autonomic Neuroscience : Basic and Clinical Control of the cardiovascular and respiratory systems during sleep. *Autonomic Neuroscience: Basic and Clinical*, *218*(January), 54–63. https://doi.org/10.1016/j.autneu.2019.01.007

Berteotti, C., Lo Martire, V., Alvente, S., Bastianini, S., Matteoli, G., Silvani, A., & Zoccoli, G. (2020). Effect of ambient temperature on sleep breathing phenotype in mice: the role of orexins. *The Journal of Experimental Biology*. https://doi.org/10.1242/jeb.219485

Berteotti, C., & Silvani, A. (2018). The link between narcolepsy and autonomic cardiovascular dysfunction: a translational perspective. In *Clinical Autonomic Research* (Vol. 28, Issue 6, pp. 545–555). https://doi.org/10.1007/s10286-017-0473-z

Beuckmann, C. T., Sinton, C. M., Williams, S. C., Richardson, J. A., Hammer, R. E., Sakurai, T., & Yanagisawa, M. (2004). Expression of a poly-glutamine-ataxin-3 transgene in orexin neurons induces narcolepsy-cataplexy in the rat. *The Journal of Neuroscience : The Official Journal of the Society for Neuroscience*, *24*(18), 4469–4477.

https://doi.org/10.1523/JNEUROSCI.5560-03.2004

Birkenhäger, A. M., & van den Meiracker, A. H. (2007). Causes and consequences of a non-dipping blood pressure profile. *The Netherlands Journal of Medicine*, *65*(4), 127–131.

Black, S. W., Sun, J. D., Santiago, P., Laihsu, A., Kimura, N., Yamanaka, A., Bersot, R., & Humphries, P. S. (2018). Partial ablation of the orexin field induces a sub-narcoleptic phenotype in a conditional mouse model of orexin neurodegeneration. *Sleep*, *41*(9). https://doi.org/10.1093/sleep/zsy116

Bristow, J. D., Honour, A. J., Pickering, T. G., & Sleight, P. (1969). Cardiovascular and respiratory changes during sleep in normal and hypertensive subjects. *Cardiovascular Research*, *3*(4), 476–485. https://doi.org/10.1093/cvr/3.4.476

Burdakov, D., Gerasimenko, O., & Verkhratsky, A. (2005). Physiological changes in glucose differentially modulate the excitability of hypothalamic melanin-concentrating hormone and orexin neurons in situ. *Journal of Neuroscience*, *25*(9), 2429–2433. https://doi.org/10.1523/JNEUROSCI.4925-04.2005

Campbell, M., & Jialal, I. (2020). *Physiology, Endocrine Hormones.*

Campen, M. J., Tagaito, Y., Jenkins, T. P., Smith, P. L., Schwartz, A. R., & O'Donnell, C. P. (2002). Phenotypic differences in the hemodynamic response during REM sleep in six strains of inbred mice. *Physiological Genomics*, *11*(3), 227–234. https://doi.org/10.1152/physiolgenomics.00031.2002

Carrington, M. J., Barbieri, R., Colrain, I. M., Crowley, K. E., Kim, Y., & Trinder, J. (2005). Changes in cardiovascular function during the sleep onset period in young adults. *Journal of Applied Physiology (Bethesda, Md. : 1985)*, *98*(2), 468–476. https://doi.org/10.1152/japplphysiol.00702.2004

Cerri, M., & Morrison, S. F. (2005). Activation of lateral hypothalamic neurons stimulates brown adipose tissue thermogenesis. *Neuroscience*, *135*(2), 627–638. https://doi.org/10.1016/j.neuroscience.2005.06.039

Chemelli, R. M., Willie, J. T., Sinton, C. M., Elmquist, J. K., Scammell, T., Lee, C., Richardson, J. A., Clay Williams, S., Xiong, Y., Kisanuki, Y., Fitch, T. E., Nakazato, M., Hammer, R. E., Saper, C. B., & Yanagisawa, M. (1999). Narcolepsy in orexin knockout mice: Molecular genetics of sleep regulation. *Cell*, *98*(4), 437–451.

https://doi.org/10.1016/S0092-8674(00)81973-X

Chen, C. T., Hwang, L. L., Chang, J. K., & Dun, N. J. (2000). Pressor effects of orexins injected intracisternally and to rostral ventrolateral medulla of anesthetized rats. *American Journal of Physiology - Regulatory Integrative and Comparative Physiology*, *278*(3 47-3), 692–697. https://doi.org/10.1152/ajpregu.2000.278.3.r692

Chokroverty, S. (1986). Sleep apnea in narcolepsy. *Sleep*, *9*(1 Pt 2), 250–253. https://doi.org/10.1093/sleep/9.1.250

Chou, T. C., Bjorkum, A. A., Gaus, S. E., Lu, J., Scammell, T. E., & Saper, C. B. (2002). Afferents to the ventrolateral preoptic nucleus. *Journal of Neuroscience*, *22*(3), 977–990. https://doi.org/10.1523/jneurosci.22-03-00977.2002

Cianci, T., Zoccoli, G., Lenzi, P., & Franzini, C. (1991). Loss of integrative control of peripheral circulation during desynchronized sleep. *The American Journal of Physiology*, *261*(2 Pt 2), R373-7. https://doi.org/10.1152/ajpregu.1991.261.2.R373

Ciriello, J., Li, Z., & De Oliveira, C. V. R. (2003). Cardioacceleratory responses to hypocretin-1 injections into rostral ventromedial medulla. *Brain Research*, *991*(1–2), 84–95. https://doi.org/10.1016/j.brainres.2003.08.008

Dampney, R. A. (1994). Functional organization of central pathways regulating the cardiovascular system. *Physiological Reviews*, *74*(2), 323–364. https://doi.org/10.1152/physrev.1994.74.2.323

Dampney, R. A. L. (2017). Resetting of the Baroreflex Control of Sympathetic Vasomotor Activity during Natural Behaviors: Description and Conceptual Model of Central Mechanisms. *Frontiers in Neuroscience*, *11*, 461. https://doi.org/10.3389/fnins.2017.00461

Dauvilliers, Y., Arnulf, I., & Mignot, E. (2007a). Narcolepsy with cataplexy. *Lancet (London, England)*, *369*(9560), 499–511. https://doi.org/10.1016/S0140-6736(07)60237-2

Dauvilliers, Y., Arnulf, I., & Mignot, E. (2007b). Narcolepsy with cataplexy. In *Lancet* (Vol. 369, Issue 9560, pp. 499–511). https://doi.org/10.1016/S0140-6736(07)60237-2

De Lecea, L., Kilduff, T. S., Peyron, C., Gao, X. B., Foye, P. E., Danielson, P. E., Fukuhara, C., Battenberg, E. L. F., Gautvik, V. T., Bartlett, F. S., Frankel, W. N., Van Den Pol, A.

N., Bloom, F. E., Gautvik, K. M., & Sutcliffe, J. G. (1998). The hypocretins: Hypothalamus-specific peptides with neuroexcitatory activity. *Proceedings of the National Academy of Sciences of the United States of America*, *95*(1), 322–327. https://doi.org/10.1073/pnas.95.1.322

De Oliveira, C. V. R., Rosas-Arellano, M. P., Solano-Flores, L. P., & Ciriello, J. (2003). Cardiovascular effects of hypocretin-1 in nucleus of the solitary tract. *American Journal of Physiology - Heart and Circulatory Physiology*, *284*(4 53-4), 1369–1377. https://doi.org/10.1152/ajpheart.00877.2002

Deng, B. S., Nakamura, A., Zhang, W., Yanagisawa, M., Fukuda, Y., & Kuwaki, T. (2007). Contribution of orexin in hypercapnic chemoreflex: Evidence from genetic and pharmacological disruption and supplementation studies in mice. *Journal of Applied Physiology*, *103*(5), 1772–1779. https://doi.org/10.1152/japplphysiol.00075.2007

Donadio, V., Liguori, R., Vandi, S., Giannoccaro, M. P., Pizza, F., Leta, V., & Plazzi, G. (2014). Sympathetic and cardiovascular changes during sleep in narcolepsy with cataplexy patients. *Sleep Medicine*, *15*(3), 315–321. https://doi.org/10.1016/j.sleep.2013.12.005

Douglas, N J, White, D. P., Weil, J. V, Pickett, C. K., Martin, R. J., Hudgel, D. W., & Zwillich, C. W. (1982). Hypoxic ventilatory response decreases during sleep in normal men. *The American Review of Respiratory Disease*, *125*(3), 286–289. https://doi.org/10.1164/arrd.1982.125.3.286

Douglas, N J, White, D. P., Weil, J. V, Pickett, C. K., & Zwillich, C. W. (1982). Hypercapnic ventilatory response in sleeping adults. *The American Review of Respiratory Disease*, *126*(5), 758–762. https://doi.org/10.1164/arrd.1982.126.5.758

Douglas, Neil J. (2010). Respiratory Physiology: Understanding the Control of Ventilation. In *Principles and Practice of Sleep Medicine: Fifth Edition* (Sixth Edit). Elsevier Inc. https://doi.org/10.1016/B978-1-4160-6645-3.00022-0

Dube, M. G., Horvath, T. L., Kalra, P. S., & Kalra, S. P. (2000). Evidence of NPY Y5 receptor involvement in food intake elicited by orexin A in sated rats. *Peptides*, *21*(10), 1557–1560. https://doi.org/10.1016/s0196-9781(00)00311-9

Fewell, J. E. (1993). Influence of sleep on systemic and coronary hemodynamics in lambs. *Journal of Developmental Physiology*, *19*(2), 71–76.

Funato, H., Tsai, A. L., Willie, J. T., Kisanuki, Y., Williams, S. C., Sakurai, T., & Yanagisawa, M. (2009). Enhanced orexin receptor-2 signaling prevents diet-induced obesity and improves leptin sensitivity. *Cell Metabolism*, *9*(1), 64–76. https://doi.org/10.1016/j.cmet.2008.10.010

Futuro-Neto, H. A., & Coote, J. H. (1982). Changes in sympathetic activity to heart and blood vessels during desynchronized sleep. *Brain Research*, *252*(2), 259–268. https://doi.org/10.1016/0006-8993(82)90393-6

Ganeshan, K., & Chawla, A. (2017). Warming the mouse to model human diseases. In *Nature Reviews Endocrinology* (Vol. 13, Issue 8, pp. 458–465). Nature Publishing Group. https://doi.org/10.1038/nrendo.2017.48

Ghule, A., Rácz, I., Bilkei-Gorzo, A., Leidmaa, E., Sieburg, M., & Zimmer, A. (2020). Modulation of feeding behavior and metabolism by dynorphin. *Scientific Reports*, *10*(1), 1–13. https://doi.org/10.1038/s41598-020-60518-0

Goforth, P. B., Leinninger, G. M., Patterson, C. M., Satin, L. S., & Myers, M. G. J. (2014). Leptin acts via lateral hypothalamic area neurotensin neurons to inhibit orexin neurons by multiple GABA-independent mechanisms. *The Journal of Neuroscience : The Official Journal of the Society for Neuroscience*, *34*(34), 11405–11415. https://doi.org/10.1523/JNEUROSCI.5167-13.2014

Gould, G. A., Gugger, M., Molloy, J., Tsara, V., Shapiro, C. M., & Douglas, N. J. (1988). Breathing pattern and eye movement density during REM sleep in humans. *The American Review of Respiratory Disease*, *138*(4), 874–877. https://doi.org/10.1164/ajrccm/138.4.874

Grimaldi, D., Calandra-Buonaura, G., Provini, F., Agati, P., Pierangeli, G., Franceschini, C., Barletta, G., Plazzi, G., Montagna, P., & Cortelli, P. (2012). Abnormal Sleep-Cardiovascular System Interaction in Narcolepsy with Cataplexy: Effects of Hypocretin Deficiency in Humans. *Sleep*, *35*(4), 519–528. https://doi.org/10.5665/sleep.1738

Grimaldi, D., Pierangeli, G., Barletta, G., Terlizzi, R., Plazzi, G., Cevoli, S., Franceschini, C., Montagna, P., & Cortelli, P. (2010). Spectral analysis of heart rate variability reveals an enhanced sympathetic activity in narcolepsy with cataplexy. *Clinical Neurophysiology*, *121*(7), 1142–1147. https://doi.org/10.1016/j.clinph.2010.01.028

Gross, V., Tank, J., Obst, M., Plehm, R., Blumer, K. J., Diedrich, A., Jordan, J., & Luft, F. C. (2005). Autonomic nervous system and blood pressure regulation in RGS2-deficient mice. *American Journal of Physiology - Regulatory Integrative and Comparative Physiology*, *288*(5 57-5), 1134–1142. https://doi.org/10.1152/ajpregu.00246.2004

Guyenet, P. G. (2006). The sympathetic control of blood pressure. *Nature Reviews. Neuroscience*, *7*(5), 335–346. https://doi.org/10.1038/nrn1902

Hakansson, M.-L.-, Lecea, L. De, Sutcliffe, J. G., Yanagisawa, M., & Meister, B. (1999). Leptin Receptor- and STAT3-Immunoreactivities in Hypocretin / Orexin Neurones of the Lateral Hypothalamus 1. *Journal of Neuroendocrinology*, *11*, 653–663.

Han, F., Mignot, E., Wei, Y. C., Dong, S. X., Li, J., Lin, L., An, P., Wang, L. H., Wang, J. S., He, M. Z., Gao, H. Y., Li, M., Gao, Z. C., & Strohl, K. P. (2010). Ventilatory chemoresponsiveness, narcolepsy-cataplexy and human leukocyte antigen DQB1*0602 status. *European Respiratory Journal*, *36*(3), 577–583. https://doi.org/10.1183/09031936.00174609

Han, Fang. (2012). Respiratory regulation in narcolepsy. *Sleep & Breathing*, *16*(1), 241–245. https://doi.org/10.1007/s11325-011-0489-x

Hara, J., Beuckmann, C. T., Nambu, T., Willie, J. T., Chemelli, R. M., Sinton, C. M., Sugiyama, F., Yagami, K., Goto, K., Yanagisawa, M., & Sakurai, T. (2001). Genetic ablation of orexin neurons in mice results in narcolepsy, hypophagia, and obesity. *Neuron*, *30*(2), 345–354. http://www.ncbi.nlm.nih.gov/pubmed/11394998

Hirano, A., Hsu, P.-K., Zhang, L., Xing, L., McMahon, T., Yamazaki, M., Ptáček, L. J., & Fu, Y.-H. (2018). DEC2 modulates orexin expression and regulates sleep. *Proceedings of the National Academy of Sciences of the United States of America*, *115*(13), 3434–3439. https://doi.org/10.1073/pnas.1801693115

Hodges, M. R., & Richerson, G. B. (2008). Interaction between defects in ventilatory and thermoregulatory control in mice lacking 5-HT neurons. *Respir Physiol Neurobiol*, *164*(3), 350–357. https://doi.org/10.1016/j.resp.2008.08.003

Hodges, M. R., Tattersall, G. J., Harris, M. B., McEvoy, S. D., Richerson, D. N., Deneris, E. S., Johnson, R. L., Chen, Z. F., & Richerson, G. B. (2008). Defects in breathing and thermoregulation in mice with near-complete absence of central serotonin neurons. *J*

Neurosci, *28*(10), 2495–2505. https://doi.org/10.1523/JNEUROSCI.4729-07.2008

Hoshino, T., Sasanabe, R., Mano, M., Nomura, A., Kato, C., Sato, M., Imai, M., Murotani, K., Guilleminault, C., & Shiomi, T. (2019). Prevalence of Rapid Eye Movement-related Obstructive Sleep Apnea in Adult Narcolepsy. *Internal Medicine*, 2601–2618. https://doi.org/10.2169/internalmedicine.2601-18

Hublin, C., Matikainen, E., & Partinen, M. (1994). Autonomic nervous system function in narcolepsy. *Journal of Sleep Research*, *3*(3), 131–137. https://doi.org/10.1111/j.1365-2869.1994.tb00119.x

Iellamo, F., Placidi, F., Marciani, M. G., Romigi, A., Tombini, M., Aquilani, S., Massaro, M., Galante, A., & Legramante, J. M. (2004). Baroreflex buffering of sympathetic activation during sleep: evidence from autonomic assessment of sleep macroarchitecture and microarchitecture. *Hypertension (Dallas, Tex. : 1979)*, *43*(4), 814–819. https://doi.org/10.1161/01.HYP.0000121364.74439.6a

Ishii, Y., Blundell, J. E., Halford, J. C. G., Upton, N., Porter, R., Johns, A., & Rodgers, R. J. (2005). Satiety enhancement by selective orexin-1 receptor antagonist SB-334867 : influence of test context and profile comparison with CCK-8S. *Behavioural Brain Research*, *160*, 11–24. https://doi.org/10.1016/j.bbr.2004.11.011

Jhaveri, K. A., Trammell, R. A., & Toth, L. A. (2007). Effect of environmental temperature on sleep, locomotor activity, core body temperature and immune responses of C57BL/6J mice. *Brain, Behavior, and Immunity*, *21*(7), 975–987. https://doi.org/10.1016/j.bbi.2007.03.007

Kannan, H., Hayashida, Y., & Yamashita, H. (1989). Increase in sympathetic outflow by paraventricular nucleus stimulation in awake rats. *The American Journal of Physiology*, *256*(6 Pt 2), R1325-30. https://doi.org/10.1152/ajpregu.1989.256.6.R1325

Karacan, I., Thornby, J. I., Anch, A. M., Williams, R. L., & Perkins, H. M. (1978). Effects of high ambient temperature on sleep in young men. *Aviation, Space, and Environmental Medicine*, *49*(7), 855–860.

Kayaba, Y., Nakamura, A., Kasuya, Y., Ohuchi, T., Yanagisawa, M., Komuro, I., Fukuda, Y., & Kuwaki, T. (2003). Attenuated defense response and low basal blood pressure in orexin knockout mice. *American Journal of Physiology - Regulatory Integrative and*

Comparative Physiology, *285*(3 54-3), 1–8. https://doi.org/10.1152/ajpregu.00671.2002

Koeppen, B. M., Stanton, B. A., Berne, R., & Levy, M. N. (2010). Il sistema cardiovascolare. In *Fisiologia di Berne & Levy* (VI). Casa Editrice Ambrosiana.

Kuwaki, T. (2008). Orexinergic modulation of breathing across vigilance states. *Respiratory Physiology and Neurobiology*, *164*(1–2), 204–212. https://doi.org/10.1016/j.resp.2008.03.011

Kuwaki, T. (2015). Thermoregulation under pressure: a role for orexin neurons. *Temperature*, *2*(3), 379–391. https://doi.org/10.1080/23328940.2015.1066921

Latorre, D., Kallweit, U., Armentani, E., Foglierini, M., Mele, F., Cassotta, A., Jovic, S., Jarrossay, D., Mathis, J., Zellini, F., Becher, B., Lanzavecchia, A., Khatami, R., Manconi, M., Tafti, M., Bassetti, C. L., & Sallusto, F. (2018). T cells in patients with narcolepsy target self-antigens of hypocretin neurons. *Nature*, *562*(7725), 63–68. https://doi.org/10.1038/s41586-018-0540-1

Laude, D., Baudrie, V., & Elghozi, J. L. (2008). Applicability of recent methods used to estimate spontaneous baroreflex sensitivity to resting mice. *American Journal of Physiology - Regulatory Integrative and Comparative Physiology*, *294*(1), 142–150. https://doi.org/10.1152/ajpregu.00319.2007

Lee, M. G., Hassani, O. K., & Jones, B. E. (2005). Discharge of Identified Orexin/Hypocretin Neurons across the Sleep-Waking Cycle. *Journal of Neuroscience*, *25*(28), 6716–6720. https://doi.org/10.1523/JNEUROSCI.1887-05.2005

Li, A., & Nattie, E. (2010). Antagonism of rat orexin receptors by almorexant attenuates central chemoreception in wakefulness in the active period of the diurnal cycle. *The Journal of Physiology*, *588*(Pt 15), 2935–2944. https://doi.org/10.1113/jphysiol.2010.191288

Li, A., & Nattie, E. (2014). Orexin, cardio-respiratory function, and hypertension. *Frontiers in Neuroscience*, *8*, 22. https://doi.org/10.3389/fnins.2014.00022

Liblau, R. S. (2018). Put to sleep by immune cells. In *Nature* (Vol. 562, Issue 7725, pp. 46–48). https://doi.org/10.1038/d41586-018-06666-w

Lin, L., Faraco, J., Li, R., Kadotani, H., Rogers, W., Lin, X., Qiu, X., de Jong, P. J., Nishino, S., & Mignot, E. (1999). The Sleep Disorder Canine Narcolepsy Is Caused by a Mutation

in the Hypocretin (Orexin) Receptor 2 Gene. *Cell*, *98*(3), 365–376. https://doi.org/10.1016/S0092-8674(00)81965-0

Lin, Y., Matsumura, K., Tsuchihashi, T., Abe, I., & Iida, M. (2002). Chronic central infusion of orexin-A increases arterial pressure in rats. *Brain Research Bulletin*, *57*(5), 619–622. https://doi.org/10.1016/s0361-9230(01)00756-0

Liu, L., Wang, Q., Liu, A., Lan, X., Huang, Y., Zhao, Z., & Jie, H. (2020). Physiological Implications of Orexins/Hypocretins on Energy Metabolism and Adipose Tissue Development. *ACS Omega*, *5*, 547–555. https://doi.org/10.1021/acsomega.9b03106

Liu, R. J., Van Den Pol, A. N., & Aghajanian, G. K. (2002). Hypocretins (orexins) regulate serotonin neurons in the dorsal raphe nucleus by excitatory direct and inhibitory indirect actions. *Journal of Neuroscience*, *22*(21), 9453–9464. https://doi.org/10.1523/jneurosci.22-21-09453.2002

Lo Martire, V., Silvani, A., Alvente, S., Bastianini, S., Berteotti, C., Valli, A., & Zoccoli, G. (2018). Modulation of sympathetic vasoconstriction is critical for the effects of sleep on arterial pressure in mice. *Journal of Physiology*, *596*(4), 591–608. https://doi.org/10.1113/JP275353

Lo Martire, V., Silvani, A., Bastianini, S., Berteotti, C., & Zoccoli, G. (2012). Effects of Ambient Temperature on Sleep and Cardiovascular Regulation in Mice: The Role of Hypocretin/Orexin Neurons. *PLoS ONE*, *7*(10). https://doi.org/10.1371/journal.pone.0047032

Lu, J., Greco, M. A., Shiromani, P., & Saper, C. B. (2000). Effect of lesions of the ventrolateral preoptic nucleus on NREM and REM sleep. *The Journal of Neuroscience : The Official Journal of the Society for Neuroscience*, *20*(10), 3830–3842. https://doi.org/10.1523/JNEUROSCI.20-10-03830.2000

Lubkin, M., & Stricker-Krongrad, A. (1998). Independent feeding and metabolic actions of orexins in mice. *Biochemical and Biophysical Research Communications*, *253*(2), 241–245. https://doi.org/10.1006/bbrc.1998.9750

Ma, X., Zubcevic, L., Brüning, J. C., Ashcroft, F. M., & Burdakov, D. (2007). Electrical inhibition of identified anorexigenic POMC neurons by orexin/hypocretin. *Journal of Neuroscience*, *27*(7), 1529–1533. https://doi.org/10.1523/JNEUROSCI.3583-06.2007

Mancia, G., Baccelli, G., Adams, D. B., & Zanchetti, A. (1971). Vasomotor regulation during sleep in the cat. *The American Journal of Physiology*, *220*(4), 1086–1093. https://doi.org/10.1152/ajplegacy.1971.220.4.1086

Marcus, J. N., Aschkenasi, C. J., Lee, C. E., Chemelli, R. M., Saper, C. B., Yanagisawa, M., & Elmquist, J. K. (2001). Differential expression of orexin receptors 1 and 2 in the rat brain. *The Journal of Comparative Neurology*, *435*(1), 6–25. http://www.ncbi.nlm.nih.gov/pubmed/11370008

Mason, D. T. (1968). The autonomic nervous system and regulation of cardiovascular performance. *Anesthesiology*, *29*(4), 670–680. https://doi.org/10.1097/00000542-196807000-00009

Matsumura, K., Tsuchihashi, T., & Abe, I. (2001). Central orexin-A augments sympathoadrenal outflow in conscious rabbits. *Hypertension (Dallas, Tex. : 1979)*, *37*(6), 1382–1387. https://doi.org/10.1161/01.hyp.37.6.1382

Mezzanotte, W. S., Tangel, D. J., & White, D. P. (1996). Influence of sleep onset on upper-airway muscle activity in apnea patients versus normal controls. *American Journal of Respiratory and Critical Care Medicine*, *153*(6 Pt 1), 1880–1887. https://doi.org/10.1164/ajrccm.153.6.8665050

Mignot, E., Lammers, G. J., Ripley, B., Okun, M., Nevsimalova, S., Overeem, S., Vankova, J., Black, J., Harsh, J., Bassetti, C., Schrader, H., & Nishino, S. (2002). The role of cerebrospinal fluid hypocretin measurement in the diagnosis of narcolepsy and other hypersomnias. *Archives of Neurology*, *59*(10), 1553–1562. https://doi.org/10.1001/archneur.59.10.1553

Miki, K., Kato, M., & Kajii, S. (2003). Relationship between renal sympathetic nerve activity and arterial pressure during REM sleep in rats. *American Journal of Physiology. Regulatory, Integrative and Comparative Physiology*, *284*(2), R467-73. https://doi.org/10.1152/ajpregu.00045.2002

Milbank, E., & López, M. (2019). Orexins/Hypocretins: Key Regulators of Energy Homeostasis. *Frontiers in Endocrinology*, *10*, 830. https://doi.org/10.3389/fendo.2019.00830

Mileykovskiy, B. Y., Kiyashchenko, L. I., & Siegel, J. M. (2005). Behavioral correlates of

activity in identified hypocretin/orexin neurons. *Neuron*, *46*(5), 787–798. https://doi.org/10.1016/j.neuron.2005.04.035

Millman, R. P., Knight, H., Kline, L. R., Shore, E. T., Chung, D. C., & Pack, A. I. (1988). Changes in compartmental ventilation in association with eye movements during REM sleep. *Journal of Applied Physiology (Bethesda, Md.: 1985)*, *65*(3), 1196–1202. https://doi.org/10.1152/jappl.1988.65.3.1196

Mochizuki, T., Klerman, E. B., Sakurai, T., & Scammell, T. E. (2006). Elevated body temperature during sleep in orexin knockout mice. *American Journal of Physiology-Regulatory, Integrative and Comparative Physiology*, *291*(3), 533–540.

Monda, M., Viggiano, A., Mondola, P., & De Luca, V. (2001). Inhibition of prostaglandin synthesis reduces hyperthermic reactions induced by hypocretin-1/orexin A. *Brain Research*, *909*(1–2), 68–74. https://doi.org/10.1016/s0006-8993(01)02606-3

Morrison, S. F., & Nakamura, K. (2011). Central neural pathways for thermoregulation. *Frontiers in Bioscience (Landmark Edition)*, *16*, 74–104. https://doi.org/10.2741/3677

Mortola, J., & Maskrey, M. (2011). Metabolism, Temperature, and Ventilation. *Comprehensive Physiology*, *1*, 1679–1709. https://doi.org/10.1002/cphy.c100008

Mortola, J. P., & Frappell, P. B. (2000). Ventilatory responses to changes in temperature in mammals and other vertebrates. *Annual Review of Physiology*, *62*, 847–874. https://doi.org/10.1146/annurev.physiol.62.1.847

Mosko, S. S., Holowach, J. B., & Sassin, J. F. (1983). The 24-hour rhythm of core temperature in narcolepsy. *Sleep*, *6*(2), 137–146. https://doi.org/10.1093/sleep/6.2.137

Nagura, S., Sakagami, T., Kakiichi, A., Yoshimoto, M., & Miki, K. (2004). Acute shifts in baroreflex control of renal sympathetic nerve activity induced by REM sleep and grooming in rats. *The Journal of Physiology*, *558*(Pt 3), 975–983. https://doi.org/10.1113/jphysiol.2004.064527

Nakamura, A., Zhang, W., Yanagisawa, M., Fukuda, Y., & Kuwaki, T. (2007). Vigilance state-dependent attenuation of hypercapnic chemoreflex and exaggerated sleep apnea in orexin knockout mice. *Journal of Applied Physiology*, *102*(1), 241–248. https://doi.org/10.1152/japplphysiol.00679.2006

Nambu, T., Sakurai, T., Mizukami, K., Hosoya, Y., Yanagisawa, M., & Goto, K. (1999). Distribution of orexin neurons in the adult rat brain. *Brain Research*, *827*(1–2), 243–260. https://doi.org/10.1016/S0006-8993(99)01336-0

Neil-Dwyer, G., Bartlett, J., McAinsh, J., & Cruickshank, J. M. (1981). Beta-adrenoceptor blockers and the blood-brian barrier. *British Journal of Clinical Pharmacology*, *11*(6), 549–553. https://doi.org/10.1111/j.1365-2125.1981.tb01169.x

Nishino, S., Ripley, B., Overeem, S., Lammers, G. J., & Mignot, E. (2000). Hypocretin (orexin) deficiency in human narcolepsy. *Lancet*, *355*(9197), 39–40. https://doi.org/10.1016/S0140-6736(99)05582-8

Ohayon, M. M., Priest, R. G., Zulley, J., Smirne, S., & Paiva, T. (2002). Prevalence of narcolepsy symptomatology and diagnosis in the European general population. *Neurology*, *58*(12), 1826–1833. https://doi.org/10.1212/WNL.58.12.1826

Ohno, K., & Sakurai, T. (2008). Orexin neuronal circuitry: role in the regulation of sleep and wakefulness. *Frontiers in Neuroendocrinology*, *29*(1), 70–87. https://doi.org/10.1016/j.yfrne.2007.08.001

Parmeggiani, P. L. (1986). Interaction Between Sleep and Thermoregulation: An Aspect of the Control of Behavioral States. *Sleep*, *10*(5), 426–435. https://doi.org/10.1093/sleep/10.5.426

Peyron, C, Tighe, D. K., van den Pol, A. N., de Lecea, L., Heller, H. C., Sutcliffe, J. G., & Kilduff, T. S. (1998). Neurons containing hypocretin (orexin) project to multiple neuronal systems. *J Neurosci*, *18*(23), 9996–10015. http://www.ncbi.nlm.nih.gov/pubmed/9822755

Peyron, Christelle, Faraco, J., Rogers, W., Ripley, B., Overeem, S., Charnay, Y., Nevsimalova, S., Aldrich, M., Reynolds, D., Albin, R., Li, R., Hungs, M., Pedrazzoli, M., Padigaru, M., Kucherlapati, M., Jun, F., Maki, R., Lammers, G. J., Bouras, C., … Mignot, E. (2000). A mutation in a case of early onset narcolepsy and a generalized absence of hypocretin peptides in human narcoleptic brains. *Nature Medicine*, *6*(9), 991–997. https://doi.org/10.1038/79690

Qureshi, M., Khalil, M., Kwiatkowski, K., & Alvaro, R. E. (2009). Morphology of sighs and their role in the control of breathing in preterm infants, term infants and adults. *Neonatology*, *96*(1), 43–49. https://doi.org/10.1159/000201738

Reading, P. J. (2019). Update on narcolepsy. *Journal of Neurology*, *266*(7), 1809–1815. https://doi.org/10.1007/s00415-019-09310-3

Redgate, E. S., & Gellhorn, E. (1958). Respiratory activity and the hypothalamus. *The American Journal of Physiology*, *193*(1), 189–194. https://doi.org/10.1152/ajplegacy.1958.193.1.189

Ren, J., Ding, X., Funk, G. D., & Greer, J. J. (2012). Anxiety-related mechanisms of respiratory dysfunction in a mouse model of Rett syndrome. *J Neurosci*, *32*(48), 17230–17240. https://doi.org/10.1523/JNEUROSCI.2951-12.2012

Roussel, B., Turrillot, P., & Kitahama, K. (1984). Effect of ambient temperature on the sleep-waking cycle in two strains of mice. *Brain Research*, *294*(1), 67–73. https://doi.org/https://doi.org/10.1016/0006-8993(84)91310-6

Sachs, C., & Kaijser, L. (1982). Autonomic regulation of cardiopulmonary functions in sleep apnea syndrome and narcolepsy. *Sleep*, *5*(3), 227–238. https://doi.org/10.1093/sleep/5.3.227

Sakurai, T. (1999). Orexins and orexin receptors: Implication in feeding behavior. *Regulatory Peptides*, *85*(1), 25–30. https://doi.org/10.1016/S0167-0115(99)00076-2

Sakurai, T. (2007). The neural circuit of orexin (hypocretin): maintaining sleep and wakefulness. *Nature Reviews Neuroscience*, *8*(3), 171–181. https://doi.org/10.1038/nrn2092

Sakurai, T., Amemiya, A., Ishii, M., Matsuzaki, I., Chemelli, R. M., Tanaka, H., Williams, S. C., Richardson, J. A., Kozlowski, G. P., Wilson, S., Arch, J. R. S., Buckingham, R. E., Haynes, A. C., Carr, S. A., Annan, R. S., McNulty, D. E., Liu, W. S., Terrett, J. A., Elshourbagy, N. A., … Yanagisawa, M. (1998). Orexins and orexin receptors: A family of hypothalamic neuropeptides and G protein-coupled receptors that regulate feeding behavior. *Cell*, *92*(4), 573–585. https://doi.org/10.1016/S0092-8674(00)80949-6

Sakurai, T., Moriguchi, T., Furuya, K., Kajiwara, N., Nakamura, T., Yanagisawa, M., Goto, K., & Gene, H. O. (1999). *Structure and Function of Human Prepro-orexin Gene *. 274*(25), 17771–17776.

Sakurai, T., Nagata, R., Yamanaka, A., Kawamura, H., Tsujino, N., Muraki, Y., Kageyama, H., Kunita, S., Takahashi, S., Goto, K., Koyama, Y., Shioda, S., & Yanagisawa, M. (2005).

Input of orexin/hypocretin neurons revealed by a genetically encoded tracer in mice. *Neuron*, *46*(2), 297–308. https://doi.org/10.1016/j.neuron.2005.03.010

Sansa, G., Iranzo, A., & Santamaria, J. (2010). Obstructive sleep apnea in narcolepsy. *Sleep Medicine*, *11*(1), 93–95. https://doi.org/10.1016/j.sleep.2009.02.009

Saper, Clifford B., S. T. E. & L. J. (2005). Hypothalamic regulation of sleep and circadian rhythms. *Nature*, *437*, 1257–1263. https://doi.org/10.1038

Sarkanen, T., Alakuijala, A., Julkunen, I., & Partinen, M. (2018). Narcolepsy Associated with Pandemrix Vaccine. *Current Neurology and Neuroscience Reports*, *18*(7). https://doi.org/10.1007/s11910-018-0851-5

Saternos, H. C., Almarghalani, D. A., Gibson, H. M., Meqdad, M. A., Antypas, R. B., Lingireddy, A., & AbouAlaiwi, W. A. (2018). Distribution and function of the muscarinic receptor subtypes in the cardiovascular system. *Physiological Genomics*, *50*(1), 1–9. https://doi.org/10.1152/physiolgenomics.00062.2017

Scammell, T. E. (2003). The neurobiology, diagnosis, and treatment of narcolepsy. *Annals of Neurology*, *53*(2), 154–166. https://doi.org/10.1002/ana.10444

Scammell, T. E. (2015). Narcolepsy. *New England Journal of Medicine*, *373*(27), 2654–2662. https://doi.org/10.1056/NEJMra1500587

Scammell, T. E., Willie, J. T., Guilleminault, C., Siegel, J. M., & International Working Group on Rodent Models of Narcolepsy. (2009). A consensus definition of cataplexy in mouse models of narcolepsy. *Sleep*, *32*(1), 111–116. http://www.ncbi.nlm.nih.gov/pubmed/19189786

Schäfer, T., & Schläfke, M. E. (1998). Respiratory changes associated with rapid eye movements in normo- and hypercapnia during sleep. *Journal of Applied Physiology*, *85*(6), 2213–2219. https://doi.org/10.1152/jappl.1998.85.6.2213

Schneider, H., Schaub, C. D., Andreoni, K. A., Schwartz, A. R., Smith, P. L., Robotham, J. L., & O'Donnell, C. P. (1997). Systemic and pulmonary hemodynamic responses to normal and obstructed breathing during sleep. *Journal of Applied Physiology (Bethesda, Md. : 1985)*, *83*(5), 1671–1680. https://doi.org/10.1152/jappl.1997.83.5.1671

Schuld, A., Hebebrand, J., Geller, F., & Pollmacher, T. (2000). Increased body-mass index in

patients with narcolepsy. In *Lancet* (Vol. 355, Issue 9211, pp. 1274–1275). Elsevier Limited. https://doi.org/10.1016/S0140-6736(05)74704-8

Schulz, H. (2008). Rethinking sleep analysis. In *Journal of clinical sleep medicine : JCSM : official publication of the American Academy of Sleep Medicine* (Vol. 4, Issue 2, pp. 99–103).

Sei, H., Morita, Y., Morita, H., & Hosomi, H. (1989). Long-term profiles of sleep-related hemodynamic changes in the postoperative chronic cat. *Physiology & Behavior*, *46*(3), 499–502. https://doi.org/10.1016/0031-9384(89)90027-9

Sei, H., Morita, Y., Tsunooka, K., & Morita, H. (1999). Sino-aortic denervation augments the increase in blood pressure seen during paradoxical sleep in the rat. *Journal of Sleep Research*, *8*(1), 45–50. https://doi.org/10.1046/j.1365-2869.1999.00135.x

Sei, H., Sakai, K., Kanamori, N., Salvert, D., Vanni-Mercier, G., & Jouvet, M. (1994). Long-term variations of arterial blood pressure during sleep in freely moving cats. *Physiology & Behavior*, *55*(4), 673–679. https://doi.org/10.1016/0031-9384(94)90043-4

Sellayah, D., Bharaj, P., & Sikder, D. (2011). Orexin is required for brown adipose tissue development, differentiation, and function. *Cell Metabolism*, *14*(4), 478–490. https://doi.org/10.1016/j.cmet.2011.08.010

Sellayah, D., & Sikder, D. (2012). Orexin receptor-1 mediates brown fat developmental differentiation. *Adipocyte*, *1*(1), 58–63. https://doi.org/10.4161/adip.18965

Sellayah, D., & Sikder, D. (2014). Orexin restores aging-related brown adipose tissue dysfunction in male mice. *Endocrinology*, *155*(2), 485–501. https://doi.org/10.1210/en.2013-1629

Shahid, I. Z., Rahman, A. A., & Pilowsky, P. M. (2011). Intrathecal orexin A increases sympathetic outflow and respiratory drive, enhances baroreflex sensitivity and blocks the somato-sympathetic reflex. *British Journal of Pharmacology*, *162*(4), 961–973. https://doi.org/10.1111/j.1476-5381.2010.01102.x

Sheng, Z., Santiago, A. M., Thomas, M. P., & Routh, V. H. (2014). Metabolic regulation of lateral hypothalamic glucose-inhibited orexin neurons may influence midbrain reward neurocircuitry. *Molecular and Cellular Neurosciences*, *62*, 30–41. https://doi.org/10.1016/j.mcn.2014.08.001

Sherin, J. E., Elmquist, J. K., Torrealba, F., & Saper, C. B. (1998). Innervation of histaminergic tuberomammillary neurons by GABAergic and galaninergic neurons in the ventrolateral preoptic nucleus of the rat. *The Journal of Neuroscience : The Official Journal of the Society for Neuroscience*, *18*(12), 4705–4721. https://doi.org/10.1523/JNEUROSCI.18-12-04705.1998

Shih, C. D., & Chuang, Y. C. (2007). Nitric oxide and GABA mediate bi-directional cardiovascular effects of orexin in the nucleus tractus solitarii of rats. *Neuroscience*, *149*(3), 625–635. https://doi.org/10.1016/j.neuroscience.2007.07.016

Shirasaka, T, Nakazato, M., Matsukura, S., Takasaki, M., & Kannan, H. (1999). Sympathetic and cardiovascular actions of orexins in conscious rats. *The American Journal of Physiology*, *277*(6), R1780-5. https://doi.org/10.1152/ajpregu.1999.277.6.R1780

Shirasaka, Tetsuro, Miyahara, S., Kunitake, T., Jin, Q. H., Kato, K., Takasaki, M., & Kannan, H. (2001). Orexin depolarizes rat hypothalamic paraventricular nucleus neurons. *American Journal of Physiology - Regulatory Integrative and Comparative Physiology*, *281*(4 50-4), 1114–1118. https://doi.org/10.1152/ajpregu.2001.281.4.r1114

Shirasaka, Tetsuro, Takasaki, M., & Kannan, H. (2003). Cardiovascular effects of leptin and orexins. *American Journal of Physiology - Regulatory Integrative and Comparative Physiology*, *284*(3 53-3). https://doi.org/10.1152/ajpregu.00359.2002

Sieminski, M., & Partinen, M. (2016). "Non-dipping" is equally frequent in narcoleptic patients and in patients with insomnia. *Sleep and Biological Rhythms*, *14*, 31–36. https://doi.org/10.1007/s41105-015-0004-z

Silvani, A. (2008). Physiological sleep-dependent changes in arterial blood pressure: Central autonomic commands and baroreflex control. In *Clinical and Experimental Pharmacology and Physiology* (Vol. 35, Issue 9, pp. 987–994). https://doi.org/10.1111/j.1440-1681.2008.04985.x

Silvani, A., Bastianini, S., Berteotti, C., Franzini, C., Lenzi, P., Lo Martire, V., & Zoccoli, G. (2009). Sleep modulates hypertension in leptin-deficient obese mice. *Hypertension*, *53*(2), 251–255. https://doi.org/10.1161/HYPERTENSIONAHA.108.125542

Silvani, A., Bastianini, S., Berteotti, C., Lo Martire, V., & Zoccoli, G. (2012). Control of cardiovascular variability during undisturbed wake-sleep behavior in hypocretin-deficient

mice. *American Journal of Physiology - Regulatory Integrative and Comparative Physiology*, *302*(8), 958–964. https://doi.org/10.1152/ajpregu.00668.2011

Silvani, A., Berteotti, C., Bastianini, S., Cohen, G., Lo Martire, V., Mazza, R., Pagotto, U., Quarta, C., & Zoccoli, G. (2014). Cardiorespiratory anomalies in mice lacking CB1cannabinoid receptors. *PLoS ONE*, *9*(6), e100536. https://doi.org/10.1371/journal.pone.0100536

Silvani, A., Calandra-Buonaura, G., Dampney, R. A. L., & Cortelli, P. (2016). Brain-heart interactions: physiology and clinical implications. *Philosophical Transactions. Series A, Mathematical, Physical, and Engineering Sciences*, *374*(2067). https://doi.org/10.1098/rsta.2015.0181

Silvani, A., & Dampney, R. A. L. (2013). Central control of cardiovascular function during sleep. *American Journal of Physiology. Heart and Circulatory Physiology*, *305*(12), H1683-92. https://doi.org/10.1152/ajpheart.00554.2013

Silveira, N. P., Moreira, E. D., Drager, L. F., Silva, G. J. J., & Krieger, E. M. (2008). Effects of sinoaortic denervation on hemodynamic parameters during natural sleep in rats. *Sleep*, *31*(3), 328–333. https://doi.org/10.1093/sleep/31.3.328

Skatrud, J. B., Dempsey, J. A., Badr, S., & Begle, R. L. (1988). Effect of airway impedance on CO2 retention and respiratory muscle activity during NREM sleep. *Journal of Applied Physiology (Bethesda, Md. : 1985)*, *65*(4), 1676–1685. https://doi.org/10.1152/jappl.1988.65.4.1676

Smith, P. M., Connolly, B. C., & Ferguson, A. V. (2002). Microinjection of orexin into the rat nucleus tractus solitarius causes increases in blood pressure. *Brain Research*, *950*(1–2), 261–267. https://doi.org/10.1016/s0006-8993(02)03048-2

Smyth, H. S., Sleight, P., & Pickering, G. W. (1969). Reflex regulation of arterial pressure during sleep in man. A quantitative method of assessing baroreflex sensitivity. *Circulation Research*, *24*(1), 109–121. https://doi.org/10.1161/01.res.24.1.109

Somers, V. K., Dyken, M. E., Mark, A. L., & Abboud, F. M. (1993). Sympathetic-nerve activity during sleep in normal subjects. *The New England Journal of Medicine*, *328*(5), 303–307. https://doi.org/10.1056/NEJM199302043280502

Sullivan, C. E., Murphy, E., Kozar, L. F., & Phillipson, E. A. (1979). Ventilatory responses to

CO2 and lung inflation in tonic versus phasic REM sleep. *Journal of Applied Physiology: Respiratory, Environmental and Exercise Physiology*, *47*(6), 1305–1310. https://doi.org/10.1152/jappl.1979.47.6.1304

Székely, M., Pétervári, E., Balaskó, M., Hernádi, I., & Uzsoki, B. (2002). Effects of orexins on energy balance and thermoregulation. *Regulatory Peptides*, *104*(1–3), 47–53. https://doi.org/10.1016/s0167-0115(01)00348-2

Tabuchi, S., Tsunematsu, T., Black, S. W., Tominaga, M., Maruyama, M., Takagi, K., Minokoshi, Y., Sakurai, T., Kilduff, T. S., & Yamanaka, A. (2014). Conditional ablation of orexin/hypocretin neurons: a new mouse model for the study of narcolepsy and orexin system function. *The Journal of Neuroscience : The Official Journal of the Society for Neuroscience*, *34*(19), 6495–6509. https://doi.org/10.1523/JNEUROSCI.0073-14.2014

Tabuchi, S., Tsunematsu, T., Kilduff, T. S., Sugio, S., Xu, M., Tanaka, K. F., Takahashi, S., Tominaga, M., & Yamanaka, A. (2013). Influence of inhibitory serotonergic inputs to orexin/hypocretin neurons on the diurnal rhythm of sleep and wakefulness. *Sleep*, *36*(9), 1391–1404. https://doi.org/10.5665/sleep.2972

Takahashi, Y., Zhang, W., Sameshima, K., Kuroki, C., Matsumoto, A., Sunanaga, J., Kono, Y., Sakurai, T., Kanmura, Y., & Kuwaki, T. (2013). Orexin neurons are indispensable for prostaglandin E2-induced fever and defence against environmental cooling in mice. *J Physiol*, *591*(22), 5623–5643. https://doi.org/10.1113/jphysiol.2013.261271

Tang, X., & Dworkin, B. R. (2010). Baroreflexes of the rat. VI. Sleep and responses to aortic nerve stimulation in the dmNTS. *American Journal of Physiology. Regulatory, Integrative and Comparative Physiology*, *298*(5), R1428-34. https://doi.org/10.1152/ajpregu.00486.2009

Tank, J., Jordan, J., Diedrich, A., Obst, M., Plehm, R., Luft, F. C., & Gross, V. (2004). Clonidine Improves Spontaneous Baroreflex Sensitivity in Conscious Mice through Parasympathetic Activation. *Hypertension*, *43*(5), 1042–1047. https://doi.org/10.1161/01.HYP.0000125884.49812.72

Terada, J., Nakamura, A., Zhang, W., Yanagisawa, M., Kuriyama, T., Fukuda, Y., & Kuwaki, T. (2008). Ventilatory long-term facilitation in mice can be observed during both sleep and wake periods and depends on orexin. *Journal of Applied Physiology*, *104*(2), 499–507. https://doi.org/10.1152/japplphysiol.00919.2007

Thannickal, T. C., Moore, R. Y., Nienhuis, R., Ramanathan, L., Gulyani, S., Aldrich, M., Cornford, M., & Siegel, J. M. (2000). Reduced number of hypocretin neurons in human narcolepsy. *Neuron*, *27*(3), 469–474. http://www.ncbi.nlm.nih.gov/pubmed/11055430

Tsujino, N., & Sakurai, T. (2009). Orexin/hypocretin: A neuropeptide at the interface of sleep, energy homeostasis, and reward system. *Pharmacological Reviews*, *61*(2), 162–176. https://doi.org/10.1124/pr.109.001321

Tupone, D., Madden, C. J., Cano, G., & Morrison, S. F. (2011). An orexinergic projection from perifornical hypothalamus to raphe pallidus increases rat brown adipose tissue thermogenesis. *Journal of Neuroscience*, *31*(44), 15944–15955. https://doi.org/10.1523/JNEUROSCI.3909-11.2011

Uschakov, A., Gong, H., McGinty, D., & Szymusiak, R. (2006). Sleep-active neurons in the preoptic area project to the hypothalamic paraventricular nucleus and perifornical lateral hypothalamus. *The European Journal of Neuroscience*, *23*(12), 3284–3296. https://doi.org/10.1111/j.1460-9568.2006.04860.x

Valham, F., Sahlin, C., Stenlund, H., & Franklin, K. A. (2012). Ambient Temperature and Obstructive Sleep Apnea: Effects on Sleep, Sleep Apnea, and Morning Alertness. *Sleep*, *35*(4), 513–517. https://doi.org/10.5665/sleep.1736

Vander, A. J., Sherman, J. H., & Luciano, D. S. (1986). *Human Physiology. The mechanism of body function* (Fourth Edi). McGraw-Hill.

Venner, A., Karnani, M. M., Gonzalez, J. A., Jensen, L. T., Fugger, L., & Burdakov, D. (2011). Orexin neurons as conditional glucosensors: paradoxical regulation of sugar sensing by intracellular fuels. *The Journal of Physiology*, *589*(Pt 23), 5701–5708. https://doi.org/10.1113/jphysiol.2011.217000

Wall, A., & Volkoff, H. (2013). General and Comparative Endocrinology Effects of fasting and feeding on the brain mRNA expressions of orexin , tyrosine hydroxylase (TH), PYY and CCK in the Mexican blind cavefish (Astyanax fasciatus mexicanus). *General and Comparative Endocrinology*, *183*, 44–52. https://doi.org/10.1016/j.ygcen.2012.12.011

Wallin, B. G., & Charkoudian, N. (2007). Sympathetic neural control of integrated cardiovascular function: insights from measurement of human sympathetic nerve activity. *Muscle & Nerve*, *36*(5), 595–614. https://doi.org/10.1002/mus.20831

Williams, R. H., Jensen, L. T., Verkhratsky, A., Fugger, L., & Burdakov, D. (2007). Control of hypothalamic orexin neurons by acid and CO2. *Proceedings of the National Academy of Sciences of the United States of America*, *104*(25), 10685–10690. https://doi.org/10.1073/pnas.0702676104

Willie, J. T., Chemelli, R. M., Sinton, C. M., Tokita, S., Williams, S. C., Kisanuki, Y. Y., Marcus, J. N., Lee, C., Elmquist, J. K., Kohlmeier, K. A., Leonard, C. S., Richardson, J. A., Hammer, R. E., & Yanagisawa, M. (2003). Distinct Narcolepsy Syndromes in Orexin Receptor-2 and Orexin Null Mice : Molecular Genetic Dissection of Non-REM and REM Sleep Regulatory Processes. *Neuron*, *38*, 715–730. https://doi.org/10.1016/s0896-6273(03)00330-1

Willie, J. T., M., C. R., & Masashi, S. C. M. Y. (2001). To eat or to sleep? Orexin in the regulation of feeding and wakefulness. *Annual Review of Neuroscience*, *24*(1), 429–458. https://doi.org/Annu. Rev. Neurosci. 2001. 24:429–58

Won, C., Mahmoudi, M., Qin, L., Purvis, T., Mathur, A., & Mohsenin, V. (2014). The impact of gender on timeliness of narcolepsy diagnosis. *Journal of Clinical Sleep Medicine : JCSM : Official Publication of the American Academy of Sleep Medicine*, *10*(1), 89–95. https://doi.org/10.5664/jcsm.3370

Yamanaka, A., Beuckmann, C. T., Willie, J. T., Hara, J., Tsujino, N., Mieda, M., Tominaga, M., Yagami, K. I., Sugiyama, F., Goto, K., Yanagisawa, M., & Sakurai, T. (2003). Hypothalamic orexin neurons regulate arousal according to energy balance in mice. *Neuron*, *38*(5), 701–713. https://doi.org/10.1016/S0896-6273(03)00331-3

Yamanaka, A., Kunii, K., Nambu, T., Tsujino, N., Sakai, A., Matsuzaki, I., Miwa, Y., Goto, K., & Sakurai, T. (2000). Orexin-induced food intake involves neuropeptide Y pathway. *Brain Research*, *859*(2), 404–409. https://doi.org/10.1016/S0006-8993(00)02043-6

Yamanaka, A., Muraki, Y., Tsujino, N., Goto, K., & Sakurai, T. (2003). Regulation of orexin neurons by the monoaminergic and cholinergic systems. *Biochemical and Biophysical Research Communications*, *303*(1), 120–129. https://doi.org/10.1016/s0006-291x(03)00299-7

Yamanaka, A., Tsujino, N., Goto, K., Sakurai, T., Funahashi, H., Guan, J. L., Wang, Q. P., Shioda, S., Honda, K., & Tominaga, M. (2002). Orexins activate histaminergic neurons via the orexin 2 receptor. *Biochemical and Biophysical Research Communications*,

290(4), 1237–1245. https://doi.org/10.1006/bbrc.2001.6318

Yoshida, K., McCormack, S., España, R. A., Crocker, A., & Scammell, T. E. (2006). Afferents to the orexin neurons of the rat brain. *Journal of Comparative Neurology*, *494*(5), 845–861. https://doi.org/10.1002/cne.20859

Yoshimoto, M., Sakagami, T., Nagura, S., & Miki, K. (2004). Relationship between renal sympathetic nerve activity and renal blood flow during natural behavior in rats. *American Journal of Physiology. Regulatory, Integrative and Comparative Physiology*, *286*(5), R881-7. https://doi.org/10.1152/ajpregu.00105.2002

Yoshimoto, M., Yoshida, I., & Miki, K. (2011). Functional role of diverse changes in sympathetic nerve activity in regulating arterial pressure during REM sleep. *Sleep*, *34*(8), 1093–1101. https://doi.org/10.5665/SLEEP.1168

Zhang, S., Zeitzer, J. M., Sakurai, T., Nishino, S., & Mignot, E. (2007). Sleep/wake fragmentation disrupts metabolism in a mouse model of narcolepsy. *Journal of Physiology*, *581*(2), 649–663. https://doi.org/10.1113/jphysiol.2007.129510

Zhang, W, Fukuda, Y., & Kuwaki, T. (2005). Respiratory and cardiovascular actions of orexin-A in mice. *Neurosci Lett*, *385*(2), 131–136. https://doi.org/10.1016/j.neulet.2005.05.032

Zhang, Wei, Shimoyama, M., Fukuda, Y., & Kuwaki, T. (2006). Multiple components of the defense response depend on orexin: Evidence from orexin knockout mice and orexin neuron-ablated mice. *Autonomic Neuroscience: Basic and Clinical*, *126–127*, 139–145. https://doi.org/10.1016/j.autneu.2006.02.021

Zhang, Wei, Sunanaga, J., Takahashi, Y., Mori, T., Sakurai, T., Kanmura, Y., & Kuwaki, T. (2010). Orexin neurons are indispensable for stress-induced thermogenesis in mice. *The Journal of Physiology*, *588*(Pt 21), 4117–4129. https://doi.org/10.1113/jphysiol.2010.195099

Zhu, Y, Yamanaka, A., Kunii, K., Tsujino, N., Goto, K., & Sakurai, T. (2002). Orexin-mediated feeding behavior involves both leptin-sensitive and -insensitive pathways. *Physiology & Behavior*, *77*(2), 251–257. https://doi.org/https://doi.org/10.1016/S0031-9384(02)00843-0

Zhu, Yun, Miwa, Y., Yamanaka, A., Yada, T., Shibahara, M., Abe, Y., Sakurai, T., & Goto, K. (2003). Orexin receptor type-1 couples exclusively to pertussis toxin-insensitive G-

proteins, while orexin receptor type-2 couples to both pertussis toxin-sensitive and -insensitive G-proteins. *Journal of Pharmacological Sciences*, *92*(3), 259–266. https://doi.org/10.1254/jphs.92.259

Zinkovska, S. M., Rodriguez, E. K., & Kirby, D. A. (1996). Coronary and total peripheral resistance changes during sleep in a porcine model. *The American Journal of Physiology*, *270*(2 Pt 2), H723-9. https://doi.org/10.1152/ajpheart.1996.270.2.H723

LIST OF ABBREVIATIONS

A

ACT *Activity signal*

AgRP *Agouti-related protein*

ANS *Autonomic nervous system*

AP *Arterial pressure*

ARC *Arcuate nucleus*

AV *Atrioventricular*

B

BAT *Brown adipose tissue*

BF *Basal forebrain*

BMI *Body mass index*

BMR *Basal metabolic rate*

BP *Blood pressure*

BST *Bed nucleus of the stria terminalis*

C

CART *Cocaine- and amphetamine-related transcript*

CSF *Cerebrospinal fluid*

CVLM *Caudal ventrolateral medulla*

D

DMH *Dorsomedial hypothalamus*

DR *Dorsal raphe*

ΔMAP *Differences in mean arterial pressure*

E

EEG *Electroencephalographic*

EMG *Electromyographic*

EOG *Electrooculographic*

F

GABA *Gamma Amino-butyric acid*

GPCRs *G-protein-coupled cell surface receptors*

H

HLA *Human leukocyte antigen*

HP *Heart period*

HR *Heart rate*

I

ICV *Intracerebroventricular*

IP *Intraperitoneal*

L

LC *Locus coeruleus*

LHA *Lateral area of hypothalamus*

LTF *Long-term facilitation*

M

MAP *Mean arterial pressure*

MSLT *Multiple sleep latency test*

N

NO *Nitric oxide*

NPY *Neuropeptide Y*

NREM *Non-rapid eye movement*

NT1 *Narcolepsy type 1*

NT2 *Narcolepsy type 2*

NTS *Nucleus tractus solitarii*

O

ORX-A *Orexin A*

ORX-AB *ORX neurons-ablated*

ORX-B *Orexin B*

ORX-KO *Prepro-ORX knockout*

ORXs *Orexins*

OSA *Obstructive Sleep Apnea*

OX1R *ORX-1 receptor*

OX2R *ORX-2 receptor*

OX2R-KO *OX2R knockout*

OXRs *Orexin receptors*

P

PCR *Polymerase chain reaction*

PFA *Perifornical area*

POMC *Pro-opiomelanocortin*

prepro-ORX *Prepro-orexin*

PVN *Paraventricular nucleus*

R

REM *Rapid-eye-movement*

rRPa *Rostral raphe pallidus*

RSNA *Renal sympathetic nerve activity*

RVLM *Rostral ventrolateral medulla*

S

s.d.1 *Short-term variability*

s.d.2 *Long-term variability*

SA *Sinoatrial*

SAD *Sinoaortic denervation*

SD *Sleep deprivation*

SLD *Sublateral dorsal*

SOREMP *Sleep-onset REM period*

T

Ta *Ambient temperature*

Tb	*Body temperature*
TMN	*Tuberomammillary nucleus*
	V
VE	*Minute ventilation*
vlPAG	*Ventrolateral periaqueductal gray*
VMH	*Ventromedial hypothalamic nucleus*
VO2	*Rates of oxygen consumption*
VP	*Ventilatory period*
Vt	*Tidal volume*
VTA	*Ventral tegmental area*
	W
W	*Wakefulness*
WBP	*Whole-body plethysmography*
WT	*Wild type*